PROTEIN-RESISTANT POLYURETHANE PREPARED BY SURFACE-INITIATED ATRP OF WATER-SOLUBLE POLYMERS

PROTEIN-RESISTANT POLYURETHANE PREPARED BY SURFACE-INITIATED ATOM TRANSFER RADICAL POLYMERIZATION OF WATER-SOLUBLE POLYMERS

By

ZHILIN JIN, B.Eng., D.Sc.

A Thesis
Submitted to the School of Graduate Studies
In Partial Fulfillment of the Requirements
For the Degree
Doctor of Philosophy

McMaster University

DOCTOR OF PHILOSOPHY (2010) McMaster University
(Chemical Engineering) Hamilton, Ontario

TITLE: Protein-Resistant Polyurethane Prepared by Surface-Initiated Atom Transfer Radical Polymerization of Water-Soluble Polymers

AUTHOR: Zhilin Jin
B.Eng. (Shandong University)
D.Sc. (Shandong University)

SUPERVISORS: Professor Shiping Zhu
Professor John L. Brash

NUMBER OF PAGES: 186

ABSTRACT

This work focused on grafting water-soluble polymers with well-controlled properties such as tuneable polymer chain length and high graft density to improve the biocompatibility of polymer surfaces via surface-initiated atom transfer radical polymerization (s-ATRP); and on gaining improved fundamental understanding of the mechanisms and factors (e.g., graft chain length and surface density of monomer units) in protein resistance of the water-soluble grafts.

Protein-resistant polyurethane (PU) surfaces were prepared by grafting water-soluble polymers including poly(oligo(ethylene glycol) methacrylate) (poly(OEGMA)) and poly(1-methacryloyloxyethyl phosphorylcholine) (poly(MPC)) via s-ATRP. A typical three-step procedure was used in the ATRP grafting. First, the substrate surface was treated in an oxygen plasma and reactive sites (-OH and -OOH) were formed upon exposure to air. Second, the substrate surface was immersed in 2-bromoisobutyryl bromide (BIBB)-toluene solution to form a layer of ATRP initiator. Finally, target polymer was grafted from the initiator-immobilized surface by s-ATRP with Cu(I)Br/2bpy complex as catalyst. The graft chain length was adjusted by varying the molar ratio of monomer to sacrificial initiator in solution. The modified PU surfaces were characterized by water contact angle, X-ray photoelectron spectroscopy (XPS), and atomic force microscopy (AFM).

Protein adsorption experiments were carried out to evaluate the protein-resistance of the surfaces. Adsorption from single and binary protein solutions as well as from plasma decreased significantly after poly(OEGMA) grafting, and decreased with

increasing poly(OEGMA) main chain length. Fibrinogen (Fg) adsorption on the most resistant surfaces (chain length 200 units) was in the range of 3-33 ng/cm^2, representing a reduction of more than 96% compared to the control surfaces.

OEGMA monomers with three different molecular weights (MW 300, 475, 1100 g/mol) were used to achieve different side chain lengths of poly(OEGMA). Fibrinogen (Fg) and lysozyme (Lys) were used as model proteins in adsorption experiments. The effects of side chain length as well as main chain length were then investigated. It was found that adsorption to the poly(OEGMA)-grafted PU (PU/PO) surfaces was protein size dependent. Resistance was greater for the larger protein. For grafts of a given side chain length, the adsorption of both proteins decreased with increasing polymer main chain length. For a given main chain length, the adsorption of Fg, the larger protein, was independent of side chain length. Surprisingly, however, Lys (the smaller protein) adsorption increased with increasing side chain length. A reasonable explanation is that graft main chain density decreased as monomer size and footprint on the surface increased. Protein size-based discrimination suggests that the chain density was lower than required to form layers in the "brush" regime in which protein size is expected to have little effect on protein adsorption.

In order to achieve high surface densities of ethylene oxide (EO) units, we used a sequential double grafting approach whereby the surface was grafted first with poly(2-hydroxyethyl methacrylate) (HEMA) by s-ATRP. OEGMA grafts were then grown from the hydroxyl groups on HEMA chains by a second ATRP. The effect of EO density on protein-resistant properties was then investigated. Protein adsorption on the sequentially-grafted poly(HEMA)-poly(OEGMA) surfaces (PU/PH/PO) was not only significantly lower than on the unmodified PU as expected, but also much lower than on the PU/PO surfaces with the same poly(OEGMA) chain length. Moreover, protein adsorption decreased with increasing EO density for these grafts. On the PU/PH/PO surface with a poly(OEGMA) chain length of 100, the adsorption of Lys and Fg were reduced by ~98%

and >99%, respectively, compared to the unmodified PU. Binary protein adsorption experiments showed that suppression of protein adsorption on the PU/PH/PO surfaces was essentially independent of protein size. The double-grafted OEG layers resisted both proteins equally.

The general applicability of this approach which combines oxygen plasma treatment and ATRP grafting was also studied. Various kinds of polymers such as PU, silicone hydrogel, and polydimethylsiloxane (PDMS) were chosen as substrates. Poly(MPC) grafts with different chain lengths were achieved by the three-step ATRP-grafting procedure. It was found that protein adsorption levels on the poly(MPC) grafts were significantly lower than on the respective unmodified surfaces. Protein adsorption decreased with increasing poly(MPC) chain length. Among the surfaces investigated, PU/MPC showed the highest protein resistance for a given chain length.

ACKNOWLEDGEMENTS

I would like to take this opportunity to express my sincere thanks to the following people who helped me and supported me throughout my journey to complete this work.

I have had the pleasure to work with two excellent supervisors, Dr. Shiping Zhu and Dr. John L. Brash. They encouraged and guided me with great patience and sincerity throughout the course of this study. I would like to express my deep and sincere gratitude to my supervisors for their constant guidance and generous support.

I am deeply grateful to Dr. Raja Ghosh and Dr. Harald D. H. Stöver for serving on my supervisory committee. Their valuable suggestions and help are greatly appreciated. I warmly thank Dr. Heather Sheardown for her kind support and friendly help.

I would like to thank Rena M. Cornelius and W. Glenn McClung for the tremendous assistance and valuable discussion around my work. Thank Dr. Wei Feng for training me in polymer synthesis and protein adsorption experiments and all the valuable advices. Thank Dr. Santiago Faucher for his great suggestions and strong help. Many thanks to my colleagues, Hualong Pan, Renxu Chen, Xiang Gao, Jen Mahon, Yixin Gong, Hongyan Gu, Kyla Sask, Sara Alibeik, Junwei Zhang, Mark Machado, Mohammad Haj Abed, Jason Doggart and many others for their friendship and assistance.

I would also like to thank my parents and brother for their continuous support and encouragement over the years. I would like to dedicate this thesis to my husband, my best friend, Weian Zhao. Without his steadfast support and love, this study could not have been completed.

The financial supports through the Ontario Graduate Fellowship, the Natural Sciences and Engineering Research Council of Ca

nada (NSERC), Canadian Foundation of Innovation (CFI), the Canadian Institutes of Health Research (CIHR) and McMaster University are gratefully acknowledged.

TABLE OF CONTENTS

LIST OF FIGURES

LIST OF TABLES

LIST OF SCHEMES

LIST OF ABBREVIATIONS

AFM	atomic force microscopy
ATRP	atom transfer radical polymerization
BIBB	2-bromoisobutyryl bromide
BMA	n-butyl methacrylate
CRP	controlled radical polymerization
DLVO	Derjaguin-Landau-Verwey-Overbeek
DMA	n-dodecyl methacrylate
DMAEMA	2-(dimethylamino)ethyl methacrylate
DMAPAAm	dimethylaminopropyl acrylamide
EO	ethylene oxide
Et_3N	triethylamine
Fg	fibrinogen
FTIR	Fourier transform infrared spectroscopy
GMA	glycidyl methacrylate
HEMA	2-hydroxyethyl methacrylate
Lac	lactalbumin
Lys	lysozyme
MAA	methacrylic acid
MDI	4,4'-diphenylmethane diisocyanate
MMA	methyl methacrylate
MPC	2-methacryloyloxyethyl phosphorylcholine
MPEOMA	methoxy PEO monomethacrylate

MW	molecular weight
NIPAAm	N-isopropylacrylamide
NMRP	nitroxide mediated radical polymerization
OEG	oligo(ethylene glycol)
PAA	polyacrylic acid
PBS	phosphate buffered saline
PC	phosphorylcholine
PDMS	poly(dimethylsiloxane)
PE	polyethylene
PEG	poly(ethylene glycol)
PEO	poly(ethylene oxide)
PET	poly(ethylene terephthalate)
Poly(HEMA)	poly(2-hydroxyethyl methacrylate)
Poly(MEA)	poly(2-methoxyethylacrylate)
Poly(MPC)	poly(1-methacryloyloxyethyl phosphorylcholine)
Poly(OEGMA)	poly(oligo(ethylene glycol) methyl ether methacrylate)
PP	polypropylene
PS	polystyrene
PU/PO	poly(OEGMA)-grafted PU
PU/PH/PO	poly(HEMA)-poly(OEGMA)-grafted PU
PU	polyurethane
PVP	poly(vinylpyrrolidone)
RAFT	reversible addition-fragmentation chain transfer
SAM	self-assembled monolayer
s-ATRP	surface-initiated atom transfer radical polymerization
SEM	scanning electron microscopy

SMMs	surface-modifying macromolecules
TBAEMA	2-(tert-butylamino)ethyl methacrylate
TBS	tris-buffered saline
THF	tetrahydrofuran
VSA	vinyl sulfonic acid sodium salt
XPS	X-ray photoelectron spectroscopy

CHAPTER 1 Introduction and Literature Review

Biomaterials are widely used in medical devices such as contact lenses, orthopaedic implants, blood pumps, pacemakers, vascular grafts and catheters.[1-3] For these applications, biocompatibility is a crucial requirement. It is generally accepted that protein adsorption is the initiating event in tissue-material interactions and is strongly detrimental to biocompatibility.[4] Adsorbed proteins may induce many adverse effects such as coagulation, thrombosis, bacterial infection, and the foreign body reaction, leading to the failure of the device.[5-7] Therefore, an important strategy to improve biocompatibility is to reduce or eliminate non-specific protein adsorption.

Surface physical and chemical properties play very important roles in mediating protein adsorption[8] and the hydrophobic effect is generally believed to be a particularly important driving force for protein-surface interactions.[9] Some hydrophilic or water soluble polymers such as PEO have relatively low interfacial free energy[10] and can reduce protein and cell interactions at the tissue-material interface.[11,12]

Several approaches have been developed to incorporate protein resistant polymers into biomaterial surfaces, including physisorption, chemical grafting, blending etc.[13-15] Among these approaches, surface-initiated atom transfer radical polymerization (s-ATRP) has attracted much attention due to numerous advantages such as tolerance of impurities, versatility of monomer type, and mild reaction conditions.[16] Most importantly of all, uniform and tuneable graft chain length and relatively high graft density are achievable using s-ATRP.[17-19] The ability to vary grafting density, chain length and functional groups is of great importance for the optimization of protein-resistant properties.[20,21]

In recent years, well-defined polymer grafts have been successfully achieved using s-ATRP on model surfaces such as gold, silicon and titanium.[22,23] However, surface-initiated ATRP grafting of water-soluble polymers with well-controlled grafting density and chain length on polymeric biomaterials such as polyurethane remains challenging. The aim of the research described in this thesis was to develop protein resistant polymeric biomaterials using s-ATRP grafting, and to improve our understanding of the effects of protein and polymer graft properties on protein resistance.

1.1 Polyurethanes as Biomaterials

Polyurethanes (PUs) have been widely used in biomedical applications such as blood bags, vascular catheters, intra-aortic balloon pumps, and pacemaker lead insulation.[24] The benefits of PUs come from their outstanding physical and mechanical properties, which include flexibility, durability, fatigue resistance, shape retention, elasticity, and tensile strength. The versatility in PU physical properties is also a key attribute and arises from the variability of their physical structures and chemical composition. Although PUs have relatively good biocompatibility,[25,26] they are by no means problem free when used as biomaterials. In particular, as for other polymeric materials, they provoke coagulation and thrombosis in contact with blood.

Polyurethanes are block copolymers typically formed by the addition reactions between a diisocyanate such as 4,4'-diphenylmethane diisocyanate (MDI), a polyester, polyether or polycarbonate polyol, and a chain extender.[27] The diisocyanate and chain extender form relatively stiff and hard chain segments while polyols form amorphous or semi-crystalline soft segments. In the solid state the hard and soft segments tend to separate into respective domains or microphases. The segment chemical composition determines the nature of the domains, such as hydrophilic/hydrophobic, amorphous, semi-crystalline or crystalline. The variable nature of the domains and the extent of phase separation give polyurethanes a broad range of physical and mechanical properties.[28]

Although "inert" PUs have relatively good biocompatibility, they are by no means ideal as already indicated. Properties required for an ideal biomaterial include biodurability, biostability, blood compatibility (including thromboresistance), and infection resistance among others. Modification of PUs, especially surface modification, for improved biocompatibility has been extensively studied. For example, polyurethane was blended with phospholipid-containing polymers for improved blood compatibility.[29] Biologically active species such as anticoagulants,[30] recombinant peptides[31] and collagen[32] were attached to polyurethane surfaces via chemical coupling to improve tissue compatibility. Among the numerous modification methods, surface modification is generally believed to be the method of choice to improve biocompatibility while maintaining excellent bulk properties such as mechanical strength.

1.2 Protein Adsorption and Biocompatibility

Blood is a biological fluid containing water, salts, minerals, lipids, other organics, proteins and cells. This complex composition gives a wide range of possible interactions and competitive processes when blood is in contact with a biomaterial. It is well accepted that the first event following blood-material contact is the rapid adsorption of a layer of proteins.[33-35] The composition and other properties of the adsorbed protein layer strongly affect subsequent blood interactions including platelet adhesion and activation, initiation of blood coagulation, complement activation, erythrocyte interactions and leukocyte interactions.[36] These interactions may eventually lead to thrombosis, the foreign body reaction, and bacterial infection. Therefore, it is very important to be able to control protein adsorption to minimize these adverse effects.

1.2.1 Protein Structure

Proteins are naturally occurring polypeptides composed of more than 20 different amino acids. There are four levels of protein structure. The primary structure

refers to the linear sequence of amino acid residues and the location of any disulfide bridges. The secondary protein structure, such as α-helix and β-sheet, describes the conformation of the polypeptide chain and is determined mainly by intramolecular and intermolecular hydrogen bonding. The tertiary structure refers to the complete three-dimensional structure of the polypeptide, including chain folding, and describes the spatial relationship of different domains/secondary structures within a protein. For proteins containing more than one polypeptide chain, the way in which the peptide chains combine comprises the quaternary structure. The tertiary and quaternary structures of a protein are maintained by noncovalent interactions including hydrogen bonds, hydrophobic interactions, disulfide bonds, electrostatic forces and van de Waals forces. Factors such as pH, ionic strength, temperature and the presence of organic solvents have an impact on these noncovalent interactions and hence on the three dimensional structures of proteins.[37,38]

1.2.2 Thermodynamics of Protein Adsorption

Protein adsorption is driven by the various interactions among protein, surface, water and other components in the system. The driving forces include van der Waals interactions, electrostatic interactions, hydration forces, hydrophobic forces and Brownian motion.[39]

The adsorption of protein occurs only if the Gibbs free energy of the process is negative. The expression for the Gibbs free energy is:

$$\Delta G = \Delta H - T\Delta S \qquad 1.1$$

where H, S and T are the enthalpy, entropy and absolute temperature, respectively. A loss of enthalpy (exothermic) and/or a sufficient gain of entropy favor the occurrence of protein adsorption. The enthalpy and entropy contributions result from the combination of

the various interactions in the system and are applicable to a qualitative discussion of protein or macromolecule adsorption.[39]

The enthalpic contribution includes van der Waals interactions, electrostatic interactions, and hydrophobic forces. The entropic contribution comes from the loss of ordered structure in the protein such as the release of counterions and bound water (dehydration),[40] and conformational change.[41-44] Dehydration is driven by the hydrophobic interactions between hydrophobic domains of protein and the surface (hydrophobic effect), resulting in the release of the ordered water layers and an increase in entropy.[45] In many cases, the entropy contribution from dehydration provides the main driving force for protein adsorption.[41] However, protein adsorption can be either entropically driven or enthalpically driven or a combination of both, depending on the nature of protein and solid surface, pH, ionic strength, and other factors.[42]

1.2.3 Kinetics of Protein Adsorption

Protein adsorption at an aqueous/solid interface comprises the following steps:[46-55] (1) transport/diffusion of protein from bulk of solution to interface where interactions between protein and surface become effective, (2) attachment/adsorption of protein onto surface, (3) rearrangement of protein on surface (spreading, re-orientation, denaturation), (4) detachment/desorption of protein from surface, (5) transport/diffusion of protein away from surface to bulk. The protein adsorption rate depends on whether the process is transport-controlled or reaction-controlled. It is generally agreed that protein adsorption is transport-controlled when the protein surface coverage is lower than 10%.[36,38] Since the transport of protein in a nonflowing system is mainly driven by diffusion, the rate of adsorption in the transport-controlled regime is simply correlated to the rate of diffusion (Equation 1.2):[56]

$$\frac{d\Gamma}{dt} = C_0 \left(\frac{D}{\pi t}\right)^{\frac{1}{2}} \qquad 1.2$$

where $d\Gamma/dt$ is the rate of adsorption, C_0 is the bulk protein concentration, D is the diffusion coefficient of protein in solution, t is time. The surface protein concentration Γ is then given by Equation 1.3:

$$\Gamma = 2C_0\left(\frac{Dt}{\pi}\right)^{\frac{1}{2}} \qquad 1.3$$

When protein coverage is relatively high, the rate of protein adsorption is reaction-controlled, i.e. controlled by the intrinsic kinetics of adsorption.[56,57] The rate of adsorption is given in general by Equation 1.4:

$$\frac{d\Gamma}{dt} = f(C_0, \theta) \qquad 1.4$$

where C_0 is the bulk protein concentration and θ is the fractional surface coverage. For example the Langmuir kinetic model gives the rate of adsorption as:

$$\frac{d\Gamma}{dt} = k_a C_0(1-\theta) - k_d\theta \qquad 1.5$$

where k_a and k_d are the rate constants of adsorption and desorption, respectively.

1.2.4. Models of Protein Adsorption[56,58]

Protein adsorption from solution has been described by various models such as the Langmuir model, the random sequential adsorption model (RSA), the Freundlich model and the Temkin model.[59] The Langmuir model is generally applicable to describe single protein adsorption from dilute solution onto a biomaterial surface. It assumes that adsorption is reversible, that adsorption is limited to a monolayer, that the adsorption of one molecule does not affect any other molecule and that the solid surface is energetically uniform.[46] Based on these assumptions, the Langmuir model is then given by Equation 1.5. Solving for fractional coverage θ:

$$\theta = \frac{\Gamma}{\Gamma_{max}} = \frac{KC_p}{1+KC_p} \qquad 1.6$$

where Γ is the surface protein concentration; Γ_{max} is the surface protein concentration at the plateau (monolayer adsorption); C_p is the solution concentration at equilibrium; $K = k_a/k_d$ is the adsorption equilibrium constant.

Langmuir type isotherms have been observed in many studies,[36, 60-63] despite the fact that the assumptions of the model are generally invalid for protein adsorption. Thus it has been generally found that protein adsorption is irreversible on a reasonable time scale, that lateral interactions occur between adsorbed proteins and that surfaces in general are energetically heterogeneous.[64-66] Other observations not in agreement with the Langmuir model, include the occurrence protein conformational change and denaturation, and the involvement of multiple sites in a single adsorption event given the large size of protein molecules.

The random sequential adsorption (RSA) model,[67] takes into account the excluded surface effect (the earlier adsorbed molecules preventing later-arriving molecules from approaching the surface) and irreversible adsorption. The basic assumptions of the model include:[68,69] (1) Particles adsorb at random on a homogeneous adsorption plane, i.e., every position is statistically equivalent. (2) If the adsorbing particle overlaps with any preadsorbed particles, it is not adsorbed and a new adsorption attempt is made. (3) Otherwise the particle adsorbs with unit probability (hard sphere model) or with the probability calculated from the Boltzman distribution. (4) Once the particle is adsorbed, its position and orientation are permanently fixed: localized, irreversible adsorption. (5) The process is continued until no additional particle can be accommodated, thus the jamming or maximum parking limit is attained characterized by the fractional surface coverage θ_∞. The RSA kinetics of hard spheroids follow the scaling law:[70,71]

$$\theta_\infty - \theta(t) \propto t^{-\frac{1}{d}} \quad 1.7$$

where $\theta(t)$ and θ_∞ are the surface coverages at time t and in the jamming limit, respectively. The exponent d corresponds to the dimensionality of the substrate ($d = 2$ for a plane). However, this model is limited in that it does not allow protein diffusion over surface which has been shown to occur and to be an important effect in protein adsorption.[72]

A number of empirical models have been used to describe single protein adsorptions with non-Langmuir type isotherms. One is the Freundlich isotherm:[63]

$$\theta = kC_p^{\frac{1}{n}} \quad 1.8$$

where k and n are empirical constants of the system at a given temperature. k is related to adsorption capacity and $1/n$ is related to adsorption energy. This model assumes an exponentially decaying sorption site energy distribution.[73-75] The Temkin model assumes that the binding energy decreases linearly with increasing surface coverage.[76,77]

1.2.4 Multi-Protein Systems: the Vroman Effect

Biological fluids such as blood contain large numbers of proteins, and adsorption in these multi-protein systems is competitive. The composition of the adsorbed protein layer is generally a function of adsorption time and the relative concentrations of the component proteins.[78,79] The properties of the proteins, the surface and the solvent are also important factors in competitive adsorption.[38]

Adsorption is initially a diffusion-controlled process strongly affected by protein concentration. In general proteins of high concentration are expected to dominate the surface in the early stages. These initially adsorbed proteins may later be displaced by

proteins of lower concentration and higher binding affinity. At longer time, the surface is expected to be dominated by proteins of high affinity.[38,80] This dynamic behaviour is referred to as the "Vroman effect"[78,81] and has been observed for many surfaces and proteins.[82-90]

It has been found that adsorption of fibrinogen and other abundant proteins such as albumin and IgG exhibit Vroman effects in plasma. These are manifested as maxima in adsorption as a function of concentration at a given time, or of time at a given concentration.[78,90] The Vroman effect implies that exchange and displacement occur in the competitive adsorption process; for example, fibrinogen initially adsorbed from plasma is rapidly displaced by other proteins, notably high molecular weight kininogen (HMWK).[80,91] It is well known that the adsorbed fibrinogen promotes platelet adhesion and aggregation on the surface. The protein dynamics clearly affects the composition and structure of the adsorbed protein layer and thus is expected to be of significance for blood contacting devices.

1.3 Water-soluble Polymers as Protein-resistant Materials

Nonspecific protein adsorption is believed to be the initiating event that occurs when a biomaterial implant comes into contact with the biological environment, and is strongly detrimental to biomcompatibility.[4] A general strategy for reducing protein adsorption is to provide a well-hydrated hydrophilic polymer layer on the biomaterial surface, which "shields" the surface, makes it hydrophilic, and thus reduces the interfacial free energy. Hydrophilic or water-soluble polymers that have been used for this purpose include poly(vinylpyrrolidone) (PVP),[92-94] poly(2-methoxyethylacrylate) (poly(MEA)),[95] polyacrylic acid (PAA),[96-98] poly(ethylene oxide) (PEO),[99] poly(2-hydroxyethylmethacrylate) (PHEMA),[100-102] polysaccharides,[103] poly(sulfobetaine methacrylate), poly(carboxybetaine methacrylate),[104] poly(2-methacryloyloxyethyl phosphorylcholine) (poly(MPC)) and its copolymers.[105,106] Among these water-soluble

polymers, PEO and phosphorylcholine (PC)-based polymers have been widely used and verified to be among the most effective ones for the prevention of non-specific protein adsorption. However, the underlying mechanism is not well understood, and it remains challenging to achieve practical biomaterial surfaces that are strongly protein-resistant.

1.3.1 Polyethylene Oxide (PEO) as a Protein-resistant Material

Polyethylene oxide (PEO, H-(O-CH_2CH_2)$_n$-OH) is a neutral polyether that is miscible with water in all proportions at room temperature. PEO chains have considerable flexibility, mobility and thus a large excluded volume in water.[107,108] Moreover, PEO coatings or grafts on a surface cause a reduction in free energy of the interface between solid surface and water, and thus reduce the thermodynamic driving force for protein adsorption.[11,109-110] In addition, PEO is an attractive FDA-approved biomaterial; it is non-toxic, only weakly immunogenic, compatible with living cells, and does not cause inactivation or denaturation of proteins.[11,111]

Two main mechanisms have been proposed to explain the ability of PEO chains to resist protein adsorption: (1) steric repulsion, (2) the effect of the tightly bound hydration layer which creates a "barrier" to protein contact.[112,113] Steric repulsion results from loss of entropy (chain compression), osmotic pressure and elastic restoring forces when a protein approaches the PEO chains or other hydrophilic macromolecule.[22,114,115] It is probably important for longer polymer grafts. For shorter chains or oligomers, the tight water layer is probably the dominant factor.[116-118] This highly ordered hydration layer is formed via strong hydrogen bonds between PEO and water and provides an effective energy barrier against protein adsorption requiring displacement of the bound water.[119-121] The hydration force depends on both density of EO moieties and chain conformation.[122]

Protein adsorption can be influenced not only by the properties of the polymer grafts such as chain density, chain length, and chain conformation, but also by protein-protein interactions, protein size, solution properties (pH, ionic strength), and temperature, thus making the protein adsorption process much more complex than implied by the models described above. The interrelationships of these factors with protein adsorption have been widely studied. For example, Gombotz et al.[123] reported that the adsorption of serum albumin and fibrinogen decreased with increasing chain length of surface-modifying PEO. Resistance to adsorption increased up to molecular weight 3500 Da; but further increase gave little extra reduction in protein adsorption. Gölander et al.[124] observed qualitatively similar behaviour and found an optimum PEO MW of 1500 Da for protein resistance. Others[125-128] have reported an optimum value in the range of 2000-3000 Da. The discrepancies in optimal molecular weight in these studies may be due to different grafting densities. It was suggested that the phenomenon of a minimum length of PEO chains required for significant protein resistance is due to the water barrier associated with EO units, which becomes stronger with increasing density of EO units up to a certain value.[129]

The effect of PEO graft density on protein adsorption has been found to be of critical importance.[119,130-132] McPherson et al.[130,133] showed that protein adsorption decreased with increasing PEO density, and suggested that the efficiency of PEO grafts in preventing adsorption is based on effective covering of the surface, thereby blocking protein binding sites with PEO segments.

Normally, a surface with long grafts and sufficiently high graft density is expected to have strong resistance to protein adsorption. However, some densely packed short oligo(ethylene glycol) (OEG) self-assembled monolayers (SAMs), where the chains have only a few EO units, have also been found to repel proteins.[119,122,134,135] In Prime and Whitesides' work,[119] OEG with a single EO unit was shown to reduce protein adsorption significantly, given a sufficiently high graft density, suggesting that high

coverage of EO units is important for protein resistance. Despite extensive research on the protein-resistance of PEO grafts, there is still a debate as to which of chain length and grafting density is the more important.

1.3.2 Phosphorylcholine (PC)-containing Polymers as Protein-resistant Materials

Phosphorylcholine (PC)-based polymers, which mimic the outer surface of cell membranes, have been shown to have non-thrombogenic properties and generally good biocompatibility.[106,136] Ishihara et al.[30,105,137] observed that PC-polymer modified surfaces were strongly resistant to protein adsorption, and adhesion of cells including platelets, bacteria and other cells. Although the exact mechanism of resistance to fouling of these materials is not well understood, it is believed that the tightly bound hydration layer associated with the PC groups plays a critical role.[138] PC-based surfaces have high free water content associated with the PC groups, which is believed to allow proteins to contact the surface reversibly without conformational change.[138,139,140] In addition, the flexibility and mobility of PC-based polymers was suggested as responsible for their protein resistance.[106,141,142]

1.4 Surface Modification for Improved Biocompatibility

A variety of approaches have been used to incorporate modifiers such as PEO or PC-based molecules into biomaterial surfaces. Methods include physical adsorption,[143-147] surface coating,[148-150] blending[151-154] and chemical grafting[116,132,155-161], providing modified surfaces with a variety of structures and properties. These methods and their advantages and disadvantages are briefly reviewed here.

1.4.1 Physical Adsorption

Physical adsorption of a block copolymer or surfactant which contains biocompatible segments onto a substrate is a simple and rapid method of surface

modification. For example, Bohner et al.[145] modified polystyrene (PS) latex particles by physical-adsorption of the PEO-PPO-PEO triblock polymer Pluronic F108 (PEO129-PPO56-PEO129). It was observed that fibrinogen adsorption decreased exponentially with the copolymer surface concentration. As well, the particle size was found to have a significant effect on the fibrinogen uptake, with larger particles showing greater uptake.

Another important modification method based on adsorption was developed by Elbert et al.[10,144, 146,162] Comb copolymers with a poly(L-lysine) backbone (PLL) and PEO grafts were adsorbed to metal oxide surfaces including TiO_2, $Si_{0.4}Ti_{0.6}O_2$ and Nb_2O_5. The positively charged PLL component adsorbed to the metal oxides electrostatically leaving the PEO grafts "free" to interact with the bio-environment. The resulting surfaces were highly effective in inhibiting non-specific protein adsorption, and the higher the PEG surface density, the greater the inhibition.[146]

Adsorption methods are limited in that they cannot provide surfaces that are stable over long periods. It is to be expected that the adsorbed molecules will be displaced by other molecules of greater affinity.[163]

1.4.2 Surface Coating

PEO- and PC-containing copolymers and others can also be coated (e.g. from solution) onto various substrates for improved biocompatibility. The surface coating method has advantages such as simplicity, rapidity, and capability to prepare multi-functional surfaces.

In recent work, Lee and Oh synthesized random copolymers of methyl methacrylate (MMA), methoxy PEO monomethacrylate (MPEOMA, PEO Mw 1000) and vinyl sulfonic acid sodium salt (VSA) and coated them onto polyurethane and poly(MMA) films by spin coating.[148,149] The hydrophobic MMA segments and long carbon backbone of the copolymers provided strong interactions with the hydrophobic substrates. The

coated MMA/ MPEOMA/VSA surface with a monomer molar ratio 8:1:1 was found to be particularly effective in preventing both protein adsorption and platelet adhesion, which was suggested to be due to the combined effects of the hydrophilic PEO and the negatively charged VSA side chains. In other work, a tri-block copolymer PEO99-PPO65-PEO99 (Pluronic F-127) was applied to silicone rubber by solution coating.[164] Studies of the kinetics of bacterial growth showed that the PEO-containing coating reduced initial adhesion of bacteria (staphylococci) and delayed biofilm growth.

MPC-based copolymers such as MPC-co-MMA, MPC-co-n-butyl methacrylate (BMA), or MPC-co-n-dodecyl methacrylate (DMA) have been widely used as coating materials on a variety of substrates.[105,106,165-167] For example, Fujii and Ishihara et al.[167,168] applied poly(MPC-co-BMA) coatings to stainless steel and to polymers such as poly(ethylene telephthalate) (PET) and polyurethane. It was observed that the coated surfaces reduced fibronectin adsorption and cell adhesion, and that adsorption and adhesion decreased with increasing MPC content in the copolymers.[168] Moreover, bacterial adhesion and biofilm formation were inhibited on the poly(MPC)-containing surfaces.[167]

Although surface coating has been widely used, it does have disadvantages including difficulty of application to devices/substrates with complex shapes, poor stability and loss of coating over time. Some crosslinkable copolymers have been developed to improve the stability and physical properties of coatings.[105,106,166]

1.4.3 Blending

Blending is a simple and convenient process, in which components of high surface activity such as amphiphilic PEO- or PC-containing copolymers are mixed with a base material or matrix. The surface active component is expected to migrate to the surface. Tan et al.[169] prepared PEO-rich surfaces by blending triblock copolymers PEO-

PU-PEO with a segmented polyurethane. The protein resistance of the blend surfaces was found to increase with increasing copolymer content up to 20 wt%, and reductions in adsorption greater than 95% were observed on the blend surfaces with 20% copolymer content. Another example of blending is the work of Ishihara and Iwasaki in which MPC copolymers were blended with a segmented polyurethane.[153] These surfaces were shown to reduce the adsorption of plasma proteins and to suppress platelet adhesion and activation. Santerre et al.[170-175] synthesized fluorinated surface-modifying macromolecules (SMMs) containing poly(tetramethylene oxide) or poly(propylene oxide) polyol segments and oligomeric fluorocarbon (CF_2) segments, and blended the SMMs with polyurethanes. The fluorinated SMM blend materials showed reduced hydrolysis by enzymes,[173,174] and also exhibited significant reductions in non-specific protein adsorption, platelet adhesion and activation[175].

The blending approach also has disadvantages: (1) While it is generally believed that the blended polymeric additives are stabilized by chain entanglements with the matrix, they can be lost over time; (2) For a bioactive component, its biological activity can be compromised or lost in the blending process. (3) The mechanical properties of the material can be altered with increased loading of the blended component.

1.4.4 Surface Grafting

As discussed above, a major disadvantage of physical adsorption, surface coating and blending approaches is the instability of the surface modifier or additive. In this respect, chemical grafting is superior since the surface active component is covalently bonded to the surface, thus improving stability. Another advantage of this method is that the bulk properties remain unchanged since grafting occurs exclusively on the surface. Surface grafting of polymers can be achieved either by 'grafting to' or 'grafting from'.

1.4.4.1 'Grafting to' Approach

The 'grafting to' approach has been widely employed to tether pre-formed chain end-functionalized polymers to an appropriate substrate to form polymer brushes.[176-179] For example, Sofia et al.[132] coupled hydroxy-terminated linear and star PEO molecules to aminosilane-treated silicon wafers. Murthy et al.[160] grafted amphiphilic PEO-silanes onto silicon wafers to form PEO brushes. Chain-end-thiolated PEO has been widely used to form self-assembled monolayers on gold and silver surfaces.[116,157,158,180] Unsworth et al. prepared PEO layers of various MW on gold by chemisorption (effectively "grafting to"). For PEO brushes of MW 750 and 2000, fibrinogen adsorption was found to decrease with increasing chain density up to ~0.5 chains/nm^2, and to increase again as the density increased beyond 0.5 chains/nm^2. It was suggested that the PEO chains become dehydrated at very high chain density giving a surface that is hydrophobic and no longer protein resistant. The PEO surfaces with the optimal chain density were shown to reduce fibrinogen adsorption by 80% compared to a control.[157] Experiments on protein adsorption from plasma on OH- and CH_3O-terminated PEO brushes suggested a chain end group effect: the hydroxyl terminated PEO layers inhibited fibrinogen adsorption and/or facilitated protein displacement more effectively.[157] Further studies showed that the adsorption of both fibrinogen and lysozyme from buffer to the hydroxy-terminated PEO surfaces levelled off at a critical chain density, but showed increasing adsorption beyond the critical value on the methoxy terminated surfaces, indicating a role of chain end chemistry at chain densities greater than the critical value.[158] In other work, Archambault et al.[181] grafted amine-terminated PEO chains to a polyurethane substrate using methylene di-p-phenyl diisocyanate MDI as a coupling agent giving a modified surface that reduced protein adsorption significantly.

Although the 'grafting to' approach is an effective way to create a permanent, stable polymer-grafted surface, the surface density of grafts is limited by the hindrance of

initially immobilized chains to the attachment of additional chains. This is a significant disadvantage.

1.4.4.2 'Grafting from' Approach

The 'grafting from' approach, also referred to as surface-initiated polymerization, is a very promising method for the preparation of grafted surfaces of high graft density. The general procedure includes immobilization of an initiator layer on the substrate surface followed by polymerization from the initiator sites.[182] Polymerization methods include conventional free radical polymerization,[100,183-189] anionic polymerization,[190] cationic polymerization,[191,192] ring-opening polymerization,[193,194] and controlled radical polymerization (CRP).[17,178,195]

Conventional free radical polymerization is the most widely used method to produce high molecular weight polymers. Various techniques have been used to initiate conventional free radical polymerization on surfaces, including photo-induced polymerization, plasma post-polymerization, and ammonium persulfate- or ceric ammonium nitrate-initiated polymerization. For example, Chen et al.[185] prepared poly(OEGMA) surfaces on emeraldine base films via UV-induced graft polymerization. The graft density increased with increasing polymerization time and monomer concentration. Kim et al.[187,196] grafted acrylated phospholipids from a methacryloyl-terminated substrate by in situ polymerization with the water-soluble initiator, 2,2'-azobis(2-methylpropionamidine) dihydrochloride. The grafted surfaces greatly reduced the adsorption of proteins such as albumin, fibrinogen and IgG, in vitro, and the adhesion of macrophages and formation of foreign body giant cells, in vivo. Korematsu et al.[188] grafted poly(MPC) from PU surfaces via ceric ammonium nitrate-initiated conventional free radical polymerization. The poly(MPC) grafted surfaces showed reduced platelet adhesion and activation compared to the unmodified PU.

Although conventional free radical polymerization has been used extensively to prepare PEO- and PC-grafted surfaces, its use is limited by poor control of graft density, chain length and polydispersity, and the difficulty of forming block copolymers and other defined chain architectures. In order to overcome these limitations, surface-initiated living polymerization methods have been developed, including anionic, cationic, ring-opening polymerization and CRP techniques.[176] For anionic, cationic, and ring-opening polymerization, restrictive experimental conditions and/or the requirement for sophisticated catalysts which are often sensitive to moisture and impurities, limit their use for surface modification. In recent years, controlled/living radical polymerization (CRP) has attracted much interest not only because of its effectiveness in producing polymer graft surfaces of well-defined composition, architecture, functionality, and high density, but also its less stringent experimental requirements. The CRP techniques include nitroxide mediated radical polymerization (NMRP),[197] reversible addition-fragmentation chain transfer (RAFT) polymerization,[198,199] and metal-catalyzed living radical polymerizations.[17,200-204] Of the CRP methods, atom transfer radical polymerization (ATRP) has proved to be one of the most successful for preparing well-defined and narrowly dispersed polymer brushes.[177] It is much easier to prepare ATRP initiator layers on target substrates using commercially available initiators such as *a*-haloesters or benzyl halides than to synthesize functional alkoxyamine initiators for NMRP and dithioesters (chain transfer agents) for RAFT polymerization. In addition, ATRP is feasible for a wide range of monomers and solvents, and can be carried out at room temperature, which renders it compatible with a variety of substrate materials. In the following section, recent developments in biocompatible, antifouling surfaces prepared by ATRP are reviewed.

1.5 Bioactive and Biocompatible Surfaces via ATRP

The surface properties of biomaterials govern their interactions with blood, tissue and other biological environments.[205-208] Therefore, surface modification to

control these interactions is a valid approach for the improvement of biocompatibility.[209-211] Examples of such control are to minimize undesirable interactions (non-fouling surface), or to modify the surface such that it promotes beneficial interactions (bioactive surface). Surface initiated ATRP has been used extensively for the preparation of bioactive and biocompatible surfaces. As a chemical process its attributes include tolerance of impurities, versatility with respect to monomer type and solvent, and ability to proceed under mild reaction conditions.[17,203] s-ATRP is a controlled, 'living' polymerization method and allows preparation of polymer-grafted surfaces having well-controlled graft density and grafts of predetermined, uniform length.[17,203] Graft density and length are the two key parameters governing protein resistance,[19,212] so ATRP is of great interest in this connection.

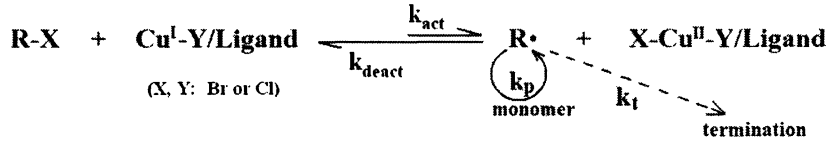

Scheme 1.1 General mechanism of atom transfer radical polymerization.

The essential mechanism of ATRP is shown in Scheme 1.1.[16,203] The catalyst complex, comprising a transition metal halide and a suitable nitrogen-based ligand, establishes a dynamic equilibrium between dormant species and growing radicals. This reversible activation-deactivation with rate constants k_{act} and k_{deact} is controlled by a redox reaction of the transition metal salt. Polymer chains grow by the addition of monomers to the intermediate radicals with rate constant k_p. Termination reactions (k_t) also occur in ATRP, mainly through radical coupling and disproportionation; however, by keeping the concentration of propagating radicals sufficiently low in comparison to the dormant species, termination can be suppressed with no more than a few percent (generally <5%) of terminated chains throughout the polymerization process.[16,182]

The main requirements for a well-controlled ATRP include: (1) initiation should be fast to provide a constant concentration of growing polymer chains; (2) the majority of the dormant polymer chains should retain the ability to grow; (3) reversible deactivation should be fast to keep the concentration of propagating radicals sufficiently low. Uniform growth of all the chains can be achieved in a successful ATRP, due to fast initiation, rapid reversible deactivation and suppressed termination. Due to the reversibility of the initiator-catalyst reaction, dormant polymer chains retain the ability to grow, allowing the synthesis of block copolymers and polymers with generally well-controlled architecture. Moreover, ATRP can be readily initiated from various surfaces, such as planar surfaces, particles, polymer chains and networks.[177,195,202,213-215]

In the process of preparing functional polymer brushes via surface-initiated ATRP, the first step, i.e., immobilization of the ATRP initiator on the substrate surface, is of crucial importance. Versatile initiator immobilization methods have been developed for various surfaces.[183,216] Most of this work is focused on hard inorganic or metallic surfaces such as silicon,[19,193,209,212,217-223] silica,[224-226] gold,[13,23,210,227-232] titanium,[233-235] Fe_3O_4[236-242] and stainless steel.[233,243] For example, on a hydride (Si-H) silicon surface, Xu et al.[217] used a simple two-step method to immobilize ATRP initiator, i.e UV-induced coupling of 4-vinylaniline followed by reaction of the amino group with 2-bromoisobutyryl bromide (BIBB). Poly(OEGMA) and poly(N-isopropylacrylamide (NIPAAm)) polymers and copolymers were grafted from the initiator layer by ATRP. The poly(NIPAAm) and poly(NIPAAm)-co-poly(OEGMA) brushes were shown to act as stimuli-responsive modifiers of cell adhesion: above the lower critical solution temperature (LCST) of the grafts, cells adhered, mainly on the NIPAAm segments; below the LCST, the cells detached spontaneously. Stadler et al.[222] reacted silicon wafers with 2-bromo-2-methyl-N-propyltriethoxysilyl isobutyramide as initiator and prepared various graft copolymer films of OEGMA and MMA via ATRP. Well defined hydrophobic domains were observed on copolymer films containing 10-40 mol% OEGMA. However,

loss of protein-resistant properties was observed only for surfaces having 15 mol% OEGMA or lower. Feng et al.[19,212] prepared poly(MPC) brushes with graft density 0.06-0.39 chains/nm^2 and chain length 5-200 monomer units on silicon wafer surfaces by combining self-assembly of initiator (10-(2-bromo-2-methyl) propionyloxy decyltrichlorosilane) and surface-initiated ATRP. The graft chain length was varied via the ratio of monomer to sacrificial initiator in solution. The graft density of the poly(MPC) brushes was controlled via the surface initiator density using different combinations of initiator and decyltrichlorosilane as "diluting agent". The graft densities of poly(MPC) brushes and initiator were calculated from the thickness values determined by ellipsometry. Protein adsorption decreased with increasing graft density and chain length. Grafts of chain length 200 and density 0.39 chains/nm^2 gave adsorption levels of 7 and 2 ng/cm^2, respectively, for fibrinogen and lysozyme at 1 mg/mL protein concentration, corresponding to reductions of >98% compared to the unmodified silicon.

In other work, bromomethyl-terminated catechol[233,234] was immobilized on titanium and stainless steel surfaces, and chloromethyl-terminated silanes[235] on oxidized titanium (TiOH) as ATRP initiators. Three types of poly(OEGMA) brushes (side chain lengths of 4, 9 and 23 EG units) with thickness of about 100 nm were grafted from the initiator layers.[233,234] Cell adhesion experiments showed the complete inhibition of cell attachment on all these surfaces with little dependence on EG side chain length. Resistance to fouling was maintained up to three weeks, beyond which it decreased; the decrease was more rapid with decreasing EG side chain length. Ignatova et al.[243,244] electrografted poly(2-(2-chloropropionate)ethyl acrylate (cPEA)) on stainless steel to form an ATRP initiator layer. Subsequent ATRP of 2-(t-butylamino)ethyl methacrylate (TBAEMA) or copolymerization of TBAEMA with either OEGMA or acrylic acid or styrene gave surfaces with protein resistant and antibacterial properties.

ATRP initiators such as bromomethyl-terminated thiols have been immobilized directly on gold surfaces by gold-thiol reaction.[23,227-229] The chain length and surface

density of polymers grafted from these initiators were independently controlled by adjustment of polymerization time and initiator density on the gold surface.[23] Protein adsorption on poly(OEGMA) surfaces prepared by these methods was below the detection limit of the surface plasmon resonance (SPR) method used. In addition, cell adhesion was inhibited for up to a month under typical cell culture conditions.[229]

Although ATRP has been used extensively to modify "hard" inorganic and metallic surfaces, much less work has been done on "soft" organic or polymer surfaces. For hydroxyl-containing polymeric surfaces (e.g. poly(HEMA-co-MMA), some hydrogels, cellulose), ATRP initiator can be attached by the esterification reaction between hydroxyl groups and 2-bromopropionyl bromide.[211,245-247] However, for inert polymeric substrates with no functional groups, it is difficult to prepare an ATRP initiator layer, especially one of high surface density. Huang et al have shown that poly(DMAEMA) and poly(OEGMA) can be grafted on polypropylene (PP)[248] from a layer of the ATRP initiator benzophenonyl bromoisobutyrate deposited by spin-coating followed by UV irradiation to covalently attach the initiator to the PP surface. Yao et al.[249] used ozone-induced coupling to attach the ATRP initiator 2-bromoisobutyrate to PP hollow fiber membranes. Nylon membranes have been ATRP-grafted using a two-step method for initiator attachment involving activation of the surface amide groups with formaldehyde and reaction of the resulting hydroxyl groups of the nylon-OH membrane with 2-bromoisobutyryl bromide.[182,250]

In addition to the difficulties of ATRP grafting from soft materials, surface characterization is also problematic. In particular the determination of graft density and chain length remain challenging.

1.6 References

1 Park J. B., Lakes R. S., Biomaterials: an Introduction. New York: Plenum, (1992).

2 Brash J. L., Wojciechowski P. W. (eds.), Interfacial Phenomena and Bioproducts. New York: Marcel Dekker, (1996).

3 Copper S. L., Bacterial adhesion to functionalized polyurethanes, J. Biomater. Sci. Polym. Ed., 10, 679 (1999).

4 Brash J. L., Exploiting the current paradigm of blood-material interactions for the rational design of blood-compatible materials, J. Biomater. Sci. Polym. Edn., 11, 1135 (2000).

5 Lee J. H., Ju Y. M., Kim D. M., Platelet adhesion onto segmented polyurethane film surfaces modified by addition and crosslinking of PEO-containing block copolymers, Biomaterials, 21, 683 (2000).

6 Ratner B. D., Castner D. G., Surface Modification of Polymeric Biomaterials. New York: Plenum, (1996).

7 Hanson S. R., In: Ratner B. D., Hoffman A. S., Schoen F. J., Lemon J. E. (eds.), Biomaterials science: an introduction to materials in medicine, second edition. San Diego: Elsevier Academic Press, P332 (2004).

8 Ikada Y., Shalaby W., Polymers of biological and biomedical significance, Am. Chem. Soc. Symp. Series, 540, 135 (1994)

9 Norde W., Driving forces for protein adsorption at solid surfaces, In: Biopolymers at Interfaces, Malmsten M. (ed), NY: Marcel Dekker, Inc. P21 (2003).

10 Coleman D. L., Andrade J. D., Gregonis D. E., Blood-materials interactions: the minimum interfacial free energy and the optimum polar apolar ratio hypotheses, J. Biomed. Mater. Res., 16, 381 (1982).

11 Harris J. M., Introduction to biotechnical and biomedical applications of poly(ethylene glycol), In: Poly(ethylene glycol) Chemistry: Biotechnical and Biomedical Applications, Harris J. M. (ed), Plenum Press, NY, P1-14 (1992).

12 Zhang F., Kang E. T., Neoh K. G., Huang W., Modification of gold surface by grafting of poly(ethylene glycol) for reduction in protein adsorption and platelet adhesion, J. Biomater. Sci. Polym. Edn., 12, 515 (2001).

13 Ma X., Su Y., Sun Q., Wang Y., Jiang Z., Preparation of protein-adsorption-resistant polyethersulfone ultrafiltration membranes through surface segregation of amphiphilic comb copolymer, J. of Membr. Sci., 292, 116 (2007).

14 Maechling-Strasser C., Dejardin P., Galin J. C., Schmitt A., Preadsorption of polymers on glass and silica to reduce fibrinogen adsorption, J. Biomed. Mater. Res., 23,1385 (1989).

15 Han D-K., Park K-D., Ryu G-H., Kim U-Y., Min B-G., Kim Y-H., Plasma protein adsorption to sulfonated poly(ethylene oxide)-grafted polyurethane surface, J. Biomed. Mater. Res., 30, 23, (1996).

16 Matayjaszewski K., Xia J., Atom transfer radical polymerization, Chem. Rev., 101, 2921 (2001).

17 Liu P., Su Z., Surface-initiated atom transfer radical polymerization (SI-ATRP) of MMA from PANI powders, Polym. Bullet., 55, 411 (2005).

18 Feng W., Zhu S., Ishihara K., Brash J. L., Adsorption of fibrinogen and lysozyme on silicon grafted with poly(2-methacryloyloxyethyl phosphorylcholine) via surface-initiated atom transfer radical polymerization, Langmuir, 21, 5980 (2005).

19 Zhang H., Shouro D., Itoh K., Takata T., Jiang Y., Grafting polymer from poly(ethylene terephthalate) films by surface-initiated ATRP, J. Appl. Polym. Sci., 108, 351 (2008).

20 Szleifer I., Protein adsorption on surfaces with grafted polymers: A theoretical approach, Biophys. J., 72, 595 (1997).

21 Jeon S. I., Andrade J. D., Protein-surface interactions in the presence of polyethylene oxide: II. effect on protein size, J. Coll. Interf. Sci., 142, 159 (1991).

22 Ma H., Wells M., Beebe T. P., Chilkoti A., Surface-initiated atom transfer radical polymerization of oligo(ethylene glycol) methyl methacrylate from a mixed self-assembled monolayer on gold, Adv. Funct. Mater., 16, 640 (2006).

23 Feng W., Zhu S., Ishihara K., Brash J. L., Protein resistant surfaces: Comparison of acrylate graft polymers bearing oligo-ethylene oxide and phosphorylcholine side chains, Biointerphases, 1, 50 (2006).

24 Zdrahala R. J., Zdrahala I. J., Biomedical applications of polyurethanes: a review of past promises, present realities, and a vibrant future, J. Biomater. Appl., 14, 67 (1999).

25 Boretos J. W., Past, present and future role of polyurethanes for surgical implants, Pure Appl. Chem., 52, 1851 (1980).

26 Ihlenfeld J. W., Mathis T. R., Riddle L. M., Cooper S. L., Measurements of transient thrombus deposition of polymeric materials, Thromb. Res., 14, 953 (1979).

27 Pinchuk L. J., A review of the biostability and carcinogenicity of polyurethanes in medicine and the new generation of 'biostable' polyurethanes, J. Biomater. Sci. Polym. Edn., 6, 225 (1994).

28 Lelah M. D., Cooper S. L., Polyurethanes in Medicine, CRC Press, Boca Raton, (1986).

29 Ishihara K., Shibata N., Tanaka S., Iwasaki Y., Kurosaki T., Nakabayash N., Improved blood compatibility of segmented polyurethane by polymeric additives having phospholipid polar group, II dispersion state of the polymeric additive and protein adsorption on the surface, J. Biomed. Mater. Res., 32, 401 (1996).

30 Kang I. K., Seo E. J., Huh M. W., Kim K. H., Interaction of blood components with heparin-immobilized polyurethane prepared by plasma glow discharge, J. Biomater. Sci. Polym. Ed., 12, 1091 (2001).

31 Jozwiak A. B., Kielty C. M., Black R. A., Surface functionalization of polyurethane for the immobilization of bioactive moieties on tissue scaffolds, J. Mater. Chem., 18, 2240 (2008).

32 Li Y., Huang Y., Preparation of collagen-polyurethane composite film and its subcutaneous implantation in rats: the improvement of tissue compatibility, J. Appl. Polym. Sci., 99, 1832 (2006).

33 Courtney J. M., Lamba N. M., Sundaram S., Forbes C. D., Biomaterials for blood-contacting applications, Biomaterials, 15, 737 (1994).

34 Brash J. L., Scott C. F., ten Hove P., Wojciechowski P., Colman R. W., Mechanism of transient adsorption of fibrinogen from plasma to solid surfaces: role of the contact and fibrinolytic systems, Blood, 71, 932 (1988).

35 Yung L. Y., Colman R. W., Cooper S. L., The effect of high molecular weight kininogen on neutrophil adhesion to polymer surfaces, Immuno-pharmacology, 43, 281 (1999).

36 Brash J. L., Role of plasma protein adsorption in the response of blood to foreign surfaces. In: Blood Compatible Materials and Devices, Sharma C. P., Szycher M. (eds.), Lancaster, Pennsylvania: Technomic, P3-24 (1991).

37 Petsko G. A., Ringe D., Protein Structure and Function, London: New Science Press Ltd, P26-27 (2004).

38 Andrade J. D., Principles of protein adsorption, In: Surface and Interfacial Aspects of Biomedical Polymers, Andrade J. D. (ed), Plenum Press, New York, P1-80 (1985).

39 van Oss C. J., Interfacial Forces in Aqueous Media. NY: Marcel Dekker, Inc. New York, (1994).

40 Hoffman A. S., Ratner B. D., Nonfouling surfaces, In: Biomaterials Science: An Introduction to Materials in Medicine, Ratner B. D., Hoffman A. S., Schoen F. J., Lemons J. E. (eds.), 2nd ed., Oxford, UK: Elsevier's Science & Technology, P197-200 (2004).

41 Norde W., Lyklema J., Why proteins prefer interfaces, J. Biomater. Sci. Polym. Edn., 2, 183 (1991).

42 Norde W., Haynes C. A., Reversibility and the mechanism of protein adsorption, In: Proteins at Interfaces II: Fundamentals and Applications, Horbett T. A. and Brash J. L. (eds.), American Chemical Society, Washington, DC, P26-40 (1995).

43 Haynes C. A., Norde W., Globular proteins at solid/liquid interfaces, Coll. Surf. B: Biointerf., 2, 517 (1994).

44 Duinhoven S., Poort R., Vandervoet G., Agterof W. G., Norde W., Lyklema J., Driving forces for enzyme adsorption at solid-liquid interfaces I: the serine-protease savinase, J. Coll. Interf. Sci., 170, 340 (1995).

45 Norde W., Energy and entropy of protein adsorption, J. Disper. Sci. Tech., 13, 363 (1992).

46 Andrade J. D., Hlady V., Protein adsorption and materials biocompatibility: a tutorial review and suggested hypotheses, Adv. Polym. Sci., 79, 1 (1986).

47 Wojciechowski P. W., Brash J. L., A computer-simulation for the study of macromolecular adsorption with special applications to single-component protein adsorption, J. Coll. Interf. Sci., 140, 239 (1990).

48 Lu C. F., Nadarajah A., Chittur K. K., A comprehensive model of multiprotein adsorption on surfaces, J. Coll. Interf. Sci., 168, 152 (1994).

49 Dejardin P., ten Hove P., Yu X. J., Brash J. L., Competitive adsorption of high molecular weight kininogen and fibrinogen from binary mixtures to glass surface, Langmuir, 11, 4001 (1995).

50 Calonder C., Tie Y., van Tassel P. R., History dependence of protein adsorption kinetics, Proc. Natl. Acad. Sci. U.S.A., 98, 10664 (2001).

51 Tie Y., Calonder C., van Tassel P. R., Protein adsorption: kinetics and history dependence, J. Coll. Interf. Sci., 268, 1 (2003).

52 Malmsten M., Competitive adsorption at hydrophobic surfaces from binary protein systems, J. Coll. Interf. Sci., 166, 333 (1994).

53 Malmsten M., Macromolecular adsorption: a brief introduction, In: Biopolymers at Interfaces, 2nd Ed., Malmsten M. (ed), NY: Marcel Dekker, Inc., (2003).

54 Malmsten M., Emoto K., van Alstine J. M., Effect of chain density on inhibition of protein adsorption by poly(ethylene glycol) based coatings, J. Coll. Interf. Sci., 202, 507 (1998).

55 Ramsden J. J., Protein adsorption kinetics, In: Biopolymers at Interfaces, 2nd Ed., Malmsten M. (ed), NY: Marcel Dekker, Inc., P199 (2003).

56 Lamba N. M. K., Woodhouse K. A., Copper S. L., In: Polyurethane in Biomedical Applications, New York: CRC Press, P115-117 (1998).

57 Cheng Y. L., Darst S. A., Robertson C. R., Bovine serum albumin adsorption and deadsorption rate on a solid surface with varying surface properties, J. Coll. Interf. Sci., 118, 212 (1987).

58 Plazinski W., Rudzinski W., Plazinska A., Theoretical models of sorption kinetics including a surface reaction mechanism: A review, Adv. Coll. Interf. Sci., 152, 2 (2009).

59 Silberberg A., Modeling of protein adsorption, In: Surface and Interfacial Aspects of Biomedical Polymer, Andrade J. D. (ed.), Plenum Press, New York, P321 (1985).

60 Brash J. L., Davidson V. J., Adsorption on glass and polyethylene from solutions of fibrinogen and albumin, Thromb. Res., 9, 249 (1976).

61 Brash J. L., Lyman D. J., Adsorption of proteins and lipids to nonbiological surfaces, In: The Chemistry of Biosurfaces, Vol. 1, Hair M. L. (ed.), New York: Marcel Dekker, Inc., (1971).

62 Horbett T. A., Weatherby P. K., Hoffman A. S., The preferential adsorption of hemoglobin to polyethylene, J. Bioeng., 1, 61 (1977).

63 Young B. R., Pitt W. G., Cooper S. L., Protein adsorption on polymeric biomaterials I: adsorption isotherms, J. Coll. Interf. Sci., 124, 28 (1988).

64 Brash J. L., Horbett T. A., Protein at interfaces: an overview, In: Protein at Interfaces II: Fundamentals and Applications, Horbett T. A. and Brash J. L. (eds.), American Chemical Society, Washington, D. C., P1-23 (1995).

65 Norde W., MacRitchie F., Nowicka G., Lyklema J., Protein adsorption at solid-liquid interfaces: reversibility and conformational aspects, J. Coll. Interf. Sci., 112, 447 (1986).

66 Chan B. M. C., Brash J. L., Adsorption of fibrinogen on glass: reversibility aspects, J. Coll. Interf. Sci., 82, 217 (1981).

67 Schaaf P., Talbot J., Surface exclusion effects in adsorption processes, J. Chem. Phys., 91, 4401 (1989).

68 Adamczyk Z., Weronski P., Random sequential adsorption of spheroidal particles: Kinetics and jamming limit, J. Chem. Phys., 105, 5562 (1996).

69 Adamczyk Z., Kinetics of particle and protein adsorption, In: Surface and Colloid Sciencce, Volume 17, Matijević E., Borkovec M. (eds), NY: Kluwer Academic/Plenum Publishers, P286-308 (2004).

70 Adamczyk Z., Weronski P., Kinetics of irreversible adsorption of interacting spheroidal particles, Langmuir, 11, 4400 (1995).

71 Thompson A. P., Corti D. S., Myers A. L., Glandt E. D., Irreversible adsorption in porous materials, In: Fundamentals of Adsorption: Proceedings of the Fourth International Conference on Fundamentals of Adsorption, Suzuki M. (ed), Elsevier, P671-678 (1993).

72 Tilton R. D., Mobility of biomolecules at interfaces, In: Biopolymers at Interfaces, Malmsten M. (ed), NY: Marcel Dekker, Inc., P221-258 (2003).

73 Corton E., Garcia-Calzon J. A., Diaz-Garcia M. E., Kinetics and binding properties of cloramphenicol imprinted polymers, J. Non-Crystralline Solids, 353, 974 (2007).

74 Adamson A. W., Physical Chemistry of Surfaces, Wiley-Intersciences, New York, (1990).

75 Thomson S. J., Webb G., Heterogeneous Catalysis, John Wiley & Sons, Inc., New York, (1968).

76 Sljivic M., Smiciklas I., Pejanovic S. and Plecas I., Comparative study of Cu^{2+} adsorption on a zeolite, a clay and a diatomite from Serbia, Applied Clay Science, 43, 33 (2009).

77 Johnson R. D., Arnold F. H., The temkin isotherm describes heterogeneous protein adsorption, Biochim. Biophys. Acta, 1247, 293 (1995).

78 Brash J. L., ten Hove P., Effect of plasma dilution on adsorption of fibrinogen to solid-surfaces, Thromb. Haemost., 51, 326 (1984).

79 Horbett T. A., Cheng C. M., Ratner B. D., Hoffman A. S., Hanson S. R., The kinetics of baboon fibrinogen adsorption to polymers: in vitro and in vivo studies, J. Biomed. Mater. Res., 20, 739 (1986).

80 Brash J. L., The fate of fibrinogen following adsorption at the blood-biomaterial interface, Ann. NY. Acad. Sci., 516, 206 (1987).

81 Horbett T. A., Mass action effects on competitive adsorption of fibrinogen from hemoglobin solutions and from plasma, Thromb. Haemost., 51, 174 (1984).

82 Vroman L., Methods of investigating protein interactions on artificial and natural surfaces, Ann. NY. Acad. Sci., 516, 300 (1987).

83 Vroman L., The importance of surface in contact phase reactions, Seminars in Thrombosis and Hemostasis, 13, 79 (1987).

84 Adams A. L., Fischer G. C., Munoz P. C., Vroman L., Convex-lens-on-slide: a simple system for the study of human plasma and blood in narrow spaces, J. Biomed. Mater. Res., 18, 643 (1984).

85 Wojciechowski P., ten Hove P., Brash J. L., Phenomenology and mechanism of the transient adsorption of fibrinogen from plasma (Vroman effect), J. Coll. Interf. Sci., 111, 455 (1986).

86 Slack S. M., Bohnert J. L., Horbett T. A., The effects of surface chemistry and coagulation factors on fibrinogen adsorption from plasma, Ann. NY. Acad. Sci., 516, 223 (1987).

87 Slack S. M., Horbett T. A., Physicochemical and biochemical aspects of fibrinogen adsorption from plasma and binary protein solutions onto polyethylene and glass, J. Coll. Interf. Sci., 124, 535 (1988).

88 Slack S. M., Posso S. E., Horbett T. A., Measurement of fibrinogen adsorption from blood plasma using ^{125}I-fibringen and a direct ELISA technique, J. Biomater. Sci. Polym. Edn., 3, 49 (1991).

89 Slack S. M., Posso S. E., Horbett T. A., The effects of temperature and buffer on fibrinogen adsorption from blood plasma to glass, J. Biomater. Sci. Polym. Edn., 2, 227 (1991).

90 Slack S. M., Horbett T. A., The Vroman effect: a critial review, In: Protein at Interfaces II, Fundamentals and Applications, Horbett T. A. and Brash J. L. (eds.), ACS Symposium Series No. 602, Washington DC: American Chemical Society, P112 (1995).

91 Vroman L., Adams A. L., Fisher G. C., Munoz P. C., Interaction of high molecular weight kininogen, Factor XII, and fibrinogen in plasma at interfaces, Blood, 55, 156 (1980).

92 Higuchi A., Shirano K., Harashima M., Yoon B. O., Hara M., Hattori M., et al. Chemically modified polysulfone hollow fibers with vinylpyrrolidone having improved blood compatibility, Biomaterials, 23, 2659 (2002).

93 Wetzels G. M. R., Koole L. H., Photoimmobilisation of poly(*N*-vinylpyrrolidinone) as a means to improve haemocompatibility of polyurethane biomaterials, Biomaterials, 20, 1879 (1999).

94 Wan L. S., Xu Z. K., Huang X. J., Wang Z. G., Wang J. L., Copolymerization of acrylonitrile with *N*-vinyl-2-pyrrolidone to improve the hemocompatibility of polyacrylonitrile, Polymer, 46, 7715 (2005).

95 Hirota E., Ute K., Uehara M., Kitayama T., Tanaka M., Mochizuki A., Study on blood compatibility with poly(2-methoxyethyl acrylate): Relationship between surface structure, water structure, and platelet compatibility in 2-

methoxyethylacrylate/2-Hydroxyethylmethacrylatediblock copolymer, J. Biomed. Mater. Res. A, 76A, 540 (2006).

96 Gupta B., Plummer C., Bisson I., Frey P., Hilborn J., Plasma-induced graft polymerization of acrylic acid onto poly(ethylene terephthalate) films: characterization and human smooth muscle cell growth on grafted films, Biomaterials, 23, 863 (2002).

97 Vermette P., Meagher L., Immobilization and characterization of poly(acrylic acid) graft layers, Langmuir, 18, 10137 (2002).

98 Combellas C., Fuchs A., Kanoufi F., Mazouzi D., Nunige S., Surface modification of halogenated polymers. 6. Graft copolymerization of poly(tetrafluoroethylene) surfaces by polyacrylic acid, Polymer, 45, 4669 (2004).

99 Lee J. H., Jeong B. J., Lee H. B., Plasma protein adsorption and platelet adhesion onto comb-like PEO gradient surfaces, J. Biomed. Mater. Res., 34, 105 (1997).

100 Martins M. C. L., Wang D., Ji J., Feng L., Barbosa M. A., Albumin and fibrinogen adsorption on PU-PHEMA surfaces, Biomaterials, 24, 2067 (2003).

101 Xu F. J., Zhong S. P., Yung L. Y. L., Tong Y. W., Kang E. T., Neoh K. G., Collagen-coupled poly(2-hydroxyethyl methacrylate)-Si(111) hybrid surfaces for cell immobilization, Tissue Eng., 11, 1736 (2005).

102 Joshi J. M., Sinha V. K., Graft copolymerization of 2-hydroxyethylmethacrylate onto carboxymethyl chitosan using CAN as an initiator, Polymer, 47, 2198 (2006).

103 Baumann H., Richter A., Klemm D., Faust V., Concepts for preparation of novel regioselective modified cellulose derivatives sulfated, aminated, carboxylated and acetylated for hemo-compatible ultrathin coatings on biomaterials, Macromol. Chem. Phys., 201, 1950 (2000).

104 Zhang Z., Chao T., Chen S. F., Jiang S. Y., Superlow fouling sulfobetaine and carboxybetaine polymers on glass slides, Langmuir, 22, 10072 (2006).

105 Iwasaki Y., Ishihara K., Phosphorylcholine-containing polymers for biomedical applications, Anal. Bioanal. Chem., 381, 534 (2005).

106 Lewis A. L., Phosphorylchoine-based polymers and their use in the prevention of biofouling, Coll. Surf. B: Biointerf., 18, 261 (2000).

107 Horinaka J., Amano S., Funada H., Ito S., Yamamoto M., Local chain dynamics of poly(oxyethylene) studied by the fluorescence depolarization method, Macromolecules, 31, 1197 (1998).

108 Antonsen K. P., Hoffman A. S., Water structure of PEG solutions by differential scanning calorimetry measurements, in poly(ethylene glycol) chemistry: biotechnical and biomedical applications, J. M. Harris (ed.), Plenum Press, NY, P15-28 (1992).

109 Hermans J., Excluded-volume theory of polymer-protein interactions based on polymer chain statistics, J. Chem. Phys., 77, 2193 (1982).

110 Lee J. H., Li T., Park K., Solvation interactions for protein adsorption to biomaterial surfaces, In: Water in Biomaterials Surface Science, Morra M (ed.), Chichester: John Wiley & Sons Ltd, P127-146 (2001).

111 Harris J. M., Veronese F. M., Peptide and protein pegylation II: clinical evaluation, Advanced Drug Delivery Reviews, 55, 1259 (2003).

112 Vermette P., Meagher L., Interactions of phospholipid- and poly(ethylene glycol)-modified surfaces with biological systems: relation to physico-chemical properties and mechanisms, Colloid Surf. B, 28, 153 (2003).

113 Morra M., On the molecular basis of fouling resistance, J. Biomater. Sci. Polym. Ed., 11, 547 (2000).

114 De Gennes P. G., Polymers at an Interface: a simplified view, Adv. Coll. Interf. Sci., 27, 189 (1987).

115 Jeon S. I., Lee J. H., Andrade J. D., De Gennes P. G., Protein-surface interactions in the presence of polyethylen oxide: I. simplified theory, J. Coll. Interf. Sci., 142, 149 (1991).

116 Herrwerth S., Eck W., Reinhardt S., Grunze M., Factor that determine the protein resistance of oligoether self-assembled monolayers: internal hydrophilicity,

terminal hydrophilicity, and lateral packing density, J. Am. Chem. Soc., 125, 9359 (2003).

117 Kim H. I., Kushmerick J. G., Houston J. E., Bunker B. C., Viscous "interphase" water adjacent to oligo(ethylene glycol)-terminated monolayers, Langmuir, 19, 9271 (2003).

118 Ostuni E., Grzybowski B. A., Mrksich M., Roberts C. S., Whitesides G. M., Adsorption of protein to hydrophobic sites on mixed self-assembled monolayers, Langmuir, 19, 1861 (2003).

119 Prime K. L., Whitesides G. M., Adsorption of proteins onto surfaces containing end-attached oligo(ethylene oxide): a model system using self-assembled Monolayers, J. Am. Chem. Soc., 115, 10714 (1993).

120 Feldman K., Hahner G., Spencer N. D., Harder P., Grunze M., Probing resistance to protein adsorption of oligo(ethylene glycol)-terminated self-assembled monolayers by scanning force microscopy, J. Am. Chem. Soc., 121, 10134 (1999).

121 Besseling N. A. M., Theory of hydration forces between surfaces, Langmuir, 13, 2113 (1997).

122 Harder P., Grunze M., Dahint R., Whitesides G. M., Laibinis P. E., Molecular conformation in oligo(ethylene glycol)-terminated self-assembled monolayers on gold and silver surfaces determines their ability to resist protein adsorption, J. Phys. Chem. B, 102, 426 (1998).

123 Gombotz W. R., Guanghui W., Horbett T. A., Hoffman A. S., Protein adsorption to poly(ethylene oxide) surfaces, J. Biomed. Mater. Res., 25, 1547(1991).

124 Gölander C. G., Herron J. N., Lim K., Claesson P., Stenius P, Andrade J. D., Properties of immobilized PEG films and the interaction with proteins: experiments and modeling. In: Poly(ethylene glycol) Chemistry, Biotechnological and Biomedical Applications, J. M. Harris (ed.), Plenum Press, NY, P221-246, (1992).

125 Tan J. PEO-containing block copolymers as surface modification additives in polyurethanes for protein and cell resistance, Ph.D thesis, McMaster University, Hamilton, Ontario, CA, (2004).

126 Tan J. S., Butterfield D. E., Voycheck C. L., Caldwell K. D., Li J. T., Surface modification of nanoparticles by PEO-PPO clock copolymers to minimize interactions with blood components and prolong blood circulation in rats, Biomaterials, 14, 823 (1993).

127 Bergstrom K., Osterberg E., Hoffman A. S., Schuman T. P., Harris J. M., Effects of branching and molecular weight of surface-bound poly(ethylene oxide) on protein rejection, J. Biomater. Sci. Polym. Edn., 6, 123 (1994).

128 Desai N. P., Hubbell J. A., Biological responses to polyethylene oxide modified polyethylene terephthalate surfaces, J. Biomed. Mater. Res., 25, 829 (1991).

129 Currie E. P. K., Norde W., Cohen Stuart M. A., Tethered polymer chains: surface chemistry and their impact on colloidal and surface properties, Adv. Coll. Interf. Sci., 100, 205 (2003)

130 McPherson T., Kidane A., Szleifer I., Park K., Prevention of protein adsorption by tethered poly(ethylene oxide) layers: experiments and single-chain mean field analysis, Langmuir, 14, 176 (1998).

131 Kingshott P., Thissen H., Griesser H. J., Effects of cloud-point grafting, chain length, and density of PEG layers on competitive adsorption of ocular proteins, Biomaterials, 23, 2043 (2002).

132 Sofia S. J., Premnath V., Merrill E. W., Poly(ethylene oxide) grafted to silicon surfaces: grafting density and protein adsorption, Macromolecules, 31, 5059 (1998).

133 McPherson T. B., Lee S. J., Park K., Analysis of the prevention of protein adsorption by steric repulsion theory, In: Proteins at Interfaces II: Fundamental and Applications, Horbett T. A., Brash J. L. (eds.), American Chemical Society, Washington, DC, P395-404 (1995).

134 McPherson T. B., Shim H. S., Park K., Grafting of PEO to glass, nitinol, and pyrolytic carbon surfaces by γ–irradiation, J. Biomed. Mater. Res. Appl. Biomaterials, 38, 289 (1997).

135 Wu Y. J., Timmons R. B., Jen J. S., Molock F. E., Non-fouling surfaces produced by gas phase pulsed plasma polymerization of an ultra low molecular weight ethylene oxide containing monomer, Coll. Surf. B, 18, 235 (2000).

136 Zwaal R. F. A., Comfurius P., Van Deenen L. L. M., Membrane asymmetry and blood coagulation, Nature, 268, 358 (1977).

137 Ishihara K., Oshida H., Endo Y., Watanabe A. Ueda T., Nakabayashi N., Effects of phospholipid adsorption on nonthrombogenicity of polymer with phospholipid polar group, J. Biomed. Mater. Res., 27, 1309 (1993).

138 Ishihara K., Nomura H., Mihara T., Kurita K., Iwasaki Y., Nakabayashi N., Why do phospholipid polymers reduce protein adsorption? J. Biomed. Mater. Res., 39, 323 (1998).

139 Ueda T., Ishihara K., Nakabayashi N., Adsorption-desorption of proteins on phospholipid polymer surfaces evaluated by dynamic contact angle measurement, J. Biomed. Mater. Res., 27, 381 (1995).

140 Ishihara K., Iwasaki Y., Reduced protein adsorption on novel phospholipid polymers, J. Biomater. Appl., 13, 111 (1998).

141 Murphy E. F., Lu J. R., Brewer J., Russell J. C., Penfold J., The reduced adsorption of proteins at the hydrophillic polymer water interface, Langmuir, 15, 1313 (1999).

142 Murphy E. F., Keddie J. L., Lu J. R., Brewer J., Russell J. C., The reduced adsorption of lysozyme at the phosphorylcholine incorporated polymer/aqueous solution interface studied by spectroscopic ellipsometry, Biomaterials, 20, 1501 (1999).

143 Amiji M. M., Park K., Analysis on the surface-adsorption of PEO PPO PEO triblock copolymers by radiolabeling and fluorescence techniques, J. Appl, Polym. Sci., 52, 539 (1994).

144 Kenausis G. L., Voros J., Elbert D. L., Huang N. P., Hofer R., Ruiz-Taylor L., Textor M., Hubbell J. A., Spencer N. D., Poly(L-lysine)-g-poly(ethylene glycol) layers on metal oxide surfaces: attachment mechanism and effects of polymer architecture on resistance to protein adsorption, J. Phys. Chem. B, 104, 3298 (2000).

145 Bohner M., Ring T. A., Rapoport N., Caldwell K. D., Fibrinogen adsorption by PS latex particles coated with various amounts of a PEO/PPO/PEO triblock copolymer, J. Biomater. Sci. Polym. Edn., 13, 733 (2002).

146 Michel R., Pasche S., Textor M., Castner D. G., Influence of PEG architecture on protein adsorption and conformation, Langmuir, 21, 12327 (2005).

147 Gnauck M., Jaehne E., Blaettler T., Tosatti S., Textor M., Adler H. J. P., Carboxy-terminated oligo(ethylene glycol)-alkane phosphate: synthesis and self-assembly on titanium oxide surfaces, Langmuir, 23, 377 (2007).

148 Lee J. H., Oh S. H., MMA/MPEOMA/VSA copolymer as a novel blood-comparible material: effect of PEO and negatively charged side chains on protein adsorption and platelet adhesion, J. Biomed. Mater. Res., 60, 44 (2002).

149 Lee J. H., Oh S. H., Kim W. G., MMA/MPEOMA/VSA copolymer as a novel blood-compatible material: ex vivo platelet adhesion study, J. Mater. Sci.: Mater. in Medicine, 15, 155 (2004).

150 Hildebrand H. F., Blanchemain N., Mayer G., Chai F., Lefebvre M., Boschin F., Surface coatings for biological activation and functionalization of medical devices, Surf. Coatings Techn., 200, 6318 (2006).

151 Ji J., Barbosa M. A., Feng L., Shen J., A novel urethane containing copolymer as a surface modification additive for blood contact materials, J. Mater. Sci.: Mater in Medicine, 13, 677 (2002).

152 Park J. H., Bae Y. H., Physicochemical properties and in vitro biocompatibility of PEO/PTMO multiblock copolymer/segmented polyurethane blends, J. Biomater. Sci. Polym. Edn., 13, 527 (2002).

153 Ishihara K., Iwasaki Y., Biocompatible elastomers composed of segmented polyurehtane and 2-methacryloyloxyethyl phosphorylcholine polymer, Polym. Adv. Techn., 11, 626 (2000).

154 Iwasaki Y., Sawada S., Ishihara K., Khang G., Lee H. B., Reduction of surface-induced inflammatory reaction on PLGA/MPC polymer blend, Biomaterials, 23, 3897 (2002).

155 Kidane A., McPherson T., Shim H. S., Park K., Surface modification of polyethylene terephthalate using PEO-polybutadiene-PEO triblock copolymers, Coll. Surf. B Biointerf., 18, 347 (2000).

156 Kidane A., Lantz G. C., Jo S., Park K., Surface modificaiton with PEO-containing triblock copolymer for improved biocompatibility: in vitro and ex vivo studies, J. Biomater. Sci. Polym. Edn., 10, 1089 (1999).

157 Unsworth L. D., Sheardown H., Brash J. L., Polyethylene oxide surfaces of variable chain density by chemisorption of PEO-thiol on gold: adsorption of proteins from plasma studied by radiolabelling and immunoblotting, Biomaterials, 26, 5927 (2005).

158 Unsworth L. D., Sheardown H., Brash J. L., Protein-reistant poly(ethylene oxide)-grafted surfaces: chain density-dependent multiple mechanisms of action, Langmuir, 24, 1924 (2008).

159 Sofia S. J., Merrill E. W., Grafting of PEO to polymer surfaces using electron beam irradiation, J. Biomed. Mater. Res., 40, 153 (1998).

160 Murthy R., Shell C. E., Grunlan M. A., The influence of poly(ethylene oxide) grafting via siloxane tethers on protein adsorption, Biomaterials, 30, 2433 (2009).

161 Vanderah D. J., Vierling R. J., Walkers M. L., Oligo(ethylene oxide) self-assembled monolayers, with self-limiting packing densities for the inhibition of nonspecific protein adsorption, Langmuir, 25, 5026 (2009).

162 Tosatti S., De Paul S. M., Askendal A., Vande Vondele S., Hubbell J. A., Tengvall P., Textor M., Peptide functionalized poly(L-lysine)-g-poly(ethylene glycol) on titanium: resistance to protein adsorption in full heparinized human blood plasma, Biomaterials, 24, 4949 (2003).

163 Caldwell K. D., Surface modificaitons with adsorbed poly(ethylene oxide)-based block copolymers: physical characteristics and biological use, In: Poly(ethylene glycol) Chemistry and Biological Applications, Harris J. M., Zalipsky S. (eds.), ACS Symposium Series, 680, P400-419 (1997).

164 Nejadnik M. R., van der Mei H. C., Norde W., Busscher H. J., Bacterial adhesion and growth on a polymer brush-coating, Biomaterials, 29, 4117 (2008).

165 Iwasaki Y., Yamasaki A., Ishihara K., Platelet compatible blood filtration fabrics using a phosphorylcholine polymer having high surface mobility, Biomaterials, 24, 3599 (2003).

166 Lewis A. L., In: Encyclopedia of Biomaterials and Biomedical Engineering, Wnek G. E., Bowlin G. L. (eds.), NY: Marcel Dekker Inc., P1198 (2004).

167 Fujii K, Matsumoto H. N., Koyama Y., Iwasaki Y., Ishihara K., Takakuda K., Prevention of biofilm formation with a coating of 2-methacryloyloxyethyl phosphorylcholine polymer, J. Veter. Med. Sci., 70, 167 (2008).

168 Ishihara K., Ishikawa E., Iwasaki Y.,Nakabayashi N., Inhibition of fibroblast cell adhesion on substrate by coating with 2-methacryloyloxyethyl phosphorylcholine polymers, J. Biomater. Sci. Polym. Edn., 10, 1047 (1999).

169 Tan J., McClung W. G., Brash J. L., Nonfouling biomaterials based on polyethylene oxide-containing amphiphilic triblock copolymers as surface modifying additives: protein adsorption on PEO-copolymer/polyurethane blends, J. Biomed. mater. Res. A, 85A, 873 (2008).

170 McCloskey C. B., Yip C. M., Santerre J. P., Effect of fluorinated surface-modifying macromolecules on the molecular surface structure of a polyether poly(urethane urea), Macromol., 35, 914 (2002).

171 Jahangir A., McCloskey C., McClung W. G., Brash J. L, Labow R. S., Santerre J. P., The influence of protein adsorption and surface modifying macromolecules on the hydrolytic degradation of a polyether-urea-urethane by cholesterol esterase, Biomaterials, 24, 121 (2003).

172 Massa T. M., Yang M. L., Ho J. Y. C., Brash J. L., Santerre J. P., Fibrinogen surface distribution correlates to platelet adhesion patterns on fluorinated surface-modified polyetherurethane, Biomaterials, 35, 7367 (2005).

173 Tang Y. W., Santerre J. P., Labow R. S., Taylor D. G., The use of surface modifying macromolecules to improve the biostability of segmented polyurethanes, J. Biomed. Mater. Res., 35, 371 (1997).

174 Tang Y. W., Santerre J. P., Labow R. S., Taylor D. G., Application of macromolecular additives to reduce the hydrolytic degradation of polyurethanes by lysosomal enzymes, Biomaterials, 18, 37 (1997).

175 Jahangir A. R., McClung W. G., Cornelius R. M., McCloskey C. B., Brash J. L., Santerre J. P., Fluorinated surface-modifying macromolecules: Modulating adhesive protein and platelet interactions on a polyether-urethane, J. Biomed. Mater. Res. A, 60, 135 (2002)

176 Zhao B., Brittain W. J., Polymer brushes: surface-immobilized macromolecules, Prog. Polym. Sci., 25, 677 (2000).

177 Edmondson S., Osborne V. L., Huck W. T. S., Polymer brushes via surface-initiated polymerizations, Chem. Soc. Rev., 33, 14 (2004).

178 Senaratne W., Andruzzi L., Ober C. K., Self-assembled monolayers and polymer brushes in biotechnology: current applications and future perspectives, Biomacromolecules, 6, 2427 (2005).

179 Goddard J. M., Hotchkiss J. H., Polymer surface modification for the attachment of bioactive compounds, Prog. Polym. Sci., 32, 698 (2007).

180 Unsworth L. D., Sheardown H., Brash J. L., Protein resistance of surfaces prepared by sorption of end-thiolated poly(ethylene glycol) to gold: Effect of surface chain density, Langmuir, 21, 1036 (2005).

181 Archambault J. G., Brash J. L., Protein resistant polyurethane surfaces by chemical grafting of PEO: amino-terminated PEO as grafting reagent, Coll. Surf. B Biointerf., 39, 9 (2004).

182 Xu F. J., Neoh K. G., Kang E. T., Bioactive surfaces and biomaterials via atom transfer radical polymerization, Prog. Polym. Sci., 34, 719 (2009).

183 Zhang F., Kang E. T., Neoh K. G., Wang P., Tan K. L., Modification of Si(100) surface by the grafting of poly(ethylene glycol) for reduction in protein adsorption and platelet adhesion, J. Biomed. Mater. Res., 56, 324 (2001).

184 Goda T., Konno T., Takai M., Moro T., Ishihara K., Biomimetic phosphorylcholine polymer grafting from polydimethylsiloxane surface using photo-induced polymerization, Biomaterials, 27, 5151 (2006).

185 Chen Y., Kang E. T., Wang P., Tan K. L., Surface modification of polyaniline film by grafting of poly(ethylene glycol) for reduction in protein adsorption and platelet adhesion, Synth. Met., 110, 47 (2000).

186 Iwasaki Y., Nakabayashi N., Ishihara K., Preservation of platelet function on 2-methacryloyloxyethyl phosphorylcholine-graft polymer as compared to various water-soluble graft polymers, J. Biomed. Mater. Res., 57, 72 (2001).

187 Kim K., Kim C., Byun Y., Biostability and biocompatibility of a surface-grafted phospholipid monolayer on a solid substrate, Biomaterials, 25, 33 (2004).

188 Korematsu A., Takemoto Y., Nakaya T., Inoue H., Synthesis, characterization and platelet adhesion of segmented polyurethanes grafted phospholipid analogous vinyl monomer on surface, Biomaterials, 23, 263 (2002).

189 Moro T., Takatori Y., Ishihara Y., Konno T., Takigawa Y., Matsushita T., Chung U. I., Nakamura K., Kawaguchi H., Surface grafting of artificial joints with a biocompatible polymer for preventing periprosthetic osteolsis, Nat. Mater., 3, 829 (2004).

190 Jordan R., Ulman A., Kang J. F., Rafailovich M. H., Sokolov J., Surface-initiated anionic polymerization of styrene by means of self-assembled monolayers, J. Am. Chem. Soc., 120, 1016 (1999).

191 Zhao B., Brittain W. J., Synthesis of tethered polystyrene-block-poly(methyl methacrylate) monolayer on a silicate substrate by sequential carbocationic polymerization and atom transfer radical polymerization, J. Am. Chem. Soc., 121, 3557 (1999).

192 Jordan R., UIman A., Surface initiated living cationic polymerization of 2-oxazolines, J. Am. Chem. Soc., 120, 243 (1998).

193 Yu W. H., Kang E. T., Neoh, K. G., Zhu S., Controlled grafting of well-defined polymers on hydrogen-terminated silicon substrates by surface-initiated atom transfer radical polymerization, J. Phys. Chem. B, 107, 10198 (2003).

194 Juang A., Scherman O. A., Grubbs R. H., Lewis N. S., Formation of covalently attached polymer overlayers on Si(111) surfaces using ring-opening metathesis polymerization methods, Langmuir, 17, 1321 (2001).

195 Pyun J., Kowalewski T., Matyjaszewski K., Synthesis of polymer brushes using atom transfer radical polymerization, Macromol. Rapid Commun., 24,1043 (2003).

196 Kim K., Kim C., Byun Y., Preparation of a stable phospholipid monolayer grafted onto a methacryloyl-terminated substrate as blood compatible materials, J. Biomater. Sci. Polym. Edn., 14, 887 (2003).

197 Hawker C. J., Bosman A. W., Harth E., New polymer synthesis by nitroxide mediated living radical polymerizations, Chem. Rev., 101, 3661 (2001).

198 Chiefari J., Chong Y. K., Ercole F., Krstina J., Jeffery J., Le T. P. T., Mayadunne R. T. A., Meijs G. F., Moad C. L., Moad G., Rizzardo E., Thang S. H., Living free

radical polymerization by reversible addition-fragmentation chain transfer: the RAFT process, Macromolecules, 31, 5559 (1998).

199 York A. W., Kirkland S. E., McCormick C. L., Advances in the synthesis of amphiphilic block copolymers via RAFT polymerization: Stimuli-responsive drug and gene delivery, Advanced Drug Delivery Reviews, 60, 1018 (2008).

200 Kamigaito M., Ando T., Sawamoto M., Metal-catalyzed living radical polymerization, Chem. Rev., 101, 3689 (2001).

201 Coessens V., Pintauer T., Matyjaszewski K., Functional polymers by atom transfer radical polymerization, Prog. Polym. Sci. 26, 337 (2001).

202 Carlmark A., Malmström E., Atom transfer radical polymerization from cellulose fibers at ambient temperature, J. Am. Chem. Soc., 124, 900 (2002).

203 Braunecker W. A., Matayjaszewski K., Controlled/living radical polymerization: features, developments, and perspectives, Prog. Polym. Sci., 32, 93 (2007).

204 Tsarevsky N. V., Matyjaszewski K., "Green" atom transfer radical polymerization: from process design to preparation of well-defined environmentally friendly polymeric materials, Chem. Rev., 107, 2270 (2007).

205 Croll T. I., O'Connor A. J., Stevens G. W., Cooper-White J. J., Controllable surface modification of poly(lactic-co-glycolic acid) (PLGA) by hydrolysis or aminolysis I: physical, chemical, and theoretical aspects, Biomacromolecules, 5, 463 (2004).

206 Cheng Z., Teoh S. H., Surface modification of ultra thin poly(ε-caprolactone) films using acrylic acid and collagen, Biomaterials, 25, 1991 (2004).

207 Gustavsson M. T., Persson P. V., Iversen T., Martinelle M., Hult K., Teeri T. T., Brumer H., Modification of cellulose fiber surfaces by use of a lipase and a xyloglucan endotransglycosylase, Biomacromolecules, 6, 196 (2005).

208 Alferiev I. S., Connolly J. M., Stachelek S. J., Ottey A., Rauova L., Levy R. J., Surface heparinization of polyurethane via bromoalkylation of hard segment nitrogens, Biomacromolecules, 7, 317 (2006).

209 Xu F. J., Li Y. L., Kang E. T., Neoh K. G., Heparin-coupled poly(poly(ethylene glycol) monomethacrylate)-Si(111) hybrids and their blood compatible surfaces, Biomacromolecules, 6, 1759 (2005).

210 Singh N., Cui X., Boland T., Husson S. M., The role of independently variable grafting density and layer thickness of polymer nanolayers on peptide adsorption and cell adhesion, Biomaterials, 28, 763 (2007).

211 Bozukova D., Pagnoulle C., De Pauw-Gillet M. C., Ruth N., Jérôme R., Jérôme C., Imparting antifouling properties of poly(2-hydroxyethyl methacrylate) hydrogels by grafting poly(oligoethylene glycol methyl ether acrylate), Langmuir, 24, 6649 (2008).

212 Feng W., Brash J. L., Zhu S., Non-biofouling materials prepared by atom transfer radical polymerization grafting of 2-methacryloloxyethyl phosphorylcholine: separate effects of graft density and chain length on protein repulsion, Biomaterials, 27, 847 (2006).

213 Pyun J., Matyjaszewski K., Synthesis of nanocomposite organic/inorganic hybrid materials using controlled/"living" radical polymerization, Chem. Mater., 13, 3436 (2001).

214 Ejaz M., Yamamoto S., Ohno K., Tsujii Y., Fukuda T., Controlled graft polymerization of methyl methacrylate on silicon substrate by the combined use of the Langmuir-Blodgett and atom transfer radical polymerization techniques, Macromolecules, 31, 5934 (1998).

215 Ejaz M., Tsujii Y., Fukuda T., Controlled grafting of a well-defined polymer on a porous glass filter by surface-initiated atom transfer radical polymerization, Polymer, 42, 6811 (2001).

216 Hucknall A., Rangarajan S., Chilkoti A., In pursuit of zero: polymer brushes that resist the adsorption of proteins, Adv. Mater., 21, 1 (2009).

217 Xu F. J., Zhong S. P., Yung L. Y. L., Kang E. T., Neoh K. G., Surface-active and stimuli-responsive polymer-Si(100) hybrids from surface-initiated atom transfer

radical polymerization for control of cell adhesion, Biomacromolecules, 5, 2392 (2004).

218 Xu F. J., Kang E. T., Neoh K. G., UV-induced coupling of 4-vinylbenzyl chloride on hydrogen-terminated Si(100) surfaces for the preparation of well-defined polymer-Si hybrids via surface-initiated ATRP, Macromolecules, 38, 1573 (2005).

219 Xu F. J., Cai Q. J., Kang E. T., Neoh K. G., Surface-initiated atom transfer radical polymerization from halogen-terminated Si(111) (Si-X, X = Cl, Br) surfaces for the preparation of well-defined polymer-Si hybrids, Langmuir, 21, 3221 (2005).

220 Gao X., Feng W., Zhu S., Sheardown H., Brash J. L., A facile method of forming nanoscale patterns on poly(ethylene glycol)-based surfaces by self-assembly of randomly grafted block copolymer brushes, Langmuir, 24, 8303 (2008).

221 Ma H., Li D., Sheng X., Zhao P., Chilkoti A., Protein-resistant polymer coatings on silicon oxide by surface-initiated atom transfer radical polymerization, Langmuir, 22, 3751 (2006).

222 Stadler V., Kirmse R., Beyer M., Breitling F., Ludwig T., Bischoff F. R., PEGMA/MMA copolymer graftings: generation, protein resistance, and a hydrophobic domain, Langmuir, 24, 8151 (2008).

223 Iwata R., Suk-In P., Hoven V. P., Takahara A., Akiyoshi K., Iwasaki Y., Control of nanobiointerfaces generated from well-defined biomimetic polymer brushes for protein and cell manipulations, Biomacromolecules, 5, 2308 (2004).

224 Tugulu S., Arnold A., Sielaff I., Johnsson K., Klok H. A., Protein-functionalized polymer brushes, Biomacromolecules, 6, 1602 (2005).

225 Chen B., Xu F. J., Neoh K. G., Kang E. T., Wang W. N., Chan V., Engineering cell de-adhesion dynamics on thermo-responsive poly(*N*-isopropylacrylamide, Acta Biomaterialia, 4, 218 (2008).

226 Tugulu S., Klok H. A., Stability and nonfouling properties of poly(poly(ethylene glycol) methacrylate) brushes under cell culture conditions, Biomacromolecules, 9, 906 (2008).

227 Zhang Z., Chen S., Jiang S., Dual-functional biomimetic materials: nonfouling poly(carboxybetaine) with active functional groups for protein immobilization, Biomacromolecules, 7, 3311 (2006).

228 Zhang Z., Chen S., Chang Y., Jiang S., Surface grafted sulfobetaine polymers via atom transfer radical polymerization as superlow fouling coatings, J. Phys. Chem. B, 110, 10799 (2006).

229 Ma H., Hyun J., Stiller P., Chilkoti A., 'Non-fouling' oligo(ethylene glycol)-functionalized polymer brushes synthesized by surface-initiated atom transfer radical polymerization, Adv. Mater., 16, 338 (2004).

230 Yoon K. R., Ramaraj B., Lee S. M., Kim D. P., Surface initiated-atom transfer radical polymerization of a sugar methacrylate on gold nanoparticles, Surf. Interf. Anal., 40, 1139 (2008).

231 Lee B. S., Chi Y. S., Lee K. B., Kim Y. G., Choi I. S., Functionalization of poly(oligo(ethylene glycol) methacrylate) films on gold and Si/SiO_2 for immobilization of proteins and cells: SPR and QCM studies, Biomacromolecules, 8, 3922 (2007).

232 Jones D. M., Brown A. A., Huck W. T. S., Surface-initiated polymerizations in aqueous media: effect of initiator density, Langmuir, 18, 1265 (2002).

233 Fan X., Lin L., Dalsin J. L., Messersmith P. B., Biomimetic anchor for surface-initiated polymerization from metal substrates, J. Am. Chem. Soc., 127, 15843 (2005).

234 Fan X., Lin L., Messersmith P. B., Cell fouling resistance of polymer brushes grafted from Ti substrates by surface-initiated polymerization: effect of ethylene glycol side chain length, Biomacromolecules, 7, 2443 (2006).

235 Zhang F., Shi Z. L., Chua P. H., Kang E. T., Neoh K. G., Functionalization of titanium surfaces via controlled living radical polymerization: from antibacterial surface to surface for osteoblast adhesion, Ind. Eng. Chem. Res., 46, 9077 (2007).

236 Zhou Y., Wang S., Ding B., Yang Z., Modification of magnetite nanoparticles via surface-initiated atom transfer radical polymerization (ATRP), Chem. Eng. J., 138, 578 (2008).

237 Hu F., Neoh K. G., Chen L., Kang E. T., Cellular response to magnetic nanoparticles "PEGylated" via surface-initiated atom transfer radical polymerization, Biomacromolecules, 7, 809 (2006).

238 Wuang S. C., Neoh K. G., Kang E. T., Pack D. W., Leckband D. E., Heparinized magnetic nanoparticles: in-vitro assessment for biomedical applications, Adv. Funct. Mater., 16, 1723 (2006).

239 Marutani E., Yamamoto S., Ninjbadgar T., Tsujii Y., Fukuda T., Takano M., Surface-initiated atom transfer radical polymerization of methyl methacrylate on magnetite nanoparticles, Polymer, 45, 2231 (2004).

240 Bai Y., Teng B., Chen S., Chang Y., Li Z., Preparation of magnetite nanoparticles coated with an amphiphilic block copolymer: a potential drug carrier with a core-shell-corona structure for hydrophobic drug delivery, Macromol. Rapid. Commun., 27, 2107 (2006).

241 Fan Q. L., Neoh K. G., Kang E. T., Shuter B., Wang S. C., Solvent-free atom transfer radical polymerization for the preparation of poly(poly(ethyleneglycol) monomethacrylate)-grafted Fe_3O_4 nanoparticles: synthesis, characterization and cellular uptake, Biomaterials, 28, 5426 (2007).

242 Lutz J. F., Stiller S., Hoth A., Kaufner L., Pison U., Cartier R., One-pot synthesis of PEGylated ultrasmall iron-oxide nanoparticles and their in vivo evaluation as magnetic resonance imaging contrast agents, Biomacromolecules, 7, 3132 (2006).

243 Ignatova M., Voccia S., Gilbert B., Markova N., Cossement D., Gouttebaron R., Jérôme R., Jérôme C., Combination of electrografting and atom-transfer radical polymerization for making the stainless steel surface antibacterial and protein antiadhesive, Langmuir, 22, 255 (2006).

244 Ignatova M., Voccia S., Gabriel S., Gilbert B., Cossement D., Jerome R., Jerome C., Stainless steel grafting of hyperbranced polymer brushes with an antibacterial activity: synthesis, characterization, and properties, Langmuir, 25, 891 (2009).

245 Lee S. B., Koepsel R. R., Morley S. W., Matyjaszewski K., Sun Y., Russell A. J., Permanent, nonleaching antibacterial surfaces. 1. Synthesis by atom transfer radical polymerization, Biomacromolecules, 5, 877 (2004).

246 Yan L., Ishihara K., Graft copolymerization of 2-methacryloyloxyethyl phosphorylcholine to cellulose in homogeneous media using atom transfer radical polymerization for providing new hemocompatible coating materials, J. Polym. Sci. Part A: Polym. Chem., 46, 3306 (2008).

247 Singh N., Chen Z., Tomer N., Wickramasinghe S. R., Soice N., Husson S. M., Modification of regenerated cellulose ultrafiltration membranes by surface-initiated atom transfer radical polymerization, J. Membr. Sci., 311, 225 (2008).

248 Huang J., Murata H., Koepsel R. R., Russell A. J., Matyjaszewski K., Antibacterial polypropylene via surface-initiated atom transfer radical polymerization, Biomacromolecules, 8, 1396 (2007).

249 Yao F., Fu G. D., Zhao J., Kang E. T., Neoh K. G., Antibacterial effect of surface-functionalized polypropylene hollow fiber membrane from surface-initiated atom transfer radical polymerization, J. Membr. Sci., 319, 149 (2008).

250 Xu F. J., Zhao J. P., Kang E. T., Neoh K. G., Li J., Functionalization of nylon membranes via surface-initiated atom transfer radical polymerization, Langmuir, 23, 8585 (2007).

CHAPTER 2 Objectives and Contributions to Articles

2.1 Objectives

Although surface-initiated ATRP has been widely used to graft polymer chains of well-controlled structure and functionality onto some special model surfaces such as gold, titanium, silica and silicon wafer, on which it is easy to form ATRP initiator layers with high surface density, and to characterize/quantify polymer grafts, not much work has been done on ATRP grafting of well-controlled polymer brushes on more practical polymeric biomaterial substrates for improved biocompatibility. The main hindrances lie in immobilization of ATRP initiator and characterization of grafted chains on soft polymeric substrates. These substrates are not as well defined and do not have as strong contrast to grafted chains as the previously studied inorganic/metallic substrates.

The objectives of this research are two fold, (1) from a technological standpoint, we aim to prepare highly protein-resistant biomaterials by ATRP grafting of water soluble polymers such as poly(OEGMA) and poly(MPC), and to evaluate these biomaterials for blood-contacting applications; (2) from a scientific perspective, we aim to provide fundamental understanding of the molecular processes involved in functionalization and polymerization on polymeric biomaterial surfaces; and to investigate the relative roles of the functional groups, the surface density/coverage, and the chain length of polymer brushes in the protein adsorption process.

2.2 Contributions to Articles

The following describes my contribution to the articles constituting Chapters 3-6. Professors Shiping Zhu, John L. Brash and Dr. Wei Feng provided guidance with the initial research focus and idea development. I designed and performed all phases of the

project, from literature search, experiments through to data analysis. I generated the first drafts of the papers and the initial responses to the comments of the journal reviewers. I worked with my supervisors on subsequent drafts until accepted.

CHAPTER 3 Protein-resistant Polyurethane via Surface-initiated ATRP of Oligo(ethylene glycol) Methacrylate

This chapter is a reproduction of the following published article in Journal of Biomedical Materials Research A.

Authors: **Z. Jin,** W. Feng, S. Zhu, H. Sheardown, and J.L. Brash

Publication Information: Journal of Biomedical Materials Research A. **2009**, 91A, 1189-1201.

Accepted Date: Sep 04, 2008

Working Hypothesis:

After modification by water-soluble polymers, PU surfaces, which contain the same graft density (number of polymer chain per unit area), but longer polymer chain length, are more efficient in preventing protein adsorption.

Protein-resistant Polyurethane via Surface-initiated Atom Transfer Radical Polymerization of Oligo(ethylene glycol) Methacrylate

Abstract: Protein-resistant polyurethane (PU) surfaces were prepared by surface-initiated simultaneous normal and reverse atom transfer radical polymerization (s-ATRP) of poly(oligo(ethylene glycol) methacrylate) (poly(OEGMA)). Oxygen plasma treatment was employed for initial activation of the PU surface. The grafted polymer chain length was adjusted by varying the molar ratio of monomer to sacrificial initiator in solution from 5:1 to 200:1. The modified PU surfaces were characterized by water contact angle, X-ray photoelectron spectroscopy (XPS), and atom force microscopy (AFM). Protein adsorption experiments from tris-buffered saline (TBS) and plasma were carried out to evaluate the protein-resistance of the surfaces. Adsorption from single and binary protein solutions as well as from plasma was significantly reduced after modification. Adsorption decreased with increasing poly(OEGMA) chain length. Fibrinogen (Fg) adsorption on the 200:1 monomer:initiator surface was in the range of 3-33 ng/cm^2 representing 96-99% reduction compared to the unmodified PU. Fibrinogen adsorption from 0.01-10% plasma was as low as 1-5 ng/cm^2. Moreover, binary protein adsorption experiments using fibrinogen and lysozyme (Lys) showed that protein size is a factor in the protein resistance of these surfaces.

Keywords: polyurethane; surface modification; atom transfer radical polymerization (ATRP); protein resistant surface; poly(ethylene glycol).

3.1 Introduction

Biocompatibility is an essential requirement for materials used in medical devices.[1-3] It is axiomatic that when a biomaterial surface comes into contact with blood and other biological systems, protein adsorption is the first significant event.[4,5] In blood contact situations, adverse sequelae include initiation of coagulation, platelet adhesion and platelet activation leading to thrombosis.[6-7] The prevention of nonspecific protein adsorption is thus believed to be an effective strategy to improve the biocompatibility of biomaterials. Considerable efforts have been made to develop protein resistant surfaces, including incorporation of hydrophilic polymers,[8-9] phospholipids and phospholipid-like moieties.[10-13]

Polyethylene oxide (PEO) and oligo(ethylene glycol) (OEG)-containing polymers (e.g. poly(OEGMA)) have been shown to be particularly effective agents for the prevention of protein adsorption due to their low interfacial free energy, large excluded volume, and highly flexible chains.[14-16] Considerable efforts have been made to elucidate the nature and mechanism of the protein resistance of PEO- (or OEG-) containing surfaces.[17-21] It has been shown that both PEO graft density and chain length have a strong effect on protein resistance,[22,23] and that resistance generally increases with increasing PEO graft density and chain length. These effects are believed to be due to the compressibility of the PEO chains leading to steric exclusion, and to the tightly bound water layer associated with the PEO chains (water barrier).

The preparation of biomaterials grafted with polymers of well-controlled chain length and graft density remains a challenge. In the 'grafting to' method, preformed polymer chains are introduced into the surface by reaction of functional chain ends with co-reactive moieties on the surface: low graft densities are usually obtained because of steric hindrance imposed by initially grafted chains. In the 'grafting from' method, polymerization is initiated on the surface, usually by free radical methods. Conventional

free radical polymerization generally results in low graft density: again initially-grafted chains inhibit the initiation of additional chains. Moreover, the polymer chain length is uncontrolled and broadly distributed due to the random process of radical termination.

Compared to the above methods, surface-initiated atom transfer radical polymerization (s-ATRP) has clear advantages for grafting polymer chains having well-controlled, uniform chain length and high graft density, due to the absence of termination and chain transfer reactions, and rapid initiation. There are several reports on s-ATRP grafting from model substrates such as gold, silicon and glass.[24-30] However, there have been few reports on the s-ATRP grafting of hydrophilic polymers from polymeric biomaterials of practical importance such as polyurethanes (PU) and polydimethylsiloxane (PDMS).

Plasma treatment of polymer surfaces has been shown to be an effective way to introduce high concentrations of free radicals that can be used to initiate free radical polymerization,[8,31] plasma polymerization, and various plasma deposition processes.[32,33] In the work reported here, we developed a method for the surface modification of PU materials by grafting polymers with high graft density and controlled molecular weight. Oxygen plasma treatment was followed by s-ATRP. The process consists of three steps as shown in Scheme 3.1. First, high concentrations of hydro-peroxide, peroxide and hydroxyl groups were generated on the PU surface after oxygen plasma treatment and exposure to air. These active sites were then converted to initiators for normal and reverse ATRP in one simple step. Normal ATRP refers to initiation by Br atoms, while reverse ATRP refers to initiation by OOR peroxide groups. The graft polymerization of OEGMA monomer from the surfaces was then carried out by the s-ATRP method. It should be pointed out that reverse ATRP[34,35] and simultaneous normal- and reverse- ATRP[36-38] have been widely investigated in bulk, solution, and emulsion environments and that the livingness and good control of these processes have been demonstrated. The novelty of the present work is to take advantage of all types of active species generated on the

surface by the oxygen plasma treatment and to use them for initiation of graft polymerization to produce layers of high graft density and controlled molecular weight. A set of poly(OEGMA)-grafted PU surfaces of varying structure were prepared and their protein-resistant properties were assessed by studies of adsorption from buffer and plasma. The effects of protein size and charge on protein resistance were examined.

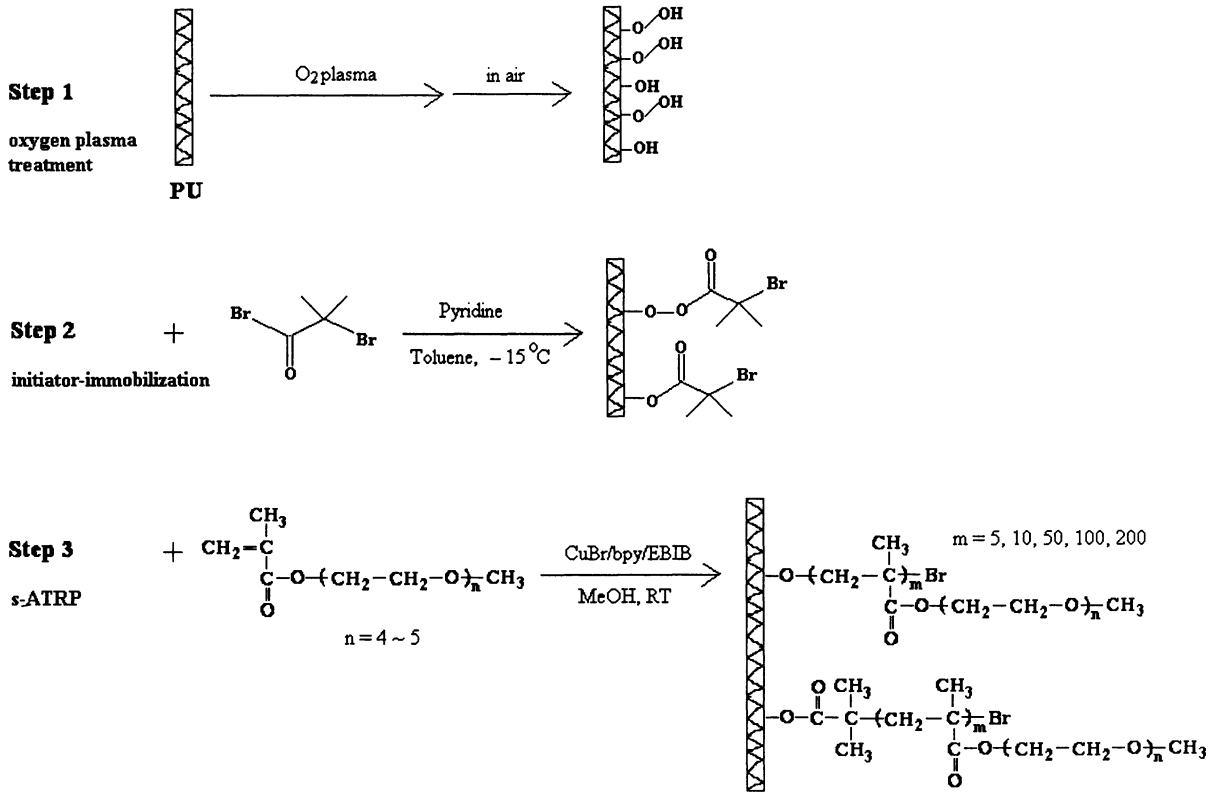

Scheme 3.1 Three-step process of PU surface modification.

3.2 Experimental

3.2.1 Materials

The polyurethane Tecothane (TT-1095A) was obtained from Thermedics and dried overnight at 65°C. OEGMA (98% purity, Mn = 300 $gmol^{-1}$; Aldrich) was distilled over CaH_2 under vacuum and stored at -15°C. 2-Bromoisobutyryl bromide (BIBB) (98%), ethyl 2-bromoisobutyrate (EBIB) (98%), 2,2'-bipyridyl (bpy) (99%), and Cu(I)Br (99.999%) were purchased from Aldrich and used as received. Pyridine (99.9%, Fisher Scientific) and N,N-dimethylformamide (DMF) (99.8%, EMD Chemicals Inc.) were also used as received. Toluene and methanol (HPLC grade) were obtained from Caledon Laboratories Ltd. Toluene was double-distilled over CaH_2. Human fibrinogen (Fg) was obtained from Enzyme Research Laboratories. Egg white lysozyme (Lys) was purchased from Sigma. Deionized water used in this study had a resistivity of 18.2 MΩ·cm and nitrogen gas was ultrahigh-purity (UHP) grade.

3.2.2 Preparation of PU Films

PU 7% w/v in DMF solution was prepared at 65°C, cast in Petri dishes and dried at 65°C for 4 days. The PU films of 0.5 mm thickness were further dried in a vacuum oven for 1 day at 65°C. PU disks of diameter 6 mm were then cut from the films, extracted in boiling toluene for 24 h to remove impurities, additives and some small molecules. After extraction, the PU disks were dried under vacuum at 65°C for 2 days.

3.2.3 Surface Treatment of PU with Oxygen Plasma

Both sides of the PU disk were treated in oxygen plasma using glow discharge technique (Biorad PT7150, East Grinstead, UK) at constant power of 100 W and pressure 200 mTorr for 30 min. The PU surfaces were then exposed to air for 5 min and stored in toluene for further modification with initiator.

3.2.4 Formation of Initiator Monolayer on PU Surfaces

The PU disks (30 pieces, 6 mm diameter and 0.5 mm thickness) freshly treated by oxygen plasma were immersed in 100 ml dry toluene. The mixture was deaerated by nitrogen for 30 min under stirring at -15°C in a NaCl- ice bath. Pyridine (52 mmol, 4.2 ml) was then added to the mixture followed by BIBB (44 mmol, 5.44 ml) added dropwise over a period of 1 h. The reaction mixture was stirred overnight at -15°C and then kept at room temperature (22°C) for 3 h. After the reaction, the PU disks functionalized with the two initiator species (see Scheme 3.1), referred to as PU/initiator, were cleaned ultrasonically for 5 min in dry toluene, and rinsed several times in toluene and methanol for 2 h. Finally the PU/initiator disks were dried in a vacuum oven at 40°C for 1 day.

3.2.5 s-ATRP of OEGMA on PU/initiator Surfaces

PU/poly(OEGMA) disks with different graft chain lengths were prepared by simultaneous normal and reverse s-ATRP. The chain lengths were controlled by varying the molar ratio of OEGMA to sacrificial EBIB (5:1, 10:1, 50:1, 100:1, 200:1). The monomer concentration was fixed at 38% w/v and the molar ratio of EBIB:Cu(I)Br:bpy at 1:1:2. For example, in an experiment with 100:1 OEGMA:EBIB ratio, Cu(I)Br (0.1 mmol, 14.3 mg) and bpy (0.2 mmol, 31.8 mg) were mixed in a dry, clean flask containing a magnetic stir bar. The solid mixture in the flask was deoxygenated by three nitrogen purge/vacuum cycles over about 30 min. OEGMA (10 mmol, 3 g) and methanol (5 ml), deaerated by nitrogen purge for 1 h, were added to the flask. The dark brown liquid mixture was transferred to a glovebox after an additional 30 min nitrogen purge. The deaerated EBIB initiator (0.1 mmol, 14.7 μL) was then added to the mixture under nitrogen protection in the glovebox. The reaction mixture was stirred intensively for 1 min, and immediately transferred to vials containing the PU/initiator disks. s-ATRP was performed on the PU/initiator disks at room temperature in the glovebox for 36 h to assure complete monomer conversion. The PU/poly(OEGMA) disks were then removed

from the glovebox, ultrasonicated, rinsed with methanol, and dried in a vacuum oven at 65°C for 2 days.

3.2.6 Characterization

OEGMA conversion in the s-ATRP reactions was measured by proton NMR spectroscopy (Bruker AC-P200 spectrometer, $CDCl_3$ solvent). The molecular weight and polydispersity index (PDI) were determined by gel permeation chromatography (GPC, Waters 2690 separations module with refractive index detector).

Water contact angle measurements were performed with a Rame-Hart NRL goniometer (Mountain Lakes, NJ) at room temperature, using the sessile drop method to obtain advancing and receding contact angles of the PU surfaces before and after each step of modification.

XPS was carried out to determine the surface chemical compositions of the PU disks (Leybold Max 200, aluminum anode non-monochromatic source). Low-resolution scans were performed to provide surface elemental analysis; high-resolution C_{1s} scans were recorded to determine the contribution of different functional groups containing carbon atoms. These scans were measured at takeoff angles of 90° and 20°.

A nanoscope IIIA multimode AFM (Digital Instruments, Inc.) was operated in tapping mode with a scan rate of 1.0 Hz to evaluate the topology of the PU surfaces before and after modification.

3.2.7 Protein Adsorption

The protein adsorption experiments were carried out at room temperature (22°C). Proteins were radioiodinated by the iodine monochloride (ICl) method using either ^{131}I or ^{125}I as described previously.[17,39] Residual unbound radioactivity was <1% for fibrinogen (^{131}I) and < 3% for lysozyme (^{125}I) as determined by trichloroacetic acid precipitation.[40]

Fibrinogen solutions containing 10% labeled protein at five concentrations ranging from 0.005 to 1.0 mg/ml were prepared in TBS, pH 7.4. For the binary protein solutions, Fg and Lys were labeled with ^{131}I and ^{125}I, respectively, and solutions of total protein concentration 0.05 mg/ml and 1.0 mg/ml were used at both 1:1 and 10:1 Lys:Fg molar ratios. For experiments in plasma, ^{125}I-labelled fibrinogen was added to pooled normal citrated human plasma as a tracer at 10% of total fibrinogen.[10,41] The plasma was diluted with TBS to obtain a series of plasmas of varying "strength".

PU disks were equilibrated in TBS overnight to achieve complete hydration, and were then incubated with the protein solutions for 2 h under static conditions. They were then washed with TBS buffer three times (5 min each time). The quantities of protein adsorbed were calculated from the radioactivity of the samples as determined by a Wizard 3″ 1480 Automatic Gamma Counter (Perkin-Elmer Life Sciences). Four replicate samples were measured for each concentration in a given experiment. Experiments were done at least twice.

3.3 Results and Discussion

3.3.1 Preparation of Poly(OEGMA)-grafted PU Surfaces

The PU/poly(OEGMA) surfaces were prepared by a three-step modification process that included oxygen plasma treatment, initiator immobilization, and s-ATRP (Scheme 3.1). In the first step, various reactive species were introduced into the PU surfaces by the oxygen plasma treatment. The treated PU surfaces were then exposed to air. The active sites, such as carbon radicals, oxygen radicals and peroxy radicals, reacted with oxygen and moisture in the air forming hydroxyl and hydro-peroxide groups.[11,32,42-45] In the second step, these hydroxyl and hydro-peroxide groups reacted with BIBB to form the initiator for normal ATRP (hydroxyl) and reverse ATRP (peroxides) respectively. In the final step, poly(OEGMA) grafts were formed by s-ATRP with

Cu(I)Br/2bpy complex as catalyst and methanol as solvent. The mechanism of s-ATRP is shown in Scheme 3.2. In order to control polymer chain length, a known amount of free/sacrificial initiator (EBIB) was added to the reaction so that ATRP of OEGMA occurred in solution as well as on the surface. The molar ratio of OEGMA to total initiator (solution EBIB, surface bromoisobutyrate groups, and surface peroxides; the latter two types being in very small amounts compared to the former) was varied. It is assumed that the poly(OEGMA) chains formed on the PU surface have the same chain length and distribution as those formed in the solution and that both are determined by the molar ratio OEGMA:EBIB.[46]

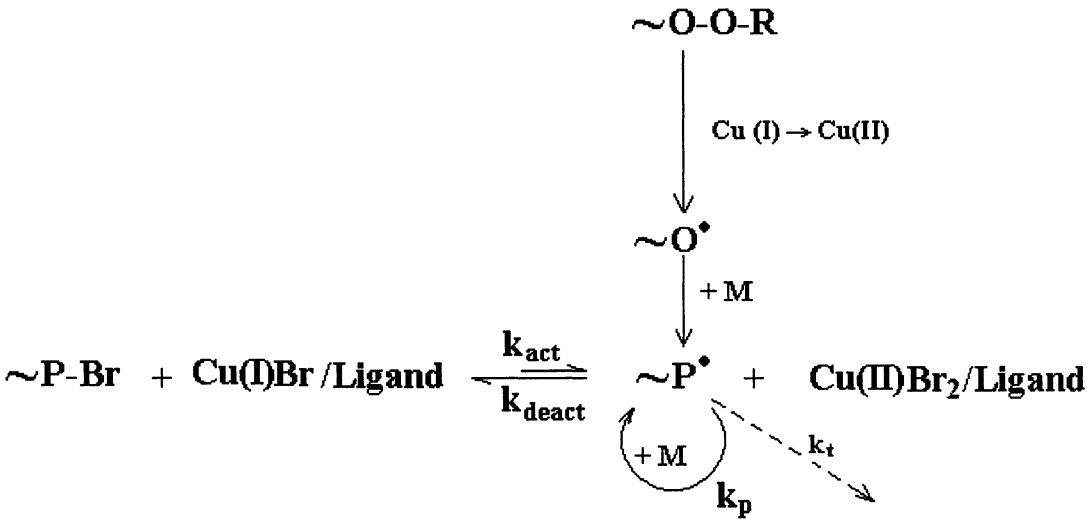

~ represents the PU surface
P is the abbr. of polymer
~P-Br acts as the normal ATRP initiator on PU surface
~O-O-R acts as the reverse ATRP initiator on PU surface

Scheme 3.2 Mechanism of s-ATRP.

The kinetics of solution ATRP of OEGMA in methanol have been studied in our previous work.[47] It was shown that the polymer molecular weight increased linearly with monomer conversion and the polydispersity was very low (in the range of 1.1-1.3). The s-ATRP of OEGMA on silicon wafer was also studied in our lab.[39,47] The graft densities of poly(OEGMA) were controlled through the initiator density on the silicon surface. It was found that the ellipsometric thickness of the grafts increased linearly with monomer conversion in solution. At a certain initiator density, the ellipsometric thickness also increased linearly with monomer:sacrificial initiator ratio, indicating constant graft density independent of this ratio in well-controlled ATRP grafting. In the present work, s-ATRP was performed on the PU/initiator surface with OEGMA:EBIB ratios of 5:1, 10:1, 50:1, 100:1 and 200:1, using the same ATRP grafting recipe (same EBIB/Cu(I)Br/bpy molar ratio and monomer concentration) as in previous work[39,47]. The conversion and molecular weight of polymers in solution are shown in Table 3.1. At complete monomer conversion, the polydispersities were in the range of 1.15 to 1.35, similar to those found for the s-ATRP of OEGMA on silicon.[47] The grafts of varying chain length are expected to have equal graft density (number of chains per area) due to the constant initiator density and similar chain growing environment, such as constant monomer concentration and EBIB:Cu(I)Br:bpy molar ratio. It is important to note that the presence of sacrificial initiator not only facilitated the control of polymer chain length by adjusting the OEGMA:sacrificial initiator ratio, but also favored the formation of sufficient deactivator ($Cu(II)Br_2$/2bpy complex) at the beginning of polymerization.[48-50]

Table 3.1 Conversion and molecular weight in s-ATRP of OEGMA from PU/initiator surface with sacrificial initiator in solution.

Surface	Molar Ratio of OEGMA:EBIB	Conversion (%)	Theoretical Mn (g/mol)	Mn by GPC[b] (g/mol)	Mw/Mn
PU/poly(OEGMA)5	5	> 99[a]	1500	1900	1.16
PU/poly(OEGMA)10	10	> 99[a]	3000	2540	1.27
PU/poly(OEGMA)50	50	> 99[a]	15000	14700	1.13
PU/poly(OEGMA)100	100	> 99[a]	30000	28600	1.14
PU/poly(OEGMA)200	200	> 99[a]	60000	56900	1.31

[a] No residual monomer signal detected in ^{1}H NMR spectrum.

[b] PEO calibration standards were used.

3.3.2 Characterization of Poly(OEGMA)-grafted PU Surfaces

The advancing (θ_{Adv}) and receding (θ_{Rec}) water contact angles of the PU surfaces before and after modification give an indication of relative hydrophilicity. As shown in Figure 3.1, there was a large difference (>20°) between the advancing and receding angles of the original PU surface, as well as the PU/poly(OEGMA) surfaces. The original PU surface showed high water contact angles (both θ_{Adv} and θ_{Rec} >65°) and was the most hydrophobic of the surfaces examined. After oxygen plasma treatment, θ_{Adv} and θ_{Rec} decreased to ~25° and 9°, respectively, attributed to the hydrophilic groups (hydroxyl, peroxyl) introduced into the surface. For the PU/initiator surface containing bromine, θ_{Adv} and θ_{Rec} were ~68° and 39°, respectively, i.e. much higher than for the oxygen plasma treated surface, but lower than for the original PU surface. After ATRP grafting of OEGMA, the water contact angles decreased with increasing poly(OEGMA) chain length, presumably due to increasing coverage of the hydrophilic OEG moieties at higher chain length. The relatively low θ_{Adv} values for PU/poly(OEGMA)100 and 200 are presumably

due to high coverage of poly(OEGMA) and more effective masking of bromine by the grafted chains.

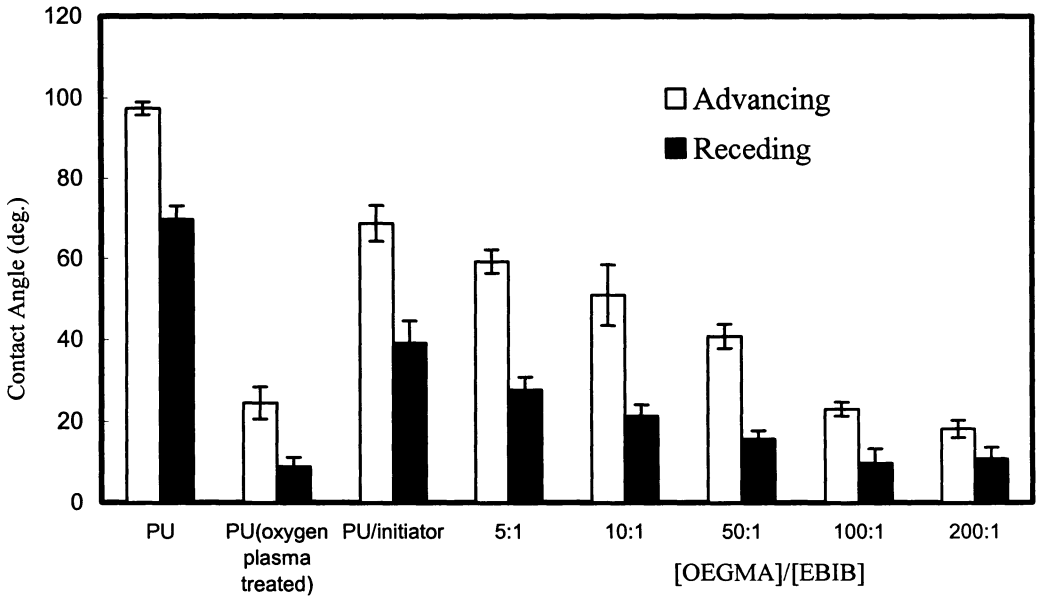

Figure 3.1 Advancing and receding water contact angles of the PU surfaces before and after modification. Error bars represent one standard deviation, n = 6.

Table 3.2 Surface roughness and surface area of the PU surfaces before and after modification obtained from AFM images.

	Samples				
	Unmodified PU	PU after O_2 Plasma	PU/Initiator	PU/Poly (OEGMA)50	PU/Poly (OEGMA)200
rms roughness (nm)	2.2	11.5	9.7	3.9	3.2
Surface area (μm^2)	1.0	1.1	1.1	1.0	1.0

The rms and surface area values were calculated from the AFM images of nominal area 1.0 μm^2.
Data are based on a single determination.

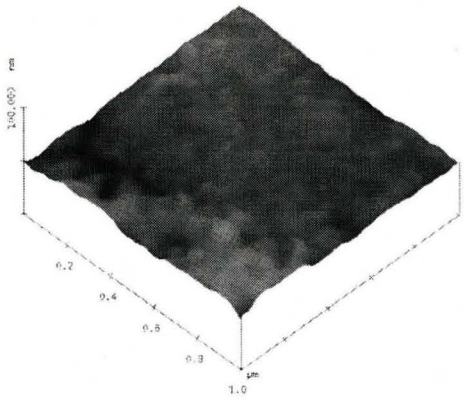

(a) Unmodified PU surface

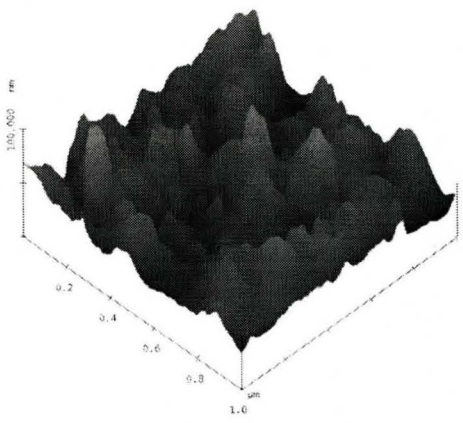

(b) PU surface after O_2 plasma treatment

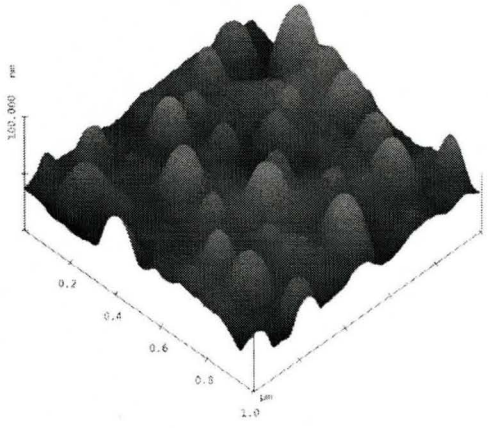

(c) PU/initiator surface

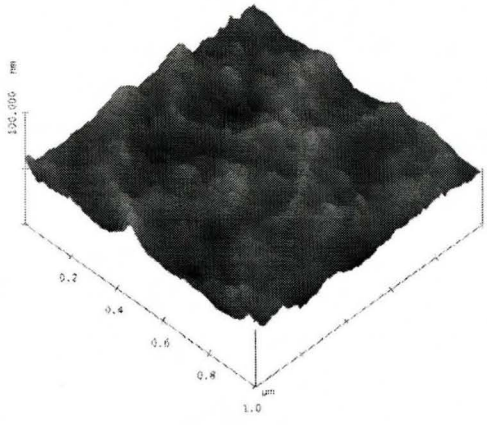

(d) PU/poly(OEGMA)50

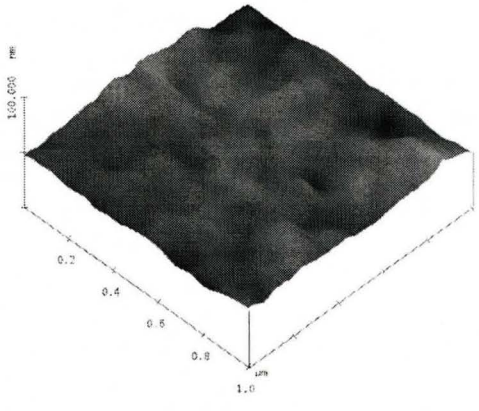

(e) PU/poly(OEGMA)200

Figure 3.2 AFM images of the PU surfaces before and after modification.

Figure 3.2 shows the morphologies of the dry PU surfaces before and after modification as measured by tapping mode AFM. The surface roughness and surface area data obtained from these images are summarized in Table 3.2. The unmodified PU surface was relatively smooth with root-mean-square (rms) roughness of 2.2 nm. The value for the oxygen plasma-treated PU surface was significantly higher at 11.5 nm, presumably due to bond-breaking and etching of the polymer surface by the plasma.[51] The formation of an initiator monolayer resulted in a smoother surface, possibly due to the fact that the polymer chains of low molecular weight formed on the PU surface upon oxygen plasma treatment were removed (toluene soluble) in the initiator immobilization step. The grafted initiator layer could also mask surface roughness. This effect was more significant for the OEGMA-grafted surfaces; for example the rms values for PU/poly(OEGMA)50 and PU/poly(OEGMA)200 were 3.9 and 3.2 nm, respectively, i.e. much lower than those for the plasma-treated PU surface. The surface area, calculated from the AFM images, showed the same trend as the surface roughness.

XPS data for the PU surfaces before and after modification are summarized in Tables 3.3 and 3.4. The PU consists of soft -$[(CH_2)_4$-O$]_n$- segments and hard urethane segments as shown in Figure 3.3. In the figure, the parameter x is the molar ratio of soft to hard segments. Based on the nitrogen content (2.9 atom percent) of the unmodified PU surface determined at 90° takeoff angle, the nx value should be about 10. However, the oxygen content was found to be close to that of the polyol moieties (20 atom%) possibly because the polyols are more hydrophobic than the urethanes and tend to dominate the air/polymer interface, especially under the vacuum condition of XPS operation.[52,53]

Table 3.3 Low-resolution XPS data for the PU surfaces before and after modification.

Surface	Takeoff angle 90°				Takeoff angle 20°			
	Elemental chemical composition (atom%)				Elemental chemical composition (atom%)			
	C	N	O	Br	C	N	O	Br
PU	76.5	2.9	20.6	0.0	77.7	2.2	20.2	0.0
PU/initiator	72.5	2.4	24.8	0.3	75.4	1.9	22.2	0.4
PU/poly(OEGMA)5	75.1	3.0	21.4	0.3	78.2	2.2	19.3	0.3
PU/poly(OEGMA)50	75.3	1.9	22.6	0.2	78.3	0.9	20.8	0.1
PU/poly(OEGMA)100	74.5	1.6	23.8	0.1	76.0	1.4	22.5	0.1
PU/poly(OEGMA)200	73.4	1.0	25.5	0.1	75.1	0.6	24.2	0.0
poly(OEGMA)[a]	68.3	0.0	31.7	0.0	68.3	0.0	31.7	0.0

[a] Theoretical composition.
Data precision ~ ±5% of the atom % values of each major peak.

Table 3.4 High-resolution C_{1s} XPS data for the PU surfaces before and after modification.

	Takeoff angle 90°			Takeoff angle 20°		
Binding energy:	285.0eV	286.5eV	288.9-289.5eV	285.0eV	286.5eV	288.9-289.5eV
C in functional groups	C-C/C-H (atom%)	C-O (atom%)	O-C=O (atom%)	C-C/C-H (atom%)	C-O (atom%)	O-C=O (atom%)
PU	58.2	36.1	5.7	59.5	35.1	5.3
PU-initiator	57.3	35.9	6.9	57.4	35.0	7.6
PU/poly(OEGMA)5	49.8	45.9	4.3	52.3	44.7	3.0
PU/poly(OEGMA)50	40.9	53.1	6.1	47.2	47.3	5.5
PU/poly(OEGMA)100	34.9	59.4	5.7	37.6	57.3	5.2
PU/poly(OEGMA)200	29.2	64.6	6.2	41.8	53.5	4.7
poly(OEGMA)[a]	21.4	71.4	7.2	21.4	71.4	7.2

[a] Theoretical composition.
Data precision ~ ±1%.

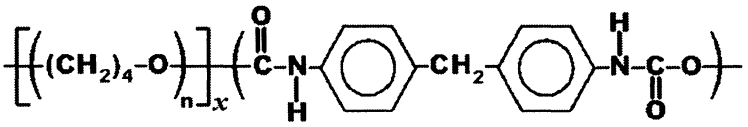

Figure 3.3 The structural unit of the PU studied in this work (Tecothane, TT-1095A). x is the molar ratio of soft to hard segments.

The Br contents of the PU/initiator and PU/poly(OEGMA) surfaces indicated, respectively, successful immobilization of the initiator moieties on the plasma-treated PU surface and the effectiveness of the initiator in s-ATRP. For the PU/poly(OEGMA) surfaces, the oxygen content increased with increasing poly(OEGMA) chain length; the nitrogen content was lower than that of the unmodified PU surface. These trends confirm the effectiveness of the grafting reactions.

As expected, the ether carbon (C–O) contents of the grafted surfaces (Table 3.4) were higher than that of the unmodified PU surface and increased with increasing poly(OEGMA) chain length. At a take off angle of 20°, the total carbon and aliphatic carbon (C–C) contents were higher, while the C–O and O–C=O contents as well as oxygen and bromine were lower than at 90°. These effects may be due to enrichment of the hydrophobic methacrylate groups and depletion of the hydrophilic groups in the outermost layer.

3.3.3 Protein Adsorption

Protein adsorption experiments were conducted to investigate the protein resistant properties of the PU/poly(OEGMA) surfaces. Fibrinogen a plasma protein which plays a key role in clot formation and platelet adhesion in thrombosis,[54,55] was used as a model protein. Adsorption experiments were conducted in both TBS and plasma. To investigate the effects of protein size and charge on adsorption behavior, experiments using binary solutions of fibrinogen and lysozyme were also carried out. Fibrinogen is a

large protein (340 kDa, 450×90×90 Å).[39] Its isoelectric point is 5.5 and thus it is negatively charged at physiologic pH. In contrast, Lys is a small protein (14.3 kDa, 45×30×30 Å) with an isoelectric point of 11.0,[39] and is positively charged at physiologic pH.

Fibrinogen adsorption from TBS

Figure 3.4 shows fibrinogen adsorption on the PU surfaces before and after modification. In Figure 3.4a, it is seen that the adsorbed amounts on the PU and PU/initiator surfaces increased rapidly with increasing fibrinogen concentration from 0.005 to 0.25 mg/ml and leveled off at higher concentrations. Adsorption on the PU/initiator surface was lower than on the unmodified PU surface, but the plateaus (~0.75 and 1.0 μg/cm^2, respectively) were in the range expected for close-packed monolayers.[56-58] The PU/poly(OEGMA) surfaces exemplified by PU/poly(OEGMA)5 in Figure 3.4a, adsorbed much less than the unmodified PU and PU/initiator surfaces and thus showed significant protein resistance.

Figure 3.4b shows the effects of graft chain length on fibrinogen adsorption. The adsorbed amounts decreased as the chain length increased at all protein concentrations. The decrease was not linear with chain length but was rapid over the shorter chain length range from 5 to 50 and slower over the longer chain length range. The lowest adsorbed amounts were seen on the PU/poly(OEGMA)200 surface. These amounts ranged from 3 ng/cm^2 at the lowest protein concentration to 33 ng/cm^2 at the highest (1.0 mg/ml), and are comparable to those seen on model silicon surfaces similarly modified by ATRP.[25,59] For example, Feng et al. reported very low fibrinogen adsorption levels of ~7 and 8 ng/cm^2 from a 1.0 mg/ml fibrinogen solution on silicon surfaces modified with poly(MPC) and poly(OEGMA) via s-ATRP.[25] It may be assumed given that the chain lengths are the same in both studies, that the chain densities are somewhat lower on the polyurethane surfaces than on the silicon.

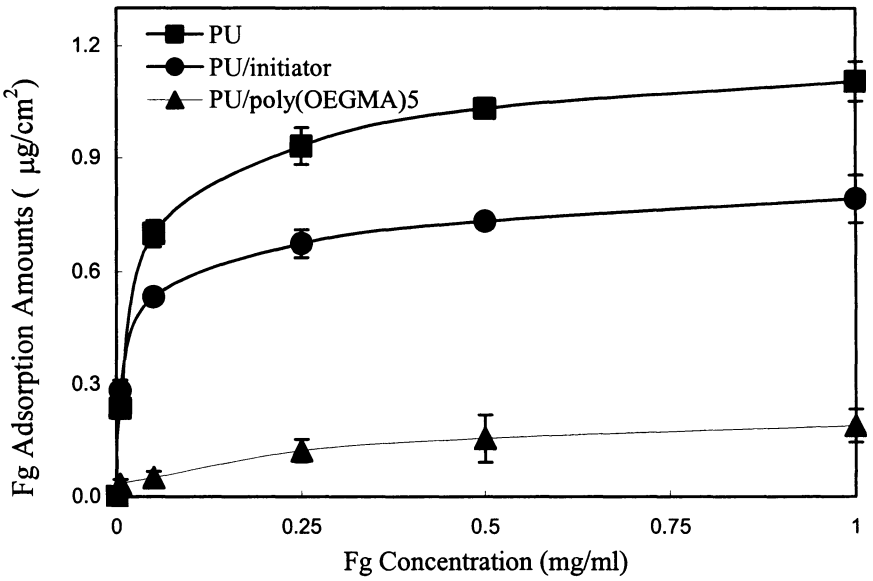

(a) Isotherms for PU control, PU/initiator, and PU/poly(OEGMA)5 surfaces. The curves are shown as a visual aid.

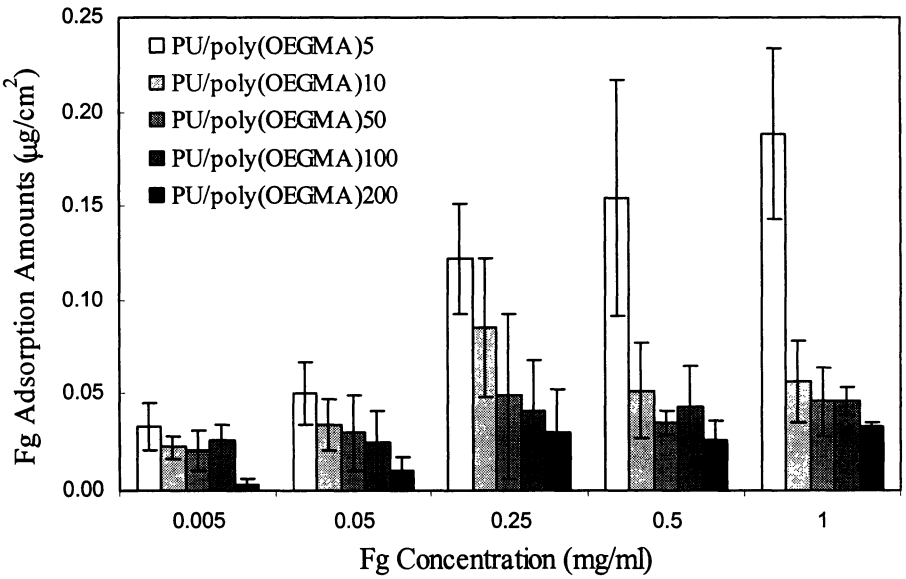

(b) Adsorption on poly(OEGMA)-grafted surfaces of varying graft length.

Figure 3.4 Fibrinogen adsorption from TBS, pH 7.4. Adsorption time 2h. Error bars represent one standard deviation, n = 6.

The clear effect of graft chain length on resistance to protein adsorption suggests that steric repulsion mechanisms may be involved. Steric repulsion is generally attributed to chain compression resulting in a repulsive interaction which increases with polymer chain length.[23,60] However, the main chains of the poly(OEGMA) grafts consist of C-C linkages, which, due to restricted rotation, give chains that are much less flexible and less compressible than the C-C-O chains of PEO. Thus steric repulsion mechanisms seem less likely for poly(OEGMA). Also the PEO side chains are all of the same length irrespective of the main chain length. It seems more likely that the water barrier mechanism[25,55,61,62] is in play. The effect of chain length may then be due to the increasing surface density of ethylene oxide residues resulting in increasing bound water content as chain length increases at constant chain density.

Fibrinogen adsorption from plasma

To assess the protein resistance of the surfaces under conditions more representative of a "real world" application, fibrinogen adsorption experiments from human plasma were also carried out (Figure 3.5). It is clear that the adsorbed amounts (highest value of 0.12 $\mu g/cm^2$ on the unmodified PU) are considerably lower than in buffer, presumably due to competition from the proteins and other components in plasma. It is also clear that the poly(OEGMA)-grafted surfaces adsorbed much less protein than the unmodified PU. Moreover, adsorption decreased with increasing graft chain length, as was observed for adsorption from buffer. In particular, adsorption to the PU/poly(OEGMA)200 surface was in the 1 to 5 ng/cm^2 range, i.e. below the value of 5 ng/cm^2 proposed by Horbett et al as the threshold for significant platelet adhesion and activation.[63]

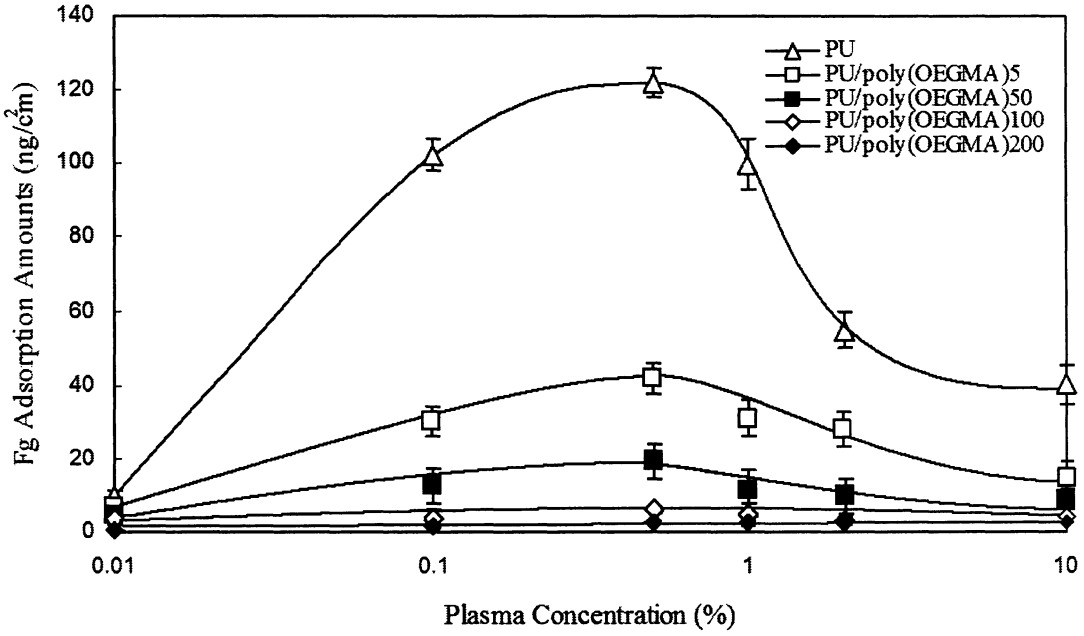

Figure 3.5 Fg adsorption from plasma on the PU surfaces before and after modification. The curves are shown only as a visual aid. Error bars represent one standard deviation, n = 6.

These plasma adsorption data show maxima at low plasma concentration, i.e. they exhibit a Vroman effect, indicating displacement of initially adsorbed fibrinogen by other proteins of higher binding affinity.[64-66] The Vroman peak was most pronounced for the unmodified PU; it was less evident for the grafted surfaces and diminished in intensity as the graft length increased. No Vroman effect was seen on the PU/poly(OEGMA)200 surface which had the longest grafts. This behavior is an additional manifestation of the protein resistance of the grafted surfaces and suggests that even at short blood contact times, where other surfaces may transiently adsorb high amounts of fibrinogen due to the Vroman Effect, these surfaces may be fibrinogen-free.

Adsorption from binary protein systems

It was of interest to investigate the protein resistance of these poly(OEGMA) grafted surfaces with respect to protein properties such as size and charge. To this end we studied adsorption from binary solutions of Lys and Fg. Solutions having Lys:Fg mol ratio 1:1 and 10:1 and total protein concentration (C_{total}) 0.05 and 1 mg/ml were used in these experiments. The composition of the adsorbed protein layers and the amount of each protein adsorbed are shown in Table 3.5 and Figure 3.6. Adsorption in the binary systems was similar to that in the single protein systems: the adsorbed amounts on the poly(OEGMA)-grafted surfaces at a given protein concentration were much lower than on the unmodified PU surface, and adsorption decreased with increasing graft chain length, particularly in the range of 5-50 monomer units.

Table 3.5 Adsorbed protein amounts (ng/cm2) from binary protein solutions with Lys:Fg molar ratios of 10:1 and 1:1.

	Binary Protein Adsorption Lys/Fg of 10:1 Molar Ratio in Solution				Binary Protein Adsorption Lys/Fg of 1:1 Molar Ratio in Solution				Single Protein Adsorption	
	0.05 mg/mL		1.0 mg/mL		0.05 mg/mL		1.0 mg/mL		Fg from TBS buffer	
	Lys	Fg	Lys	Fg	Lys	Fg	Lys	Fg	0.05 mg/mL	1.0 mg/mL
PU	93 ± 9	724 ± 41	206 ± 17	1040 ± 27	26 ± 2	810 ± 17	51 ± 5	1204 ± 54	701 ± 22	1105 ± 71
PU/initiator	116 ± 43	468 ± 66	168 ± 16	600 ± 62	27 ± 3	534 ± 38	53 ± 3	887 ± 63	534 ± 87	793 ± 63
PU/poly(OEGMA)5	16 ± 6	40 ± 22	106 ± 10	119 ± 22	2.5 ± 1.5	32 ± 9	10 ± 4	124 ± 29	50 ± 17	188 ± 45
PU/poly(OEGMA)10	14 ± 4	27 ± 7	54 ± 13	66 ± 38	2.2 ± 0.3	31 ± 6	9 ± 1	86 ± 13	34 ± 14	57 ± 21
PU/poly(OEGMA)50	8 ± 3	18 ± 4	48 ± 8	73 ± 32	0.9 ± 0.2	13 ± 4	7 ± 1	80 ± 21	30 ± 12	46 ± 18
PU/poly(OEGMA)100	7 ± 2	10 ± 7	44 ± 16	64 ± 20	0.8 ± 0.1	14 ± 1	7 ± 1	79 ± 19	25 ± 10	46 ± 7
PU/poly(OEGMA)200	6 ± 2	9 ± 1	39 ± 15	63 ± 35	1.2 ± 1.0	9 ± 5	6 ± 1	64 ± 19	10 ± 7	32 ± 2

Data are mean ± SD, n = 6.

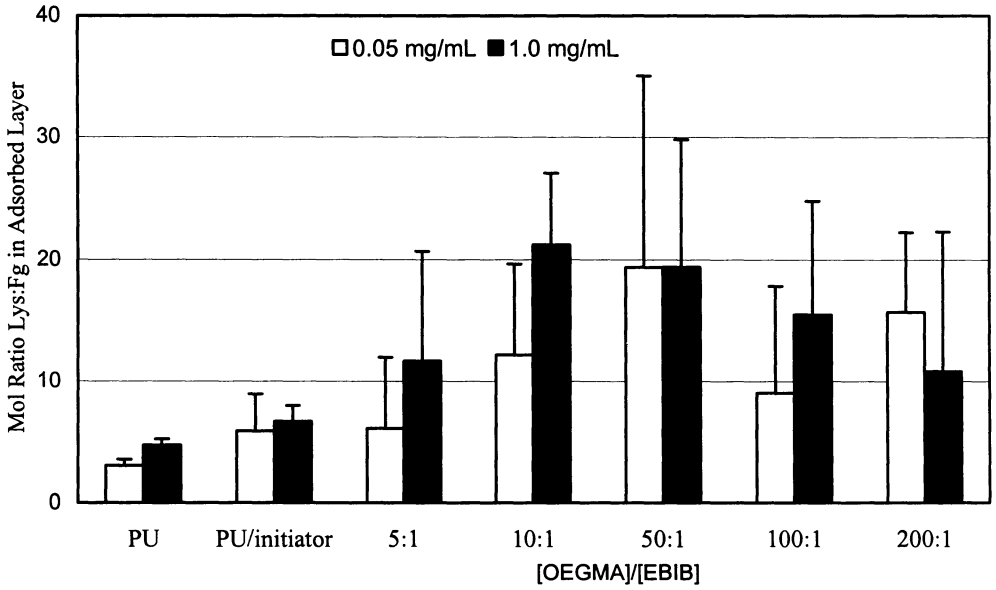

(a) Molar ratio Lys:Fg in solution = 10:1.

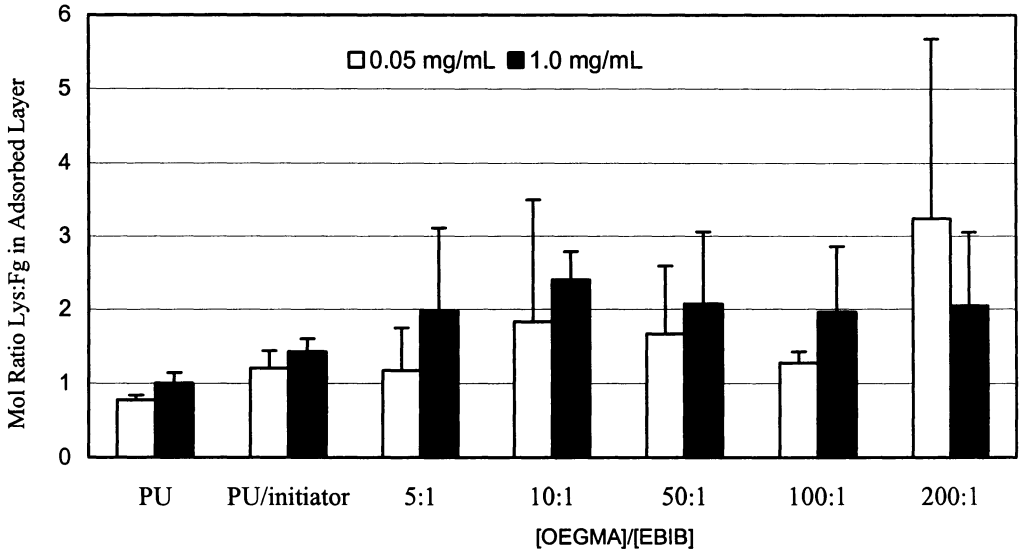

(b) Molar ratio Lys:Fg in solution = 1:1.

Figure 3.6 Fg and lys adsorption from binary protein solutions of 0.05 and 1.0 mg/ml total concentration. Error bars represent one standard deviation, n = 6.

In the binary protein experiments, as shown in Table 3.5, fibrinogen adsorption on the PU and PU/initiator surfaces was again in the range of close-packed monolayers (0.2 to 1.6 μg/cm^2) and comparable to that in the single protein experiments. By this measure the presence of Lys in the solution seemed to have no effect on Fg adsorption. Lys adsorption increased with increasing Lys concentration at a given molar ratio of the proteins. The highest Lys adsorption of 0.206 μg/cm^2 was seen on the unmodified PU surface at the higher Lys:Fg ratio and the higher C_{total}; this also is in the range of a close-packed Lys monolayer. The high adsorbed amounts of both Fg and Lys on the PU and PU/initiator surfaces suggests that mutilayers or compressed monolayers are formed on these hydrophobic surfaces.

For the PU and PU/initiator surfaces the molar ratios in the adsorbed protein layer were about 5:1 Lys:Fg at a 10:1 solution ratio (both total concentrations), reflecting enrichment of Fg on the surface and suggesting a higher affinity of fibrinogen for these hydrophobic surfaces. At a 1:1 molar ratio in solution the surface molar ratio was also in the vicinity of 1:1 (Figure 3.6b), indicating no preference for either protein under these conditions.

Adsorption on the poly(OEGMA)-grafted surfaces was significantly lower than on the PU and PU/initiator surfaces (Table 3.5). Similar to the latter surfaces, the absolute levels of fibrinogen adsorption on the grafted surfaces from the binary protein solutions were comparable to those from the single protein solutions at the same fibrinogen concentrations. The presence of lysozyme in solution did not have a great effect on fibrinogen adsorption to these surfaces.

For the PU/poly(OEGMA) surfaces at a 1:1 Lys:Fg ratio in solution, the ratio on the surface was generally greater than 1:1, suggesting that lysozyme was preferentially

adsorbed. The fact that lysozyme is smaller than fibrinogen thus indicates that the grafted surfaces are capable of discriminating among proteins based on size and that they resist bigger proteins more effectively than smaller ones. Since these PU surfaces have no permanent charge, it is reasonable to assume that the protein charge has little effect on protein adsorption; therefore the size effect seen here is consistent with the idea that steric exclusion mechanisms are at least partly responsible for the protein resistance of these surfaces. At a 10:1 Lys:Fg ratio in solution, the ratios on the grafted surfaces were higher than those on the PU and PU/initiator surfaces, again indicating preferential adsorption of Lys on these surfaces. For the PU/poly(OEGMA)10 and 50 surfaces, the ratios on the surface were ~20:1, i.e twice the solution ratio. This trend was also seen in the 1:1 solution (Figure 3.6b), where again the Lys:Fg ratios on the grafted surfaces were about twice that in the solution. The surface ratios decreased slightly with increasing graft length, but were always greater than in the solution. It appears that fibrinogen interactions with the underlying PU surface were inhibited by the poly(OEGMA) layer and that the PU/poly(OEGMA) surfaces, while they were strongly resistant to both proteins, were less resistant to the smaller protein.

Graft density may be an important factor for size-based preferential adsorption. In previous work with silicon/poly(OEGMA) grafted surfaces[25], surfaces of high graft density were found to resist both proteins (Fg and Lys) equally. For surfaces of low graft density, fibrinogen adsorbed preferentially to lysozyme, a result which was attributed to the higher affinity of fibrinogen for the substrate, not to size discrimination. In the present work, the preferential adsorption of Lys over Fg suggests that the grafted poly(OEGMA) layer at this particular graft density (the value of which is unknown) is discriminating on the basis of protein size. It seems likely that there is a graft density range where such preferentiality occurs and that at densities outside this range (both higher and lower values) there may be no differentiation between the proteins. Further work, including

variation and determination of the graft densities, would be required to establish this mechanism.

3.4 Conclusions

Polyurethanes were surface-modified by grafting poly(OEGMA) via s-ATRP. The ATRP initiator molecules were immobilized on the PU surfaces after oxygen plasma treatment. Two modes of initiation were involved: the normal mode through –OH groups and the reverse mode through –OOH groups on the PU surface. The molecular weight of the grafted polymer chains was regulated by adding free/sacrificial initiator to the reaction. The PU surfaces before and after each step of modification were characterized by water contact angle, AFM, and XPS measurements. These data indicated that high grafting densities and a range of graft lengths were achieved.

The surface-modified PU materials were evaluated for protein resistance in single and binary protein systems using Lys and Fg as model proteins. Fibrinogen adsorption from plasma was also studied. Fibrinogen adsorption on the poly(OEGMA)-grafted surfaces was significantly lower than on the unmodified PU surface, and adsorbed amounts decreased with increasing poly(OEGMA) graft length. In the plasma experiments the Vroman effect on the grafted surfaces was much less evident than on the unmodified PU surface and became weaker with increasing graft length. Adsorption levels on the most resistant surfaces were in the very low range of 1 to 5 ng/cm^2.

In experiments with mixed solutions of lysozyme and fibrinogen, the Lys:Fg ratios in the layers adsorbed to the PU/poly(OEGMA) surfaces were found to be higher than those in the solution, indicating that resistance to adsorption of the larger protein was greater than to the smaller one. Thus it appears that the mechanism of protein resistance of these surfaces is at least in part sterically based.

Acknowledgments: This work was supported by a Strategic Grant of the Natural Sciences and Engineering Research Council of Canada (NSERC). We also thank the Canada Foundation of Innovation (CFI) for supporting the research facilities in our laboratories.

3.5 References

1 Park J. B., Lakes R. S., Biomaterials: an Introduction. New York: Plenum, (1992).

2 Brash J. L., Wojciechowski P. W. (eds.), Interfacial Phenomena and Bioproducts. New York: Marcel Dekker, (1996).

3 Flemming R. G., Proctor R. A., Copper S. L., Bacterial adhesion to functionalized polyurethanes, J. Biomater. Sci. Polym. Ed., 10, 679 (1999).

4 Collier T. O., Jenney C. R., DeFife K. M., Anderson J. M., Protein adsorption on chemically modified surfaces, Biomed. Sci. Instrum., 33, 178 (1997).

5 Brash J. L., Exploiting the current paradigm of blood-material interactions for the rational design of blood-compatible materials, J. Biomater. Sci. Polym. Ed., 11, 1135 (2000).

6 Lee J. H., Ju Y. M., Kim D. M., Platelet adhesion onto segmented polyurethane film surfaces modified by addition and crosslinking of PEO-containing block copolymers, Biomaterials, 21, 683 (2000).

7 Ratner B. D., Castner D. G., Surface Modification of Polymeric Biomaterials. New York: Plenum, (1996).

8 Kingshott P., McArthur S., Thissen H., Castner D. G., Griesser H. J., Ultrasensitive probing of the protein resistance of PEG surfaces by secondary ion mass spectrometry, Biomaterials, 23, 4775 (2002).

9 Park H. D., Lee W. K., Ooya T., Park K. D., Kim Y. H., Yui N., In vitro biocompatibility assessment of sulfonated polyrotaxane-immobilized polyurethane surfaces, J. Biomed. Mater. Res., 66A, 596 (2003).

10 Cornelius R. M., Sanchez J., Olsson P., Brash J. L., Interactions of antithrombin

and proteins in the plasma contact activation system with immobilized functional heparin, J. Biomed. Mater. Res. A, 67, 475 (2003).

11 Bae J. S., Seo E. J., Kang I. K., Synthesis and characterization of heparinized polyurethanes using plasma glow discharge, Biomaterials, 20, 529 (1999).

12 Korematsu A., Takemoto Y., Nakaya T., Inoue H., Synthesis, characterization and platelet adhesion of segmented polyurethanes grafted phospholipid analogous vinyl monomer on surface, Biomaterials, 23, 263 (2002).

13 Logeart-Aviamoglou D., Jozefonvicz J., Carboxymethyl benzylamide sulfonate dextrans (CMDBS), a family of biospecific polymers endowed with numerous biological properties: a review, J. Biomed. Mater. Res., 48, 578 (1999).

14 Coleman D. L., Gregonis D. E., Andrade J. D., Blood-materials interactions: the minimum interfacial free energy and the optimum polar/apolar ratio hypotheses, J. Biomed. Mater. Res., 16, 381 (1982).

15 Knoll D., Hermans J., Polymer-protein interactions. Comparison of experiment and excluded volume theory, J. Chem. Phys., 258, 5710 (1983).

16 Han D. K., Park K. D., Ryu G. H., Kim U. Y., Min B. G., Kim Y. H., Plasma protein adsorption to sulfonated poly(ethylene oxide)-grafted polyurethane surface, J. Biomed. Mater. Res., 30, 23 (1996).

17 Archambault J. G., Brash J. L., Protein repellent polyurethane-urea surfaces by chemical grafting of hydroxyl-terminated poly(ethylene oxide): effects of protein size and charge, Coll. Surf. B, 33, 111 (2004).

18 Bearinger J. P., Terrettaz S., Michel R., Tirelli N., Vogel H., Textor M., Hubbell J. A., Chemisorbed poly(propylene sulphide)-based copolymers resist biomolecular interactions, Nat. Mater., 2, 259 (2003).

19 Liu V. A., Jastromb W. E., Bhatia S. N., Engineering protein and cell adhesivity using PEO-terminated triblock polymers, J. Biomed. Mater. Res., 60, 126 (2002).

20 Shen M. C., Wagner M. S., Castner D. G., Ratner B. D., Horbett T. A., Multivariate surface analysis characterization of plasma polymerized tetraglyme

surface chemistry for reduction of protein adsorption and monocyte adhesion, Langmuir, 19, 1692 (2003).

21 Lopez G. P., Ratner B. D., Tidwell C. D., Haycox C. L., Rapoza R. J., Horbett T. A., Glow discharge plasma deposition of tetraethylene glycol dimethyl ether for fouling-resistant biomaterial surfaces, J. Biomed. Mater. Res., 26, 415 (1992).

22 Szleifer I., Protein adsorption on surfaces with grafted polymers: a theoretical approach, Biophys. J., 72, 595 (1997).

23 Jeon S. I., Andrade J. D., Protein-surface interactions in the presence of polyethylene oxide II. effect of protein size. J. Coll. Interf. Sci., 142, 159 (1991).

24 Matyjaszewski K., Xia J. H., Atom transfer radical polymerization, Chem. Rev., 101, 2921 (2001).

25 Feng W., Zhu S. P., Ishihara K., Brash J. L., Protein resistant surfaces: comparison of ethyleneoxide and phosphorylcholine based materials, Biointerphases, 1, 50 (2006).

26 Chen R. X., Feng W., Zhu S. P., Botton G., Ong B., Wu Y. L., Surface-initiated ATRP grafting of poly(2,2,2-trifluoromethacrylate) from flat silicon wafer, J. Polym. Sci. Part A: Polym. Chem., 44, 1252 (2006).

27 Ma H. W., Wells M., Beebe Jr. T. P., Chilkoti A., Surface-initiated atom transfer radical polymerization of oligo(ethylene glycol) methyl methacrylate from a mixed self-assembled monolayer on gold, Adv. Funct. Mater., 16, 640 (2006).

28 Feng W., Brash J. L., Zhu S. P., Atom-transfer radical grafting polymerization of 2-methacryloyloxyethyl phosphorylcholine from silicon wafer surfaces, J. Polym. Sci. Part A: Polym. Chem., 42, 2931 (2004).

29 Yu W. H., Kang E. T., Neoh K. G., Controlled grafting of well-depoxide polymers on hydrogen-terminated silicon substrates by surface-initiated ATRP at ambient temperature, Langmuir, 20, 8294 (2004).

30 Tugulu S., Arnold A., Sielaff I., Johnsson K., Klok H. A., Protein functionalized polymer brushes, Biomacromolecules, 6, 1602 (2005).

31 Suzuki M., Kishida A., Iwata H., Ikada Y., Graft copolymerization of acrylamide onto a polysthylene surface prepared with glow discharge, Macromolecules, 19, 1804 (1986).

32 Siow K. S., Britcher L., Kumar S., Griesser H. J., Plasma methods for the generation of chemically reactive surfaces for biomolecule immobilization and cell colonization: A review, Plasma Process and Polym., 3, 392 (2006).

33 Chu P. K., Chen J. Y., Wang L. P., Huang N., Plasma-surface modification of biomaterials, Materials Science and Engineering R, 36, 143 (2002).

34 Xia J., Matyjaszewski K., Homogeneous reverse atom transfer radical polymerization of styrene initiated by peroxides, Macromolecules, 32, 5199 (1999).

35 Yamamoto K., Tanaka H., Sakaguchi M., Shimada S., Well-defined poly(methyl methacrylate) grafted to polyethylene with reversed atom transfer radical polymerization initiated by peroxides, Polymer, 44, 7661 (2003).

36 Min K., Li M., Matyjaszewski K., Preparation of gradient copolymers via ATRP using a simultaneous reverse and normal initiation process. I. spontaneous gradient, J. Polym. Sci. Part A: Polym. Chem. 43, 3616 (2005).

37 Li M., Jahed N. M., Min K., Matyjaszewski K., Preparation of linear and star-shaped block copolymers by ATRP using simultaneous reverse and normal initiation process in bulk and miniemulsion, Macromolecules, 37, 2434 (2004).

38 Gromada J., Matyjaszewski K., Simultaneous reverse and normal initiation in atom transfer radical polymerization, Macromolecules, 34, 7664 (2001).

39 Feng W., Zhu S. P., Ishihara K., Brash J. L., Adsorption of fibrinogen and lysozyme on silicon grafted with poly(2-methacryloyloxyethyl phosphorylcholine) via surface-initiated atom transfer radical polymerization, Langmuir, 21, 5980 (2005).

40 Regoeczi E., Iodine-Labeled Plasma Proteins, Boca Raton FL: CRC; P35-36, (1984).

41 McClung W. G., Clapper D. L., Anderson A. B., Babcock D. E., Brash J. L., Interactions of fibrinolytic system proteins with lysine-containing surfaces, J. Biomed. Mater. Res., 66A, 795 (2003).

42 Swaraj S., Oran U., Lippitz A., Friedrich J. F., Unger W. E. S., Surface analysis of plasma deposited polymer films, 6: analysis of plasma deposited allyl alcohol films before and after aging in air, Plasma Process Polym., 2, 572 (2005).

43 France R. M., Short R. D., Plasma treatment of polymers: effects of energy transfer from an argon plasma on the surface chemistry of PS, LDPE, PP and PET, J. Chem. Soc. Faraday Trans., 93, 3173 (1997).

44 Kang I. K., Kwon O. H., Lee Y. M., Sung Y. K., Preparation and surface characterization of functional group-grafted and heparinimmobilized polyurethanes by plasma glow discharge, Biomaterials, 17, 841 (1996).

45 Gugumus F., Mechanisms of photooxidation of polyolefins, Die Angewandte Makromolekulare Chemie, 176, 27 (1990).

46 Tsujii Y., Ohno K., Yamamoto S., Goto A., Fukuda T., Structure and properties of high-density polymer brushes prepared by surf ace-initiated living radical polymerization, Adv. Polym. Sci., 197, 1 (2006).

47 Feng W., Chen R. X., Brash J. L., Zhu S. P., Surface-initiated atom transfer radical polymerization of oligo(ethylene glycol) methacrylate: effect of solvent on graft density, Macromol. Rapid Commun., 26,1383 (2005).

48 Yamamoto K., Miwa Y., Tanaka H., Sakaguchi M., Shimada S., Living radical graft polymerization of methyl methacrylate to polyethylene film with typical and reverse atom transfer radical polymerization, J. Polym. Sci. Part A: Polym. Chem., 40, 3350 (2002).

49 Ejaz M., Yamamoto S., Ohno K., Tsujii Y., Fukuda T., Controlled graft polymerization of methyl methacrylate on silicon substrate by the combined use of the Langmuir-Blodgett and atom transfer radical polymerization techniques, Macromolecules, 31, 5934 (1998).

50 Feng W., Brash J. L., Zhu S. P., Non-biofouling materials prepared by atom transfer radical polymerization grafting of 2-methacryloloxyethyl phosphorylcholine: effect of graft density and chain length on protein repulsion, Biomaterials, 27, 847 (2006).

51 Vallon S., Drevillon B., Poncin-Epaillard F., In situ spectroellipsometry study of the crosslinking of polypropylene by an argon plasma, Appl. Surf. Sci., 108, 177 (1997).

52 Gray J. E., Norton P. R., Griffiths K., Mechanism of adhesion of electroless-deposited silver on poly(ether urethane), Thin Solid Films, 484, 196 (2005).

53 Chen J. H., Wei J., Chang C. Y., Laiw R. F., Lee Y. D., Studies on segmented polyetherurethane for biomedical application: effects of composition and hard-segment content on biocompatibility, J. Biomed. Mater. Res., 41, 633 (1998).

54 Herde K., Haupt H., Schwick H. G., Plasma protein fractionation, In: The Plasma Proteins, second edition. New York: Academic Press; P545-597 (1977).

55 Unsworth L. D., Sheardown H., Brash J. L., Protein resistance of surfaces prepared by sorption of end-thiolated poly(ethylene glycol) to gold: effect of surface chain density, Langmuir, 21,1036 (2005).

56 Shiba E., Lindon J. N., Kushner L., Matsueda G. R., Hawiger J., Kloczewiak M., Kudryk B., Salzman E. W., Antibody-detectable changes in fibrinogen adsorption affecting platelet activation on polymer surfaces, Am. J. Physiol. Cell. Physiol., 260, C965 (1991).

57 Feng L., Andrade J. D., Protein adsorption on low temperature isotropic carbon: III: isotherms, competitivity, desorption and exchange of human albumin and fibrinogen, Biomaterials, 15, 323 (1994).

58 Tegoulia V. A., Cooper S. L., Leukocyte adhesion on model surfaces under flow: Effects of surface chemistry, protein adsorption, and shear rate, J. Biomed. Mater. Res., 50, 291 (2000).

59 Ma H. W., Li D. J., Sheng X., Zhao B., Chilkoti A., Protein-resistant polymer

coatings on silicon oxide by surface-initiated atom Ttransfer radical polymerization, Langmuir, 22, 3751 (2006).

60 Jeon S. I., Lee J. H., Andrade J. D., De Gennes P. G., Protein-surface interactions in the presence of polyethylene oxide I: simplified theory, J. Coll. Interf. Sci., 142, 149 (1991).

61 Jon S., Seong J., Khademhosseini A., Tran T-NT., Laibinis P. E., Langer R., Construction of nonbiofouling surfaces by polymeric self-assembled monolayers, Langmuir, 19, 9989 (2003).

62 Li L., Chen S., Zheng J., Ratner B. D., Jiang S., Protein adsorption on oligo(ethylene glycol)-terminaled alkanethiolate selfassembled monolayers: the molecular basis for nonfouling behavior, J. Phys. Chem. B, 109, 2934 (2005).

63 Tsai W. B., Grunkemeier J. M., McFarland C. D., Horbett T. A., Platelet adhesion to polystyrene-based surfaces preadsorbed with plasmas selectively depleted in fibrinogen, fibronectin, vitronectin, or von Willebrand's factor, J. Biomed. Mater. Res., 60, 348 (2002).

64 Vroman L., Adams A. L., Identification of rapid changes at plasma-solid interfaces, J. Biomed. Mater. Res., 3, 43 (1969).

65 Horbett T. A., Mass action effects on competitive adsorption of fibrinogen from hemoglobin solutions and from plasma, Thromb. Haemostas., 51, 174 (1984).

66 Brash J. L., ten Hove P., Effect of plasma dilution on adsorption of fibrinogen to solid surfaces, Thromb. Haemostas., 51, 326 (1984).

CHAPTER 4 Protein-resistant Polyurethane via Surface-initiated ATRP: Effects of Main Chain and Side Chain Lengths of Grafts

This chapter is a reproduction of the following published article in Colloids and Surfaces B: Biointerfaces.

Authors: **Z. Jin,** W. Feng, K. Beisser, S. Zhu, H. Sheardown, and J.L. Brash

Publication Information: Colloids and Surfaces B: Biointerfaces. **2009**, 70, 53-59.

Accepted Date: Dec 03, 2008

Working Hypothesis:

The higher the surface coverage of water soluble polymers, the greater the protein resistance.

Protein-resistant Polyurethane via Surface-initiated ATRP: Effects of Main Chain and Side Chain Lengths of Grafts

Abstract: Water-soluble poly(oligo(ethylene glycol) methacrylate) (poly(OEGMA)) with various main chain and side chain lengths were grafted to polyurethane (PU) surface by surface-initiated atom transfer radical graft polymerization (s-ATRgP). The polymer main chain length was varied by varying the molar ratio of monomer to free initiator in solution (typically 5:1, 50:1, 100:1). Three different side chain lengths were obtained using different OEGMA monomers (MW 300, 475, 1100 g/mol). Water contact angle and x-ray photoelectron spectroscopy (XPS) were used to characterize the modified PU surfaces. The respective effects of poly(OEGMA) main chain and side chain lengths on fibrinogen (Fg) and lysozyme (Lys) adsorption were investigated in single protein systems at room temperature in TBS, pH 7.4. The poly(OEGMA)-grafted PU surfaces were found to be highly protein-resistant, with reductions of Fg and Lys adsorption in the range of 84-98% and 67-91%, respectively, compared to the unmodified PU surface. The adsorption of both proteins decreased with increasing poly(OEGMA) main chain length for a given side chain length (number of EO units). For a given main chain length, the Fg adsorption level did not change significantly with increasing side chain length. However, Lys adsorption increased with increasing side chain length, possibly due to decreasing graft density as monomer size and footprint on the surface increase. Adsorption resistance was generally greater for the bigger protein.

Keywords: polyurethane; surface modification; atom transfer radical polymerization (ATRP); protein adsorption; poly(ethylene glycol).

4.1 Introduction

Protein adsorption to biomaterial surfaces is problematic in many applications such as implants and biosensors.[1-4] It is generally believed that the ensuing adverse effects initiated by adsorbed proteins, such as general biofouling, blood coagulation, and the immune response, are responsible for most implant failures. Polyurethanes are widely used as biomaterials due to their superior physical and mechanical properties.[5] However their use in blood contacting applications is limited by their relatively poor blood compatibility resulting from protein adsorption on the hydrophobic PU surface.

Modification with various water-soluble small molecules or polymers has been proposed as a means of increasing surface hydrophilicity and thus, it is believed, inhibiting protein adsorption.[6-10] Poly(ethylene oxide) (PEO) and PEO-containing polymers have attracted much attention and have been shown to be among the most effective polymers in this regard.[11-13] The protein resistance of PEO is believed to be due to its general chemical inertness, lack of charge, water solubility, chain flexibility and large excluded volume.[14-18] A tightly bound water layer is believed to form a "barrier" around the PEO chains thus preventing the close approach of protein molecules: this constitutes the so-called "water barrier" hypothesis.[19] Steric repulsion[20] has also been invoked to explain the protein resistance of PEO: according to this theory, compression of the flexible PEO chains (configurational entropy loss) generates a repulsive interaction with an approaching protein. The "water barrier" and "steric repulsion" associated with polymer chains are expected to vary with their physical and chemical structure.[21]

Graft density (number of chains per unit area) and chain length are important factors for the protein resistance of PEO-grafted surfaces. The average distance between grafting sites (L) along with the Flory radius (R_F) of the polymer determines the conformation of the grafted polymer chains. It is generally accepted that the so-called mushroom regime, in which the grafts are present as unperturbed random coils, occurs

when $L/2R_F > 1$. By increasing graft density to reduce L and/or by increasing chain length to increase R_F, the chain conformation may go through the sequence mushroom to extended mushroom (slightly perturbed coils) to partially stretched to fully stretched ($L/2R_F < 1$, brush regime). However, details of the effects of conformation, graft density and chain length on protein resistance are still a matter of debate. The lack of techniques for control and accurate measurement of these properties is a significant barrier to their elucidation in relation to protein resistance.

Several approaches have been developed for the preparation of PEO-modified surfaces, including surface coating,[22] physical adsorption of PEO-containing block copolymers,[23] blending of PEO-containing block copolymers into the bulk material,[24] surface tethering ("grafting to" method)[25] and graft polymerization ("grafting from" method)[10]. Among these approaches, surface-initiated atom transfer radical polymerization (s-ATRP) has many advantages including versatility of monomer type, tolerance of impurities, and mild reaction conditions. In addition, uniform and tuneable graft chain length and relatively high graft density are achievable using s-ATRP.[26,27] The conformation of polymer chains grafted via s-ATRP can be fine-tuned by adjusting the graft density and chain length of the grafts, resulting in variation of the protein-resistant properties of modified surfaces. Recently, s-ATRP of PEO-containing molecules (such as oligo(ethylene glycol) methacrylate (OEGMA)) has been performed on model substrates such as silicon, gold, and other metals.[28,29] However, there is very little work on PEO-modified polymeric biomaterial surfaces prepared via s-ATRP.

In previous work[30] we developed a three-step method (oxygen plasma treatment; ATRP-initiator immobilization; s-ATRP) to graft poly(OEGMA) from PU surfaces. A set of poly(OEGMA)-grafted PU surfaces (referred to as PU/poly(OEGMA)) of varying main chain length were prepared and their protein-resistance investigated. In the present work, we investigated the effect of oligoethylene oxide side chain length using three OEGMA monomers of MW 300, 475, 1100 g/mol (~ 5, 9 and 23 ethylene oxide

residues respectively). Protein adsorption was measured in single protein experiments with two proteins (fibrinogen (Fg) and lysozyme (Lys)) differing significantly in size and charge characteristics.

4.2 Experimental

4.2.1 Materials

2-Bromoisobutyryl bromide (BIBB) (98%), ethyl 2-bromoisobutyrate (EBIB) (98%), 2,2'-bipyridyl (bpy) (99%), and Cu(I)Br (99.999%) were purchased from Sigma-Aldrich and used as received. Pyridine (99.9%, Fisher Scientific), N,N-dimethylformamide (DMF) (99.8%, EMD Chemicals) and methanol (HPLC grade, Caledon Laboratories) were also used as received. Toluene (reagent grade, Caledon Laboratories) was double-distilled over CaH_2 before use. OEGMA with molecular weights (MW) of 300, 475 and 1100, were purchased from Sigma-Aldrich and passed over a basic alumina column to remove inhibitor. Basic alumina (Brockman Activity 1, mesh 60-325) was purchased from Fisher Scientific and used as received. Polyurethane (PU) (Tecothane TT-1095A) was obtained from Thermedics and purified by Soxhlet extraction with toluene for 24 h. The freshly extracted PU was dried under vacuum at 65°C. Nitrogen gas used in this study was of ultrahigh-purity (UHP) grade.

Fibrinogen (Fg) (340 kDa, from plasminogen depleted human plasma) was purchased from Enzyme Research Laboratories and dialyzed against isotonic Tris buffer (pH 7.4), aliquoted, and stored at -70°C. Lysozyme (Lys) (14.3 kDa, from chicken egg white) was purchased from Sigma-Aldrich and used as received. Deionized water with a resistivity of 18.2 MΩ·cm was prepared using a Millipore water purification system.

4.2.2 Preparation of PU Surface

PU/DMF solution, concentration 7% (w/v), was prepared at 65°C, cast on a glass Petri dish and dried in an oven at 55°C for 4 days. The PU film was peeled from the Petri dish and further dried in a vacuum oven at 80°C for 1 day. PU disks of ~0.5 mm

thickness and 6 mm diameter were then cut from the dried PU film and extracted by Soxhlet extraction in toluene for 24 h. The freshly extracted PU disks were dried under vacuum at 65°C for 2 days and stored under vacuum.

4.2.3 Preparation of Poly(OEGMA)-grafted PU

The poly(OEGMA)-grafted PU surfaces of variable polymer main chain and PEO side chain lengths were prepared via ATRP in three steps.[30]

Step 1. Surface treatment of PU with oxygen plasma: Extracted and dried PU disks were treated in an oxygen plasma to introduce reactive sites (-O$^{\bullet}$ and -OO$^{\bullet}$) into the surface (Micro-RIE Series 800, Technics, USA).[31] Constant glow-discharge power of 100 W at a pressure of 200 mTorr was applied for a chosen time period. The PU surface was then exposed to air for 5 min giving a surface containing –OH and/or –OOH groups.

Step 2. Formation of initiator monolayer on PU surface: The freshly oxygen-plasma-treated PU disks (~40) were immersed in dry toluene (80 ml) in a round-bottomed flask. The PU-toluene mixture was stirred and de-aerated in a stream of nitrogen for 30 min and cooled to -15°C with a NaCl-ice bath. Pyridine (52 mmol, 4.2 ml) was first added via a nitrogen-purged syringe. 2-Bromoisobutyryl bromide (BIBB, 44 mmol, 5.44 ml) dissolved in 20 ml of toluene was added dropwise to the well-stirred mixture over a period of 1 h. The reaction was stirred at 0°C overnight and then at room temperature (23°C) for 3 h. The entire process of initiator immobilization was conducted under nitrogen. After the reaction, the ATRP initiator-immobilized PU disks (referred to as PU/initiator) were removed from the reaction mixture, cleaned ultrasonically for 5 min toluene, and rinsed several times with toluene and methanol. Finally the PU/initiator disks were dried in vacuum at 40°C for 1 day.

Step 3. s-ATRP of OEGMA on PU/initiator surfaces: In a typical ATRP grafting experiment, Cu(I)Br (0.1 mmol, 14.3 mg) and 2,2'-bipyridyl (bpy, 0.2 mmol, 31.8 mg) were placed in a pear-shaped flask and closed with a septum-inlet adapter (with stopcock).

The flask was de-aerated by three evacuation-backfilling cycles with nitrogen. A predetermined amount of OEGMA was dissolved in methanol, de-aerated with nitrogen for 30 min, and added to the pear-shaped flask via syringe. De-aerated methanol (bubbled with nitrogen for 30 min) was added to maintain the OEGMA concentration, which was fixed at 38% (w/v) for OEGMA of MW300 and 20% (w/v) for OEGMA of MW 475 and 1100 in separate experiments. The dark brown liquid mixture was degassed for another 10 min and transferred to a nitrogen-filled glove box. De-aerated ethyl 2-bromoisobutyrate (EBIB) initiator (0.1 mmol, 14.7 μl) was then added and the mixture was stirred vigorously for 1 min; it was then transferred to vials containing the PU/initiator disks. The graft polymerization was carried out at room temperature in the glove box for 36 h to assure complete monomer conversion. After reaction, the poly(OEGMA)-grafted PU disks were removed from the glove box, rinsed with methanol, ultrasonically cleaned in methanol for 2 min to remove physically adsorbed poly(OEGMA). The disks were then extracted (Soxhlet) with ethanol for 24 h to remove potential impurities such as catalyst complex, pyridine or BIBB. The freshly extracted PU/poly(OEGMA) disks were dried in vacuum at 65°C for 2 days.

Three different molar ratios of OEGMA:EBIB, 5:1, 50:1 and 100:1, were used to prepare PU/poly(OEGMA) of different main chain lengths. The PEG side chain length was varied by varying the OEGMA monomer MW. For OEGMA of MW 300, 475 and 1100, the corresponding PEG side chain has MW 200, 375 and 1000, respectively; the ratio of the side chain lengths (EO units) is approximately 1:2:5.

4.2.4 Graft and Surface Characterization

The OEGMA conversion in solution was determined from proton NMR spectra (Bruker AC-P200 spectrometer, D_2O solvent). The MW and polydispersity (PDI) of poly(OEGMA) produced by EBIB in solution were determined by aqueous gel permeation chromatography (GPC, Waters 2690 separations module with a Waters 2410 refractive index detector, PEO calibration standards). Static water contact angles of

unmodified and modified PU surfaces were determined using a Rame-Hart NRL goniometer (Mountain Lakes, NJ) at room temperature (sessile drop method). The surface composition of the PU disks was investigated using a Leybold Max 200 XPS with an aluminum anode non-monochromatic source. Survey spectra combined with low-resolution spectra recorded at a takeoff angle of 90° provided concentrations of the elements in the uppermost surface to a depth of ~10 nm.

4.2.5 Protein Adsorption

The adsorption of fibrinogen and lysozyme was studied by the radiolabeling method as described previously.[32] Proteins were dissolved in isotonic Tris buffered saline (TBS) (pH 7.4) and labeled with ^{125}I using the iodine monochloride (ICl) method.[33] The unbound radioiodide was removed by ion exchange chromatography on AG-1-X4 resin (Bio-Rad Laboratories) and was typically less than 1.0% for Fg, 3.0% for Lys as determined by trichloroacetic acid precipitation.[33,34] Single protein solutions for adsorption measurements were prepared by mixing radiolabeled and unlabeled protein in a 1:9 ratio. Five protein concentrations ranging from 0.005 to 1.0 mg/ml were used; these were determined by spectrophotometry at 280 nm.

Unmodified and modified PU disks were first immersed in TBS at room temperature (22°C) overnight to achieve complete hydration and then transferred to the protein solution. Adsorption was allowed to proceed under static conditions at room temperature for 2h. The disks were then immersed in fresh protein-free TBS for 5 min (three cycles) to remove solution and loosely adsorbed protein. The final samples were placed in counting vials and their radioactivity was determined (Wizard 3" 1480 automatic gamma counter, Perkin-Elmer Life Sciences). Four replicate samples were measured for each concentration in a given experiment. Experiments were done at least twice.

4.3 Results

4.3.1 Preparation of PU/poly(OEGMA) Surfaces

In the first step of the PU surface modification process, oxygen plasma treatment was carried out to introduce oxygen functional groups into the surface, resulting in a reactive and hydrophilic surface. Since the high power and long duration of plasma treatment may cause surface etching and increasing surface roughness,[31] optimal plasma exposure time and plasma power are required to maintain a smooth surface with a high concentration of reactive functional groups.

In this study, exposure time to the oxygen plasma was varied from a few seconds to several minutes at 100 W power and 200 mTorr pressure. The water contact angles of the surfaces were determined after plasma treatment (Figure 4.1). The unmodified PU surface showed an advancing angle of ~90°. After exposure to the oxygen plasma for 5 sec, the angle decreased to ~44° Additional smaller decreases were seen with increasing plasma treatment time from 5 sec to 5 min; an increasing concentration of oxygen-containing functional groups is presumably responsible for these decreases. For a plasma treatment time of 10 min the water contact angle was slightly higher than at 5 min, possibly due to increased roughness. It was observed in our previous work that the roughness of the PU surface increased significantly with increasing plasma treatment time.[30] Similar variations in water contact angle and roughness with plasma treatment time have been observed by others.[35] For PU surfaces under the plasma conditions used here, the lowest water contact angle of ~7° was achieved for a plasma treatment time of 5 min, indicating that these conditions give the maximum concentration of oxygen-containing functional groups in the polymer surface. Therefore in all subsequent work the oxygen plasma treatment time was fixed at 5 min.

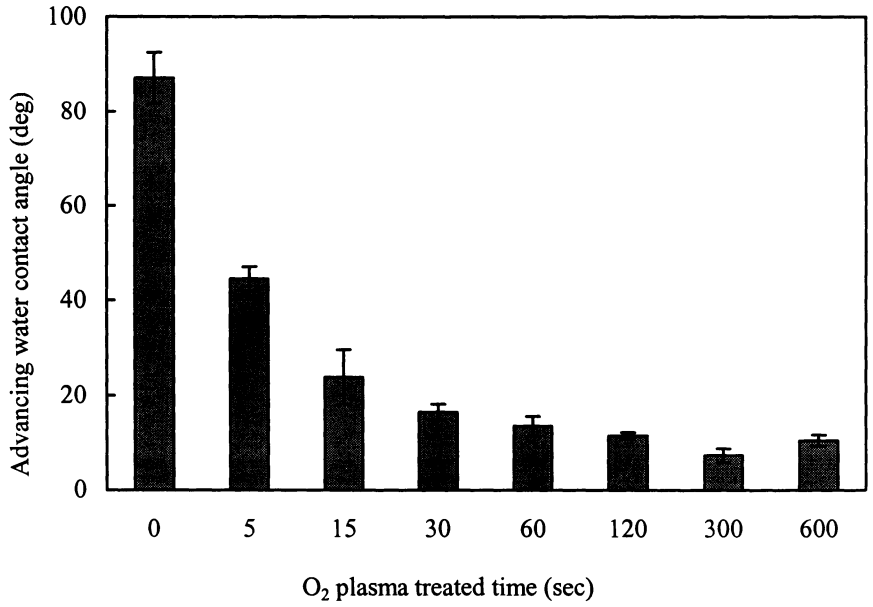

Figure 4.1 Water contact angles (advancing) of PU surfaces with various plasma treatment times. Error bars represent standard deviation, n = 6.

Table 4.1 Conversion and molecular weight in s-ATRP of OEGMA from PU/EBIB surfaces with sacrificial initiator in solution.

Surface	OEGMA MW	Molar Ratio of OEGMA:EBIB	Conversion (%)	Theoretical Mn (g/mol)	Mn by GPC (g/mol)	Mw/Mn
PU-300-5[b]	300	5	> 99[a]	1700	1900	1.16
PU-300-50[b]	300	50	> 99[a]	15200	14700	1.13
PU-300-100[b]	300	100	> 99[a]	30200	28600	1.14
PU-475-5	475	5	> 99[a]	2600	2800	1.18
PU-475-50	475	50	> 99[a]	23900	19400	1.27
PU-475-100	475	100	> 99[a]	47700	45300	1.20
PU-1100-5	1100	5	> 99[a]	5700	5300	1.17
PU-1100-50	1100	50	> 99[a]	55200	49900	1.20
PU-1100-100	1100	100	87	95900	79600	1.28

[a] No residual monomer signal detected in ^{1}H NMR spectrum.

[b] See Ref. [30].

After oxygen plasma treatment and immobilization of ATRP initiator on the PU surface, ATRP grafting of OEGMA was carried out; ATRP in solution occurred simultaneously due to the presence of free ("sacrificial") initiator. For a well-controlled ATRP process, the polymer chains formed by the free initiator in solution may be assumed to have the same properties (average molecular weight and polydispersity) as the chains grafted on the surface.[36] The polymer main chain length was varied by varying the molar ratio of monomer (OEGMA) to free initiator (EBIB). Three OEGMA:EBIB ratios, 5:1, 50:1 and 100:1, were used to prepare PU/poly(OEGMA) surfaces with different main chain length (assumed to be 5, 50 and 100 monomer units, respectively, for complete conversion). Table 4.1 shows the polymerization data, including monomer conversion as determined by ^{1}H NMR spectrometry, molecular weight and polydispersity of polymer formed in solution as determined by GPC.[30] The polymers are named by the monomer MW (first number) and the degree of polymerization (DP) or polymer main chain length (second number): thus for PU-300-5, the monomer MW is 300 and the main chain length is 5. Complete conversion was achieved after 36 h for all surfaces except PU-1100-100 where the conversion was limited to 87%. Polydisperisities were in the range of 1.10 to 1.30, indicating good control of the ATRP process. In the initial stages of polymerization, EBIB reacts with Cu(I) complex (ATRP activator) to provide sufficient Cu(II)-based deactivator for well-controlled ATRP. The residual peroxide groups on the surface introduced during oxygen plasma treatment may play a similar role as initiator, reacting with Cu(I) complex to form Cu(II) complex and radicals. The difference between the activation rate of peroxides and ATRP-initiator on the surface may increase the polydispersity slightly. However, compared to the initiator, the peroxide concentration was probably very small and thus would be expected to have little effect on the targeted main chain length. The deviation of Mn as measured by GPC from the targeted Mn may be attributed partly to the different conformations and coil sizes of the experimental polymers and the PEO standards.[37] For PU-1100-100, based on the OEGMA monomer of highest MW and largest target DP of 100, the effects of electron transfer reactions and

steric hindrance (large PEG side chains) on the functionality of bromine chain ends may become significant at high conversion (low monomer concentration). The lost initiator functionality may be the major reason for the incomplete conversion (87%).[38]

4.3.2 Characterization of PU/poly(OEGMA) Surfaces

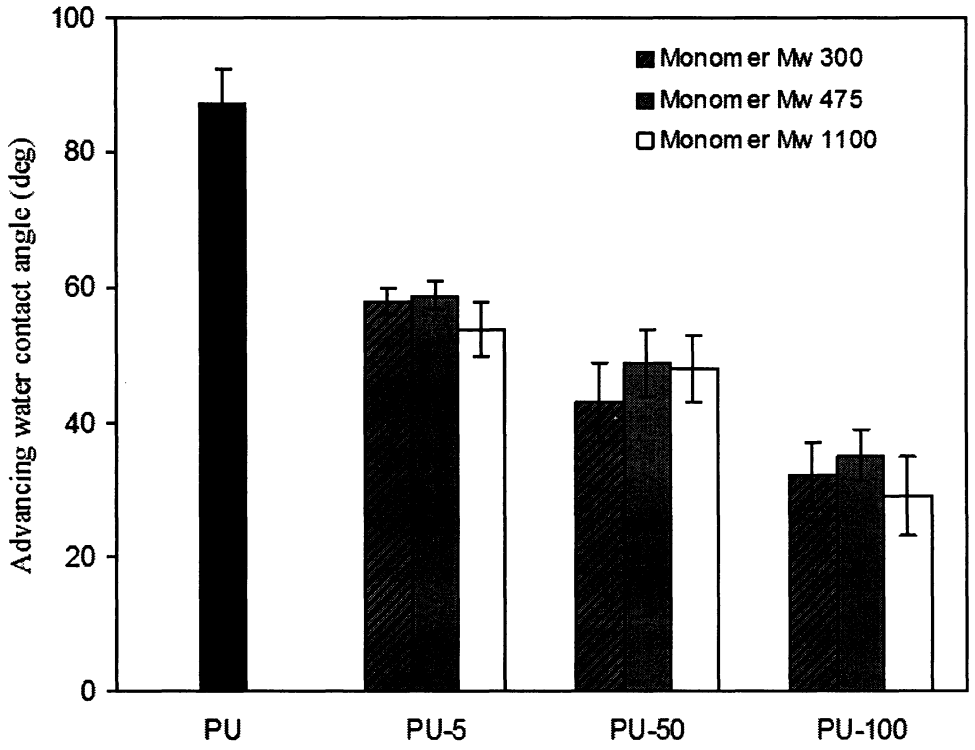

Figure 4.2 Water contact angles (advancing) of PU surfaces before and after surface modification. Error bars represent standard deviation, n = 6.

Figure 4.2 shows advancing water contact angles (θ_{Adv}) for the various experimental surfaces that were used for protein adsorption experiments. The contact angles decreased significantly after poly(OEGMA) grafting. A θ_{Adv} of ~60° was observed for the shortest graft main chain (5 monomer units) and ~30° for the longest (100 monomer units). The observation of increasing hydrophilicity with increasing graft length (at constant chain density) is presumably due to increasing coverage of hydrophilic

ethylene oxide residues. For a given main chain length, the water contact angles were independent of PEO side chain length, suggesting similar surface coverage of ethylene oxide residues (perhaps saturation coverage) despite varying side chain length. The receding water contact angles (θ_{Rec}, not shown) were found to be 12 to 20° lower than the corresponding advancing angles. These differences suggest significant chemical heterogeneity and/or roughness in these surfaces.

Table 4.2 Elemental composition of the unmodified and modified PU surfaces from XPS at 90° takeoff angle.

	Elemental Composition (atom%)			
Surfaces	C	N	O	Br
PU	73.9	3.1	23.0	0.0
PU/initiator	73.9	3.1	22.5	0.5
PU-300-5[b]	75.1	3.0	21.4	0.3
PU-300-50[b]	75.3	1.9	22.6	0.2
PU-300-100[b]	74.5	1.6	23.8	0.1
PU-475-5	71.9	3.1	24.5	0.5
PU-475-50	71.1	2.3	26.2	0.4
PU-475-100	72.7	0.0	27.2	0.1
PU-1100-5	73.7	2.5	23.3	0.4
PU-1100-50	74.0	1.7	24.0	0.3
PU-1100-100	73.8	1.3	24.6	0.2
poly(OEGMA)300[a]	68.3	0	31.7	0
poly(OEGMA)475[a]	67.7	0	32.3	0
poly(OEGMA)1100[a]	67.1	0	32.9	0

[a] Theoretical composition.

[b] See Ref. [30].

Data precision ±5%.

The elemental composition of the unmodified and modified PU surfaces was determined by XPS (Table 4.2). Whereas no bromine was detected in the unmodified PU

surface, a clear bromine signal, corresponding to an atomic concentration of 0.5%, was detected in the PU/initiator surface. For a given side chain length, the bromine content, as well as that of nitrogen (originating only from the PU), decreased slightly with increasing poly(OEGMA) main chain length. The higher coverage of the longer poly(OEGMA) may effectively "hide" the nitrogen and bromine The oxygen concentration increased with increasing main chain length for a given side chain length, suggesting increasing coverage of ethylene oxide residues.

For a given main chain length, the oxygen concentration increased in the sequence PU-300 < PU-1100 < PU-475. The oxygen content for the longest side chain length (1100) was thus lower than that for the side chain of medium length (475), even though the oxygen content for a polymer of given main chain length increases with increasing side chain length. This observation suggests that the graft density may be lower for the 1100 than for the 475 monomer, possibly due to steric hindrance. It should be noted that the graft density of the PU systems in this work is unknown due to the lack of suitable methods for its determination.

4.3.3 Protein Adsorption

Protein adsorption experiments were performed to investigate the protein resistance of the poly(OEGMA)-grafted surfaces. The poly(OEGMA) grafts with different main chain length and side chain length are expected to suppress protein adsorption to different extents, depending on protein size. According to Halperin's model for grafted surfaces in the brush regime,[39,40] small proteins should be able to access the underlying surface through the "gaps" between graft chains, while large proteins would be unable to penetrate to the substrate and would adsorb, if at all, at the outer surface of the polymer brush. To compare the adsorption behavior of proteins of different size, Fg and Lys were used in single protein adsorption experiments. The large protein fibrinogen (340 kDa, 450 × 90 × 90 Å)[31] is abundant in plasma (~3 mg/ml) and plays a crucial role in blood coagulation. The small protein lysozyme (14.3 kDa, 45 × 30 ×30 Å)[31] is found

primarily in tear fluid (normal level, 0.6 to 2.6 mg/ml)[41,42] and its adsorption is one of the major problems encountered in the use of contact lenses. It is also of interest that these two proteins have opposite net charge at physiologic pH (isoelectric points 5.5 (Fg) and 11.4 (Lys)). Although the effects of protein size and charge on the interaction of proteins with PEO-grafted surfaces have been investigated previously,[14,43,44] the present work is unique in that it is focused on PU surfaces having well-defined poly(OEGMA) grafts.

Representative protein adsorption data for the unmodified PU, PU/initiator and PU-475-5 surfaces are shown in Figure 4.3. Fg and Lys adsorption to the various surfaces increased rapidly with solution concentration in the low concentration range (0.005-0.25 mg/ml). Adsorption reached a quasi-plateau at about 0.5 mg/ml. Similar overall trends were observed on the other poly(OEGMA)-grafted PU surfaces, as have been found by other researchers on surfaces such as silicon,[45] gold,[46] PEO-modified surfaces[46] and various polymeric surfaces[47]. The highest plateau surface concentrations were obtained on the unmodified PU, i.e., 1.05 $\mu g/cm^2$ for Fg and 0.66 $\mu g/cm^2$ for Lys. The PU/initiator surface adsorbed significantly less protein than the unmodified surface, i.e., 0.77 $\mu g/cm^2$ Fg and 0.45 $\mu g/cm^2$ Lys. This decreased adsorption may be due to the increased hydrophilicity of this surface, as indicated by the decrease of water contact angle. The plateau adsorptions on the PU and PU/initiator surfaces are slightly higher than expected for close-packed monolayers with the protein molecules assumed to be rigid and non-deformable (fibrinogen 0.14 to 0.7 $\mu g/cm^2$, lysozyme 0.2 to 0.3 $\mu g/cm^2$)[31,46]. The high values observed could be due to compaction due to deformability. It is generally believed that for hydrophobic surfaces, interactions between protein and surface are likely to result in changes in secondary structure allowing higher adsorbed quantities.[48] This is supported by the Fg and Lys plateau values of 0.4 and 0.12 $\mu g/cm^2$, respectively, observed on silicon/SiO_2 under similar conditions[31], i.e. much lower than on the unmodified PU surface in the present work.

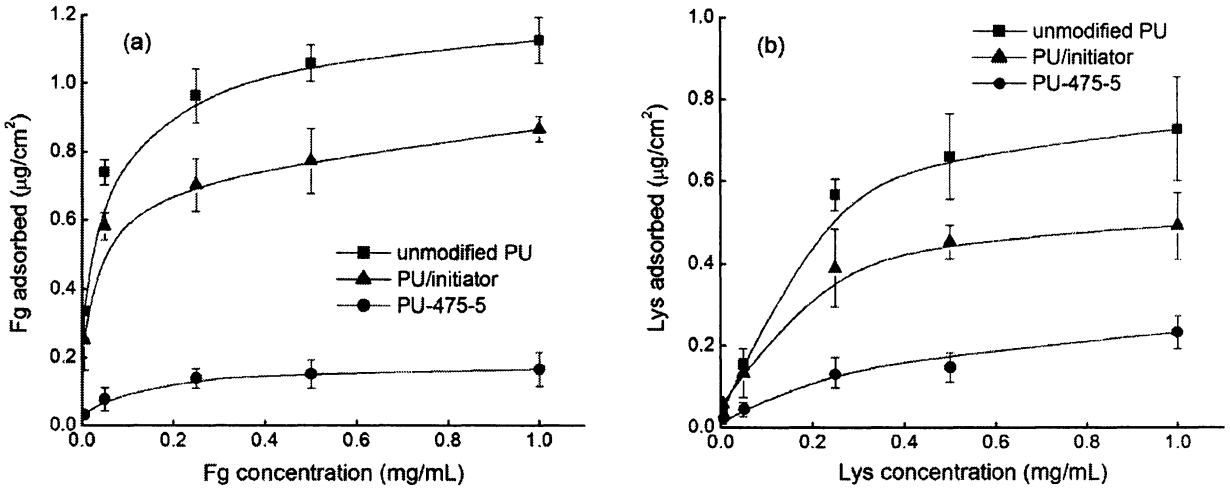

Figure 4.3 Protein adsorption on unmodified PU, PU/initiator, and poly(OEGMA)-grafted PU (PU-475-5 as example) surfaces from TBS. (a) Fg. (b) Lys. Data are mean ± S.D., n = 6. The curves are shown as a visual aid.

As shown in Figure 4.3a and 4.3b, the PU-475-5 surface with the shortest main chain length (5 monomer residues) adsorbed much less Fg and Lys than the unmodified PU and PU/initiator surfaces. The reduction in Fg and Lys adsorption was in the range of 85 to 91% and 75 to 80%, respectively, across the concentration range. Low protein adsorption was also observed on the other grafted surfaces. In addition, adsorption decreased with increasing main chain length for given side chain length as described in more detail below.

The effects of graft main chain length on protein resistance for surfaces having OEG side chain length 5 (EO residues), are shown in Figure 4.4. These data were obtained at a solution concentration of 0.5 mg/ml, generally on the plateau of the isotherm. (The same trends were observed at all concentrations.) Fg adsorption decreased sharply with increasing main chain length at shorter chain length and more gradually in the longer chain length range. No significant differences were observed among the surfaces with

chain length of 50 or above, suggesting that coverage was 'complete' for these surfaces under these conditions.

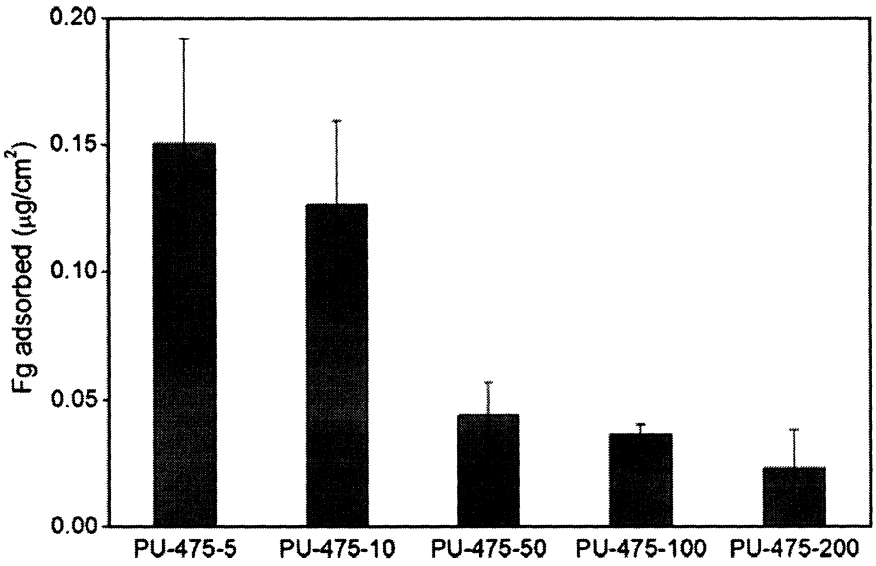

Figure 4.4 Fg adsorption from TBS on PU/poly(OEGMA) surfaces with various poly(OEGMA) main chain lengths: 5, 10, 50, 100 and 200. The OEGMA MW is 475 g/mol. Fg concentration in TBS is 0.5 mg/ml. Data are mean ± S.D., n = 6.

The OEG side chain length was varied using OEGMA of MW 300, 475 and 1100, and the effects of side chain length on protein resistance were investigated. Figure 4.5 shows "normalized" (relative to unmodified PU) protein adsorption on PU/poly(OEGMA) surfaces with various side chain and main chain lengths. For a given side chain length, both Fg and Lys adsorption decreased with increasing main chain length. For a given main chain length, Fg adsorption was relatively unaffected by side chain length, while Lys adsorption increased with increasing side chain length. The decrease in adsorption for the PU/poly(OEGMA) surfaces was in the range of 84 to 98% for Fg and 67 to 91% for Lys compared to the unmodified PU surface. For a given surface, resistance to Fg was greater than to Lys. As a smaller protein, Lys may be better able to access any gaps that may exist in the graft coverage or even the space between individual

graft points. The increase of Lys adsorption with increasing side chain length is unexpected but may indicate an increase in the effective space between chains.

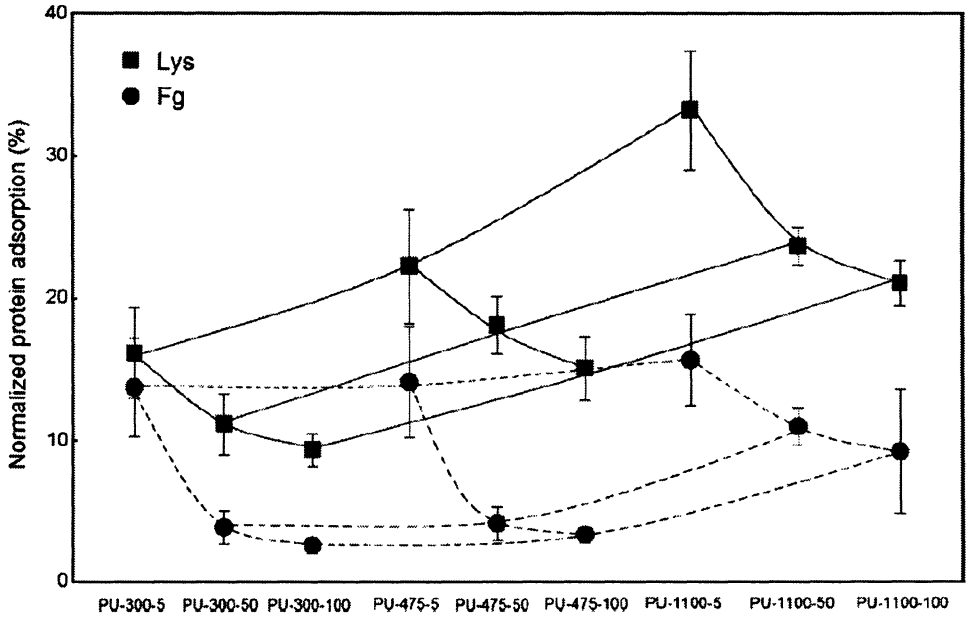

Figure 4.5 Protein adsorption on PU/poly(OEGMA) surfaces relative to unmodified PU. ■ Lys; ● Fg. Single protein concentration is 0.5 mg/ml. Data are mean ± S.D., n = 6. The curves are shown as a visual aid.

4.4 Discussion

In our previous work on s-ATRgP of OEGMA on silicon surfaces[29,37], the graft density was kept constant and was independent of polymer main chain length (equivalent to the molar ratio of monomer:sacrificial initiator). Monomer size was not varied in that work. However Ejaz et al.[49] showed that a higher graft density of poly(methyl methacrylate) (PMMA) compared to poly(3-O-methacryoyl-1,2:5,6-di-O-isopropylidene-D-glucofuranose) (PMAIpG1c) found on silicon substrate could be attributed to the size difference of the two monomers. Larger monomers, once adsorbed, may occupy more surface area (larger footprint) and exert greater steric hindrance to the access of catalyst

complex and monomer to nearby initiation sites. The reduced initiation efficiency would result in lower graft density. In the present work, the OEGMA monomer size increased with monomer MW varying from 300, 475 to 1100. Hence, the average distance between grafting sites would be expected to increase in this order. The number graft density as determined by the monomer footprint should decrease as monomer size increases; at the same time the number of ethylene oxide residues per polymer chain increases as monomer size increases. These are opposing effects for protein resistance, and since resistance decreases with monomer size (ie side chain length) it appears that the graft density change is the more important of the two.

By varying the main chain and side chain length of grafted poly(OEGMA), surfaces capable of discriminating between proteins of different size with respect to adsorption were produced. For example, as shown in Figure 4.5, superior resistance to both Fg and Lys adsorption was shown on surfaces with long main chain and short side chain length. For the PU-300-100 surface, adsorption was reduced by ~97% for Fg and ~91% for Lys adsorption compared to unmodified PU surface at a protein concentration of 0.5 mg/ml. For PU-475-100 with longer side chain length, Fg adsorption was the same as for PU-300-100, but Lys adsorption was clearly higher (97% and 85% reductions, respectively, compared to unmodified PU). For the larger protein, Fg, the poly(OEGMA) grafts appear to act as a "brush"[39], such that protein adsorption decreases with increasing main chain length of the grafted layer, but not with OEG side chain length. For the smaller protein, Lys, the poly(OEGMA) grafts appear to act more as would be expected for a layer in the mushroom regime: i.e. adsorption is sensitive to side chain length/number graft density. The relatively high adsorption of Lys is presumably due to penetration of the grafted layer to the underlying surface.

The effect of number graft density on protein adsorption has been studied by others[50-52]. However no general conclusions have been made. In particular, little is known about how surface graft density affects adsorption for proteins of different size;

this is partly due to the fact that the preparation of well-defined surfaces of known graft density is still a challenge. It was found previously that poly(MPC) grafted surfaces of high graft density, presumably in the brush regime, inhibited the adsorption of Fg and Lys to about the same extent.[31] It was also observed on PEO- and oligo(ethylene oxide) (OEO)-modified gold surfaces that an increase in graft density beyond an optimum value resulted in an increase in protein adsorption. This loss of protein resistance at higher graft density was independent of protein size and was believed to be due to a decrease in chain mobility and hydration beyond a critical chain density.[46,53] On the surfaces of very low graft density, there was also no clear effect of protein size on protein resistance. In this connection it has been suggested that surfaces formed using the 'grafting to' method may be in the mushroom regime with gaps in coverage accessible to all proteins, regardless of size.[14] In the present work, the s-ATRP of OEGMA with adjustable main chain length and side chain length seems to provide a facile way to "tune" the surface properties such that selective adsorption based on protein size is observable.

The property of size-sensitive protein adsorption could provide functions such as protein purification and separation from multi-protein mixtures. Biomaterials with such surfaces could also be useful in microfluidic devices for rapid biosensing and analysis.[54] Surprisingly there appears to be very little work on the concept/development of protein size-selective surfaces based on grafting. Recently, Albertorio et al.[55] developed a size-selective lipid bilayer by mixing a poly(ethylene glycol) (PEG)-conjugated lipid with a ligand-modified lipid. The solid-supported bilayer measures the target ligand-binding protein while filtering out other proteins larger than a certain size. The PEG moieties at a surface concentration of 1.5 mol% acted as a size-exclusion filter which rejected the bigger proteins in the mixture.

In the present work, the poly(OEGMA) grafts could in principle be tuned to adsorb small proteins preferentially, thus providing a size-selective "filter". Further work on this concept may contribute to the development of biomaterials that allow the selective

binding of target proteins in contact with blood and other biofluids. A key requirement in reaching this goal is the availability of methods to quantify polymer graft density precisely on these soft materials, especially for systems in which the properties of the substrate and the grafts are similar. Knowledge of graft density should also contribute greatly to improving our understanding of the mechanism of protein resistance of PEO and other polymer grafted surfaces.

4.5 Conclusions

Protein-resistant polyurethane surfaces were prepared by ATRP grafting of poly(OEGMA). The grafted poly(OEGMA) had different main chain and side chain lengths. The surface having the longest main chain and shortest side chain showed the highest resistance to protein adsorption. Compared to unmodified polyurethane, the adsorption of lysozyme was reduced by 91% and that of fibrinogen by 97%. Adsorption to these surfaces was also protein size dependent. The larger protein, Fg, experienced higher resistance than the small protein, Lys,. Protein discrimination based on protein size was observed for side chains of different length.

Acknowledgments: This work was supported by a Strategic Grant of the Natural Sciences and Engineering Research Council of Canada (NSERC). We also thank the Canada Foundation for Innovation (CFI) for supporting the research facilities in our laboratories.

4.6 References

1 Collier T. O., Jenney C. R., DeFife K. M., Anderson J. M., Protein adsorption on chemically modified surfaces, Biomed. Sci. Instrum., 33, 178 (1997).

2 Brash J. L., Exploiting the current paradigm of blood-material interactions for the rational design of blood-compatible materials, J. Biomater. Sci. Polym. Edn., 11, 1135 (2000).

3 Lee J. H., Ju Y. M., Kim D. M., Platelet adhesion onto segmented polyurethane film surfaces modified by addition and crosslinking of PEO-containing block copolymers, Biomaterials, 21, 683 (2000).

4 Ratner B. D., Castner D. G., Surface Modification of Polymeric Biomaterials. New York: Plenum, (1996).

5 Xue L., Greisler H. P., Biomaterials in the development and future of vascular grafts, J. Vasc. Surg., 37, 472 (2003).

6 Tan J., McClung W. G., Brash J. L., Nonfouling biomaterials based on polyethylene oxide-containing amphiphilic triblock copolymers as surface modifying additives: Protein adsorption on PEO-copolymer/polyurethane blends, J. Biomed. Mater. Res. A, 85A, 873 (2008).

7 Kingshott P., McArthur S., Thissen H., Castner D. G., Griesser H. J., Ultrasensitive probing of the protein resistance of PEG surfaces by secondary ion mass spectrometry, Biomaterials 23, 4775 (2002).

8 Parl H. D., Lee W. K., Ooya T., Park K. D., Kim Y. H., Yui N., In vitro biocompatibility assessment of sulfonated polyrotaxane-immobilized polyurethane surfaces, J. Biomed. Mater. Res., 66A, 596 (2003).

9 Bae J. S., Seo E. J., Kang I. K., Synthesis and characterization of heparinized polyurethanes using plasma glow discharge, Biomaterials, 20, 529 (1999).

10 Korematsu A., Takemoto Y., Nakaya T., Inoue H., Synthesis, characterization and platelet adhesion of segmented polyurethanes grafted phospholipid analogous vinyl monomer on surface, Biomaterials, 23, 263 (2002).

11 Coleman D. L., Andrade J. D., Gregonis D. E., Blood-materials interactions: the minimum interfacial free energy and the optimum polar apolar ratio hypotheses, J. Biomed. Mater. Res., 16, 381 (1982).

12 Knoll D., Hermans J., Polymer-protein interactions: comparison of experiment and excluded volume theory, J. Biolog. Chem., 258, 5710 (1983).

13 Han D. K., Park K. D., Ryu G. H., Kim U. Y., Min B. G., Kim Y. H., Plasma protein adsorption to sulfonated poly(ethylene oxide)-grafted polyurethane surface, J. Biomed. Mater. Res., 30, 23 (1996).

14 Archambault J. G., Brash J. L., Protein repellent polyurethane-urea surfaces by chemical grafting of hydroxyl-terminated poly(ethylene oxide): effects of protein size and charge, Coll. Surf. B, 33, 111 (2004).

15 Bearinger J. P., Terrettaz S., Michel R., Tirelli N., Vogel H., Textor M., Hubbell J. A., Chemisorbed poly(propylene sulphide)-based copolymers resist biomolecular interactions, Nat. Mater., 2, 259 (2003).

16 Liu V. A., Jastromb W. E., Bhatia S. N., Engineering protein and cell adhesivity using PEO-terminated triblock polymers, J. Biomed. Mater. Res., 60, 126 (2002).

17 Shen M. C., Wagner M. S., Castner D. G., Ratner B. D., Horbett T. A., Multivariate surface analysis of plasma-deposited tetraglyme for reduction of protein adsorption and monocyte adhesion, Langmuir, 19, 1692 (2003).

18 Lopez G. P., Ratner B. D., Tidwell C. D., Haycox C. L., Rapoza R. J., Horbett T. A., Glow discharge plasma deposition of tetraethylene glycol dimethyl ether for fouling-resistant biomaterial surfaces, J. Biomed. Mater. Res., 26, 415 (1992).

19 McPherson T. B., Shim H. S., Park K., Grafting of PEO to glass, nitinol, and pyrolytic carbon surfaces by γ–irradiation, J. Biomed. Mater. Res. Appl. Biomaterials, 38, 289 (1997).

20 Gombotz W. R., Guanghui W., Horbett T. A., Hoffman A. S., Protein adsorption to poly(ethylene oxide) surfaces, J. Biomed. Mater. Res., 25, 1547(1991).

21 Zheng J., Li L-Y., Tsao H-K., Sheng Y-J., Chen S-F., Jiang S-Y., Strong repulsive forces between protein and oligo (ethylene glycol) self-assembled monolayers: A molecular simulation study, Biophys. J., 89, 158 (2005).

22 Maechling-Strasser C., Dejardin P., Galin J. C., Schmitt A., Preadsorption of polymers on glass and silica to reduce fibrinogen adsorption, J. Biomed. Mater. Res., 23, 1385 (1989).

23 Lee J. H., Kopecek J., Andrade J. D., Protein-resistant surfaces prepared by PEO-containing block copolymer surfactants, J. Biomed. Mater. Res., 23, 351 (1989).

24 Ma X., Su Y., Sun Q., Wang Y., Jiang Z.,Preparation of protein-adsorption-resistant polyethersulfone ultrafiltration membranes through surface segregation of amphiphilic comb copolymer, J. of Membr. Sci., 292, 116 (2007).

25 Han D-K., Park K-D., Ahn K-D., Jeong S-Y., Kim Y-H., Preparation and surface characterization of PEO-grafted and heparin-immobilized polyurethanes, J. Biomed. Mater. Res., 23, 87 (1989).

26 Liu P., Su Z., Surface-initiated atom transfer radical polymerization (SI-ATRP) of MMA from PANI powders, Polym. Bullet., 55, 411 (2005).

27 Zhang H., Shouro D., Itoh K., Takata T., Jiang Y., Grafting polymer from poly(ethylene terephthalate) films by surface-initiated ATRP, J. Appl. Polym. Sci., 108, 351 (2008).

28 Ma H. W., Wells M., Beebe T. P., Chilkoti A., Surface-initiated atom transfer radical polymerization of oligo(ethylene glycol) methyl methacrylate from a mixed self-assembled monolayer on gold, Adv. Funct. Mater., 16, 640 (2006).

29 Feng W., Zhu S., Ishihara K., Brash J. L., Protein resistant surfaces: Comparison of acrylate graft polymers bearing oligo-ethylene oxide and phosphorylcholine side chains, Biointerphases, 1, 50 (2006).

30 Jin Z., Feng W., Zhu S., Sheardown H., Brash J. L., Protein-resistant polyurethane via surface-initiated atom transfer radical polymerization of oligo(ethylene glycol) methacrylate, J. Biomed. Mater. Res. A, 91A, 1189 (2009).

31 Siow K. S., Britcher L., Kumar S., Griesser H. J., Plasma methods for the generation of chemically reactive surfaces for biomolecule immobilization and cell colonization: A review, Plasma Process and Polym., 3, 392 (2006).

32 Feng W., Zhu S., Ishihara K., Brash J. L., Adsorption of fibrinogen and lysozyme on silicon grafted with poly(2-methacryloyloxyethyl phosphorylcholine) via surface-initiated atom transfer radical polymerization, Langmuir, 21, 5980 (2005).

33 Massa T. M., McClung W. G., Yang M. L., Ho J. Y. C., Brash J. L., Santerre J. P., Fibrinogen adsorption and platelet lysis characterization of fluorinated surface-modified polyetherurethanes, J. Biomed. Mater. Res. A, 81A, 178 (2006).

34 Regoeczi E., Iodine-labeled Plasma Proteins, CRC Press, Boca Raton, FL, P128 (1984).

35 Cvelbar U., Pejovnik S., Mozetie M., Zalar A., Increased surface roughness by oxygen plasma treatment of graphite/polymer composite, Appl. Surf. Sci., 210, 255 (2003).

36 Pyun J., Kowalewski T., Matyjaszewski K., Synthesis of polymer brushes using atom transfer radical polymerization, Macromol. Rapid Commun., 24,1043 (2003).

37 Feng W., Chen R., Brash J. L., Zhu S. P., Surface-initiated atom transfer radical polymerization of oligo(ethylene glycol) methacrylate: effect of solvent on graft density, Macromol. Rapid Commun., 26, 1383 (2005).

38 Braunecker W. A., Matayjaszewski K., Controlled/living radical polymerization: features, developments, and perspectives, Prog. Polym. Sci., 32, 93 (2007).

39 Halperin A., Polymer brushes that resist adsorption of model proteins: Design parameters, Langmuir, 15, 2525 (1999).

40 Malmsten M., Protein adsorption in intravenous drug delivery, In: Biopolymers at Interfaces, New York, Marcel Dekker Inc, P728, (2003).

41 Ohashi Y., Dogru M., Tsubota K., Laboratory findings in tear fluid analysis, Clinica Chimica Acta, 369, 17 (2006).

42 Avisar R., Menache R., Shaked P., Rubinstein J., Machtey I., Savir H., Lysozyme content of tears in patients with sjogrens syndrome and rheumatoid-arthritis, Am. J. Ophthalmol, 87, 148 (1979).

43 Kim Y-H., Han D-K., Park K-D., Kim S-H., Enhanced blood compatibility of polymers grafted by sulfonated PEO via a negative cilia concept, Biomaterials, 24, 2213 (2003).

44 Lee J. H., Jeong B. J., Lee H. B., Plasma protein adsorption and platelet adhesion

onto comb-like PEO gradient surfaces, J. Biomed. Mater. Res., 34, 105 (1997).

45 Mahltig B., Werner C., Muller M., Jerome R., Stamm M., Protein adsorption on preadsorbed polyampholytic monolayers, J. Biomater. Sci. Polym. Edn, 12, 995 (2001).

46 Unsworth L. D., Sheardown H., Brash J. L., Protein resistance of surfaces prepared by sorption of end-thiolated poly(ethylene glycol) to gold: Effect of surface chain density, Langmuir, 21, 1036 (2005).

47 Green R. J., Davies J., Davies M. C., Roberts C. J., Tendler S. J. B., Surface plasmon resonance for real time in situ analysis of protein adsorption to polymer surfaces, Biomaterials, 18, 405 (1997).

48 Kim J., Somorjai G. A., Molecular packing of lysozyme, fibrinogen, and bovine serum albumin on hydrophilic and hydrophobic surfaces studied by infrared-visible sum frequency generation and fluorescence microscopy, J. Am. Chem. Soc., 125, 3151 (2003).

49 Ejaz M., Ohno K., Tsujii Y., Fukuda T., Controlled grafting of a well-defined glycopolymer on a solid surface by surface-initiated atom transfer radical polymerization, Macromolecules, 33, 2870 (2000).

50 Kingshott P., Thissen H., Griesser H. J., Effects of cloud-point grafting, chain length, and density of PEG layers on competitive adsorption of ocular proteins, Biomaterials, 23, 2043 (2002).

51 Malmsten M., Emoto K., van Alstine J. M., Effect of chain density on inhibition of protein adsorption by poly(ethylene glycol) based coatings, J. Coll. Interf. Sci., 202, 507 (1998).

52 Chen H., Hu X., Zhang Y., Li D., Wu Z., Zhang T., Effect of chain density and conformation on protein adsorption at PEG-grafted polyurethane surfaces, Coll. Surf. B, 61, 237 (2008).

53 Li L., Chen S., Zheng J., Ratner B. D., Jiang S., Protein adsorption on oligo(ethylene glycol)-terminaled alkanethiolate selfassembled monolayers: the

molecular basis for nonfouling behavior, J. Phys. Chem. B, 109, 2934 (2005).

54 Lieberzeit P. A., Dickert F. L., Rapid bioanalysis with chemical sensors: novel strategies for devices and artificial recognition membranes, Anal. Bioanal. Chem., 391, 1629 (2008).

55 Albertorio F., Daniel S., Cremer P. S., Supported lipopolymer membranes as nanoscale filters: Simultaneous protein recognition and size-selection assays, J. Am. Chem. Soc., 128, 7168 (2006).

CHAPTER 5 Protein-resistant Polyurethane by Sequential Grafting of Poly(HEMA) and Poly(OEGMA) via Surface-initiated ATRP

Authors: **Z. Jin,** W. Feng, S. Zhu, H. Sheardown, and J.L. Brash

Publication Information: Submitted to Journal of Biomedical Materials Research A

Working Hypothesis:

The higher the surface density of EO units, the greater the protein resistance.

Protein-resistant Polyurethane by Sequential Grafting of Poly(HEMA) and Poly(OEGMA) via Surface-initiated ATRP

Abstract: Protein-resistant polyurethane (PU) surfaces were prepared by sequentially grafting poly(2-hydroxyethyl methacrylate) (poly(HEMA)) and poly(oligo(ethylene glycol) methacrylate) (poly(OEGMA)) via surface-initiated atom transfer radical polymerization (s-ATRP). The chain lengths of poly(HEMA) and poly(OEGMA) were regulated via the ratio of monomer to sacrificial initiator in solution. The surfaces were characterized by water contact angle and X-ray photoelectron spectroscopy (XPS). The protein resistant properties of the surfaces were assessed by single and binary adsorption experiments with fibrinogen (Fg), lysozyme (Lys) and lactalbumin (Lac). The adsorption of all three proteins on the sequentially-grafted poly(HEMA)-poly(OEGMA) surfaces (PU/PH/PO) was greatly reduced compared to the unmodified PU. Adsorption decreased with increasing poly(OEGMA) chain length. On the PU/PH/PO surface with longest poly(OEGMA) chain length (~100), the decrease in Lys adsorption was in the range of 95 to 98% and the decrease in Fg and Lac adsorption was >99% compared to the unmodified PU. Adsorption from binary protein solutions showed that the PU/PH/PO surfaces resisted these proteins more or less equally, i.e., independent of protein size.

Keywords: polyurethane; surface modification; sequential grafting; atom transfer radical polymerization (ATRP); protein resistant surface; poly(ethylene glycol).

5.1 Introduction

Nonspecific protein adsorption is believed to be the initiating event in tissue-material interactions[1,2], and is a significant limitation on the development of biomedical devices such as contact lenses, catheters, blood contacting devices and implants[3,4]. Polyethylene oxide (PEO) (or polyethylene glycol (PEG)) and PEO analogues are known for their ability to reduce protein adsorption. These attributes are due mainly to low interfacial energy, chain flexibility, large excluded volume, and generally strong interactions with water.[5-10] Thus, the preparation of PEO-based surfaces and their nonfouling behaviour have been widely investigated.

PEO-modified surfaces have been achieved by many methods such as tethering[11,12], coating[13], conventional free radical graft polymerization[14], physical adsorption, and blending of PEO-containing block copolymers with a matrix material[13,15,16]. These methods offer limited control over graft density and chain length, which are believed to be the key properties for protein resistance. Recently, surface-initiated atom transfer radical polymerization (s-ATRP), has been used to generate uniform PEO-based grafted surfaces with relatively high graft density and well-defined chain length.[17,18] The conformation of grafted polymer chains can be fine-tuned by adjusting the graft density and chain length via s-ATRP. Moreover, investigations using well-defined PEO-based grafted surfaces can potentially provide further insight into the mechanism of PEO-mediated protein resistance.

PEO-containing grafts such as poly(oligo(ethylene glycol) methacrylate) (poly(OEGMA)) have been prepared on model substrates such as silicon, gold and other metals via s-ATRP.[17,18] It was found[18] that protein adsorption decreased with increasing density and chain length of the grafts. Reductions in fibrinogen adsorption on a

poly(OEGMA)-grafted silicon surface were observed to be in the range of 20-99%, depending on the graft density and chain length. Compared to such model substrates it is more difficult to achieve well defined, high density grafts on polymeric surfaces via s-ATRP, partially due to the difficulty of forming high densities of ATRP-initiator. In previous work,[19] we developed a three-step method (oxygen plasma treatment; ATRP-initiator immobilization; s-ATRP) to graft poly(OEGMA) from a polyurethane (PU) surface. Active sites at high density were generated by oxygen plasma treatment and were then derivatized with initiators. Subsequent s-ATRP gave layers of high graft density and controlled molecular weight. These poly(OEGMA)-grafted PU surfaces (PU/PO) were shown to be highly protein resistant. For example, fibrinogen adsorption from plasma to the most resistant surface was as low as 1-5 ng/cm^2. We also prepared PU/PO surfaces with various main chain and PEO side chain lengths.[20] It was found that adsorption to these surfaces was protein size dependent. Fibrinogen (Fg), a large protein, experienced higher resistance than lysozyme (Lys), a small protein. The surfaces with the longest main chain and shortest side chain grafts showed the highest resistance to both proteins: a reduction of 91% for lysozyme and 98% for fibrinogen relative to the unmodified PU. Such protein size-based discrimination suggests that the chain density in these systems may have been less than needed to form polymer "brushes", where suppression of adsorption is expected to be independent of protein size.[21]

In this study, we investigated the surface density of ethylene oxide (EO) units as a property that may be determining for protein resistance. To achieve a range of EO density up to high values, we used a double, or sequential grafting approach whereby the surface was grafted first with poly(2-hydroxyethyl methacrylate) (HEMA) by s-ATRP. Secondary OEGMA grafts were then grown from the HEMA chains by a second ATRP. The protein resistance of the surfaces was evaluated in single and binary protein systems using fibrinogen (Fg), lysozyme (Lys) and lactalbumin (Lac) as model proteins.

5.2 Experimental

5.2.1 Materials

Tecothane polyurethane (TT-1095A) was obtained from Thermedics and purified by Soxhlet extraction with toluene and ethanol sequentially. The freshly extracted PU was dried under vacuum at 65°C. OEGMA (98% purity, Mn = 300 $gmol^{-1}$; Sigma-Aldrich) and 2-hydroxyethyl methacrylate (HEMA) (≥99% purity, Mn = 130.14 $gmol^{-1}$; Sigma-Aldrich) were passed over basic alumina columns to remove inhibitor and stored at -15°C before use. Basic alumina (Brockman Activity 1, mesh 60-325) was purchased from Fisher Scientific and used as received. 2,2'-Bipyridyl (bpy) (99%), Cu(I)Br (99.999%), 2-bromoisobutyryl bromide (BIBB) (98%), and ethyl 2-bromoisobutyrate (EBIB) (98%) were purchased from Sigma-Aldrich and used as received. Pyridine (99.9%, Fisher Scientific), N,N-dimethylformamide (DMF) (99.8%, EMD Chemicals) and methanol (HPLC grade, Caledon Laboratories) were also used as received. Toluene (reagent grade, Caledon Laboratories) was double-distilled over CaH_2 before use. Nitrogen gas was of ultrahigh-purity (UHP) grade. Poly(OEGMA)-grafted PU surfaces (referred to as PU/PO) were prepared according to the literature[19] and used for comparison purposes. All other reagents were commercially available and used as received.

Fibrinogen (Fg) (340 kDa, plasminogen-free) was purchased from Enzyme Research Laboratories and dialyzed against isotonic Tris buffer (pH 7.4), aliquoted, and stored at -70°C. Lysozyme (Lys) (14.3 kDa, from chicken egg white) and α-lactalbumin (Lac) (14.2 kDa, from bovine milk) were from Sigma-Aldrich and used as received. Deionized water with a resistivity of 18.2 MΩ·cm was prepared using a Millipore water purification system.

5.2.2 Preparation of PU Substrate Surface

PU films were prepared by solution casting as described in previous work[19]. PU/DMF (7% w/v) solution was added to a glass Petri dish and dried at 65°C for 5 days. PU disks of ~0.5 mm thickness and 6 mm diameter were then cut from the PU film and extracted in ethanol for 24 h. The freshly extracted PU disks were dried under vacuum at 65°C for 2 days and stored under vacuum.

5.2.3 Sequential Grafting of Poly(HEMA) and Poly(OEGMA) from PU Surfaces

PU surfaces with sequentially-grafted poly(HEMA) and poly(OEGMA) (referred to as PU/PH/PO) were prepared in five steps.

(1) Polyurethane disks were treated in an oxygen plasma produced by glow discharge (Micro-RIE Series 800, Technics, USA) at constant power of 100 W and pressure 200 mTorr for 5 min.[19,22] The surfaces were then exposed to air for 5 min and stored in toluene for further modification with initiator.

(2) The freshly oxygen-plasma-treated PU disks (referred to as PU/OH) were immersed in 2-bromoisobutyryl bromide (BIBB)/pyridine/toluene solution (volume ratio 1.3:1:25) to form a layer of ATRP initiator, as described in previous work.[19,20] After 16 h reaction, the ATRP-initiator-immobilized PU disks (referred to as PU/initiator) were rinsed several times with ethanol for 2 h and stored in ethanol.

(3) s-ATRP of HEMA was carried out from PU/initiator surfaces with EBIB as sacrificial initiator in solution. The molar ratio HEMA:EBIB:Cu(I)Br:bpy was fixed at 50:1:1:2. In the s-ATRP grafting procedure, a mixture of solid Cu(I)Br (0.1 mmol, 14.3 mg) and bpy (0.2 mmol, 31.8 mg) was deoxygenated with three nitrogen purge/vacuum cycles over about 30 min. HEMA (5 mmol, 650.7 mg) and ethanol (2.5 ml), de-aerated by nitrogen purge for 1h, were added to the flask. The dark brown liquid mixture was transferred to a

5.2.4 Characterization

The monomer conversion in solution was determined from proton NMR spectra (Bruker AC-P200 spectrometer). D_2O was used as solvent for OEGMA and THF-d8 for HEMA. The molecular weights of poly(OEGMA) produced by EBIB in solution were determined by gel permeation chromatography (GPC, Waters 2690 separations module, Waters 2410 refractive index detector, PEO calibration standards) using aqueous 0.2 M $NaNO_3$ and 0.1% Na_3N solution as mobile phase. The molecular weights of poly(HEMA) formed in solution were determined by GPC using three linear columns in series (Waters Styragel HR 5E, 2 Shodex KF-804L), and a Waters 410 RI detector. DMF with 0.2% (w/v) LiBr was used as solvent and narrow polystyrene standards were used to generate the calibration curve.

Water contact angle measurements were carried out on a Rame-Hart NRL goniometer (Mountain Lakes, NJ) at room temperature, using the sessile drop method. The surface composition of the PU disks was investigated using a ThermoFisher Theta Probe XPS with monochromatic Al K-alpha source. Survey scans and low-resolution spectra were recorded in standard mode via a multi-channel detector with 60° angular acceptance. The elemental compositions to ~9 nm in the uppermost surface were provided. High-resolution C 1s spectra were also obtained with the C-C peak positioned at 285.0 eV.

5.2.5 Protein Adsorption

Adsorption experiments in single and binary protein solutions (TBS buffer, pH 7.4) were carried out for 2 h at room temperature (23°C). Procedures were as described previously.[18-21] Solutions contained 10% radio-labeled (^{131}I- or ^{125}I-) protein and 90% unlabeled protein. Fibrinogen (Fg), lysozyme (Lys) and α-lactalbumin (Lac) were used in both single and binary protein experiments. All three binary combinations were studied at a molar ratio 1:1.

Surfaces were equilibrated in TBS overnight to achieve complete hydration prior to exposure to protein solutions. After 2 h protein adsorption under static conditions, the samples were immediately immersed in fresh TBS for 5 min (three cycles) to remove solution and loosely adsorbed protein. The samples were then placed in counting vials and their radioactivity was determined (Wizard 3" 1480 automatic gamma counter, Perkin-Elmer Life Sciences). The adsorbed protein amounts were calculated from the radioactivity of the samples. Four replicate samples were measured for each concentration in a given experiment. Experiments were done at least twice.

5.3 Results and Discussion

5.3.1 Preparation of PU/PH/PO Surfaces

Sequentially-grafted poly(HEMA)-poly(OEGMA) surfaces (referred to as PU/PH/PO), having the structure shown in Scheme 5.1, were prepared in five steps: oxygen plasma treatment, initiator immobilization, s-ATRP of HEMA, multi-functional macro-initiator formation, and s-ATRP of OEGMA. The first two steps were the same as in previous work.[19,20] Thus, initiator density is expected to be the same for all surfaces, PU/PH/PO and PU/PO, studied in this work. Firstly, oxygen plasma treatment was performed to introduce oxygen functions into the PU surface, resulting in a reactive and hydrophilic surface (referred to as PU/OH). Secondly, the PU/OH surface was immersed in BIBB/toluene solution to form a layer of ATRP initiator. Thirdly, s-ATRP of HEMA was carried out with Cu(I)Br/2bpy complex as catalyst. EBIB was added to the solution to initiate formation of free polymer. The molar ratio HEMA:EBIB was fixed at 50:1. The monomer conversion, molecular weight and polydispersity of the polymers formed in solution are shown in Table 5.1. HEMA conversion was essentially 100% after 48 h reaction as determined by ^{1}H NMR. The polydispersity, Mw/Mn, was 1.22, indicating good control of the ATRP process. The degree of polymerization (DP) or poly(HEMA) chain length (number 'n' in Scheme 5.1) was thus expected to be 50 and was assumed to

be the same for both the polymer chains formed in solution and those grafted on the surface. It was also found that the molecular weights (Mn) of poly(HEMA) measured by GPC using polystyrene standards were significantly higher than the theoretical value determined by NMR. The overestimation of the Mn of poly(HEMA) was also observed by Zhu et al.[23] and Matyjaszewski et al.[24], and is attributable to the much larger hydrodynamic volume of poly(HEMA) vs. polystyrene with the same Mn in DMF. Fourthly, the poly(HEMA)-grafted PU (referred to as PU/PH) was treated with BIBB to form initiator sites on the hydroxyl groups of the HEMA chains. Finally, OEGMA was grafted from the PU/PH/initiator surface in a second ATRP. Free ("sacrificial") initiator EBIB was added to adjust the poly(OEGMA) chain length formed in solution. Complete conversion was achieved after 48 h for PU/PH/PO5, and PU/PH/PO50 surfaces and 95% conversion for PU/PH/PO100 (Table 5.1). Polydispersities were in the range of 1.16 to 1.20, indicating a well-controlled ATRP process. The DPs of OEGMA in solution were thus assumed to be 5, 50 and 95. Poly(OEGMA) chain lengths (number 'm' in Scheme 5.1) in the PH/PO grafts were assumed to be the same as those for chains formed in solution.

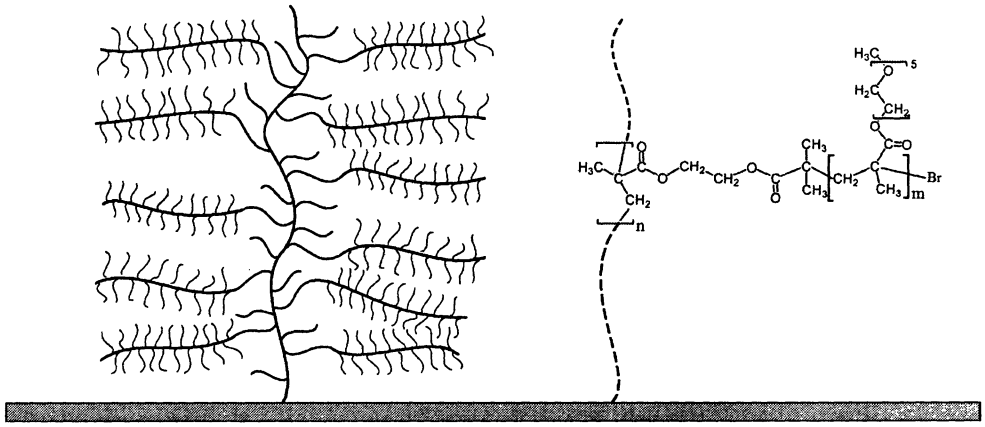

Scheme 5.1 Schematic of PU/PH/PO surfaces produced by sequential grafting of poly(HEMA) and poly(OEGMA).

Table 5.1 Conversion, molecular weight and polydispersity in s-ATRP of HEMA from PU/initiator surface and OEGMA from PU/PH/initiator surface with free initiator in solution.

Surface	Molar Ratio Monomer:EBIB	Conversion by NMR (%)	Theoretical Mn (g/mol)	Mn by GPC (g/mol)	Mw/Mn
PU/PH	50	> 99[a]	6507	17,900[b]	1.22
PU/PH/PO5	5	> 99[a]	1,500	1,340[c]	1.20
PU/PH/PO50	50	> 99[a]	15,000	12,700[c]	1.16
PU/PH/PO100	100	95	30,000	23,100[c]	1.18

[a] No residual monomer signal detected in ^{1}H NMR spectrum.

[b] Polystyrene calibration standards were used.

[c] PEO calibration standards were used.

5.3.2 Characterization of Unmodified and Modified PU Surfaces

The advancing water contact angles (θ_{Adv}) for the PU surfaces before and after modification are shown in Figure 5.1. The contact angles are consistent with the nature of the functional groups. Specifically, the unmodified PU surface showed an angle of ~90° (Figure 5.1a) and was the most hydrophobic of the surfaces examined. θ_{Adv} for the PU/OH surface was much lower due to the presence of hydrophilic groups (-OH, -OOH) introduced via oxygen plasma treatment. The angle increased significantly for the PU/initiator surface containing bromine. After the ATRP grafting of hydrophilic HEMA, θ_{Adv} decreased again with a drop of ~15° compared to the PU/initiator surface. θ_{Adv} for the PU/PH/initiator surface, containing multi-functional macro-initiators, increased to ~70°. Following ATRP grafting of OEGMA, the water contact angles decreased, and the decrease was greater the longer the graft chain length (Figure 5.1b), presumably due to the increasing density of hydrophilic OEG moieties. Compared to poly(OEGMA) single

grafted surfaces, the double-grafted PH/PO grafts had lower advancing contact angles (Figure 5.1b). This suggests high surface densities of the hydrophilic OEG moieties.

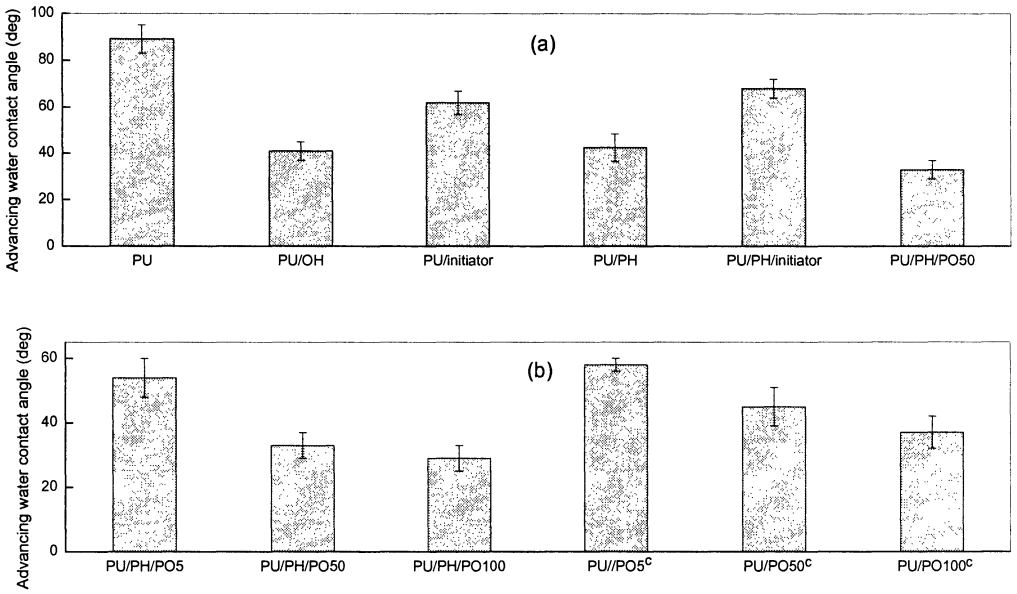

Figure 5.1 Advancing water contact angles of PU surfaces before and after modification. (a) Unmodified and initiator modified surfaces; (b) Grafted surfaces. Data are mean ± SD, n=6. [c] See Ref. [19].

The elemental compositions of the surfaces were determined by XPS (Table 5.2). Bromine was not detected on the unmodified PU surface but was clearly present on the PU/initiator (0.3%) and PU/PH/initiator (2.4%) surfaces, indicating successful attachment of the ATRP-initiator and multi-functional macro-initiator, respectively. The bromine contents of the PU/PH/PO surfaces and PU/PO surfaces were lower than those of the PU/PH/initiator and PU/initiator surfaces, presumably due to "masking" by the poly(HEMA)/poly(OEGMA) chains. Nitrogen, originating from the PU, decreased with increasing poly(OEGMA) chain length in the PU/PH/PO and PU/PO surfaces. The oxygen content for the double-grafted PU/PH/PO surfaces was higher than for the single-grafted PU/PO surfaces, and increased with increasing OEGMA chain length for both

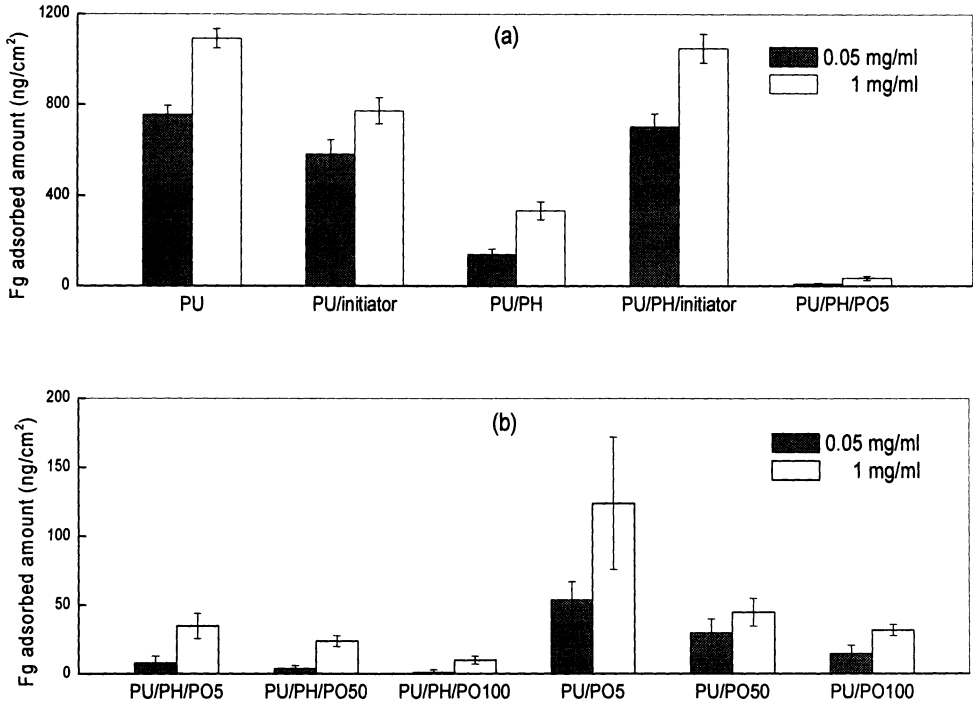

Figure 5.2 Fibrinogen adsorption from TBS with Fg concentration 0.05 and 1.0 mg/ml. (a) Unmodified and initiator modified surfaces; (b) Grafted surfaces. Adsorption time 2h. Data are mean ± SD, n = 4.

Lys, Lac and Fg adsorption data from single protein solutions are shown in Figure 5.3. Lys adsorption on PU, PU/initiator and PU/PH/initiator surfaces was in the range of 30 to 45 pmol/cm^2 (Figure 5.3a), again close to or slightly higher than expected for close-packed monolayers with the protein molecules assumed to be rigid and non-deformable.[11,20,21] These hydrophobic surfaces show Lac adsorption of 230 to 330 pmol/cm^2 (Figure 5.3a), clearly higher than Fg and Lys on a molar basis. The Lac level is much higher than for a close-packed-monolayer (0.2 to 0.4 μg/cm^2 or 14 to 28 pmol/cm^2),[29] suggesting the formation of multilayers, possibly due to adsorption-induced structural rearrangement of Lac, a relatively unstable, 'soft' protein compared to Fg and

Lys.[30,31] The adsorption levels for all three proteins decreased significantly on the hydrophilic PU/PH/PO surfaces exemplified by PU/PH/PO5 in Figure 5.3a.

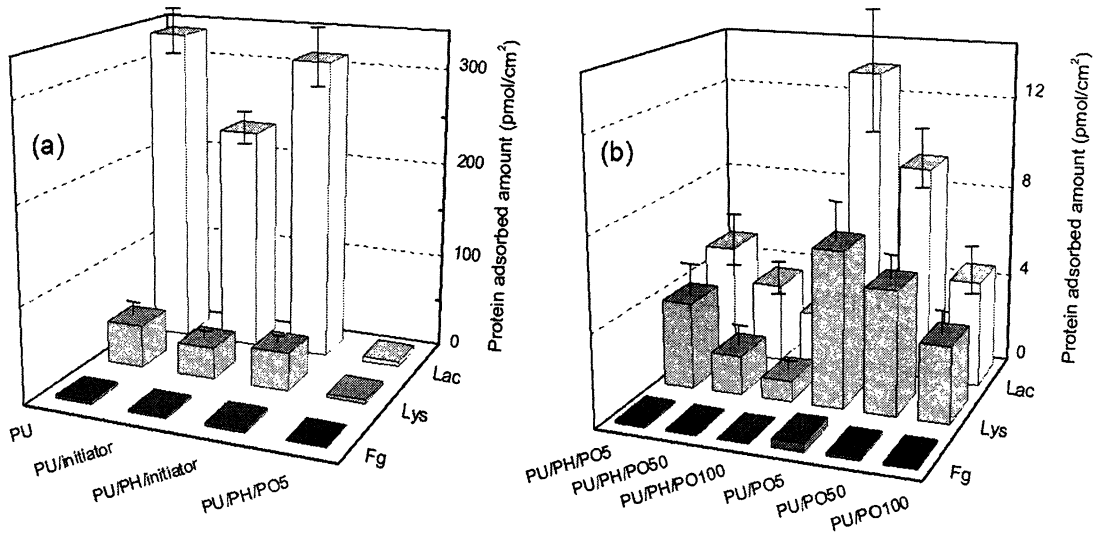

Figure 5.3 Fg, Lys and Lac adsorption from single protein solutions (1.0 mg/ml). (a) Unmodified and initiator modified surfaces; (b) Grafted surfaces. Data are mean ± SD, n = 4. (Note the difference in the z-scale for (a) and (b).)

The effects of protein type and poly(OEGMA) chain length on protein resistance for the grafted surfaces are shown in Figure 5.3b. For both the PU/PO and PU/PH/PO surfaces, the adsorbed amounts (pmol/cm^2) of Fg were significantly lower than those of Lys and Lac. The adsorption levels of all three proteins were higher on the PU/PO than on the PU/PH/PO. The PU/PH/PO surfaces showed lower 'discrimination' based on protein size, possibly due to increased surface density of hydrophilic EO residues.

As shown in Figure 5.3b, for both types of surface, the adsorption of all three proteins decreased with increasing poly(OEGMA) chain length. The highest adsorbed amounts were seen on the PU/PO5 surface with the shortest poly(OEGMA) chain length of 5 monomer units. The lowest adsorbed amounts were seen on the PU/PH/PO100

surface with the sequentially-grafted branched polymer structure and the longest poly(OEGMA) chain length. For all three proteins, the adsorbed amounts decreased in the sequence PU/PO5 > PU/PO50 > PU/PH/PO5 ≈ PU/PO100 > PU/PH/PO50 > PU/PH/PO100. This increasing protein resistance trend is in accord with the variation of the O:C ratios (Table 5.2) on these single-grafted and double-grafted OEG layers compared to the corresponding initiator surfaces. This suggests that the OEG content or surface density of EO units may be a determining property for the protein resistance of these PEO-based surfaces. The reduction in Lys adsorption on the PU/PH/PO100 surface was in the range of 95 to 98%, and the reduction in Fg and Lac adsorption was more than 99% compared to the unmodified PU.

Adsorption from binary protein systems

All three binary systems (Lys:Fg, Lac:Fg, Lac:Lys) were investigated at a molar ratio of 1:1. Total protein concentrations of 0.05 and 1 mg/ml were used; under these conditions the protein coverage would be expected to be incomplete and close to complete, respectively, for a "normally adsorbing" (not adsorption resistant) surface. Adsorbed quantities for all experiments are shown in Table 5.4. The trends are similar to those seen for the single protein systems. At a given protein concentration adsorption on the PU/PH/PO surfaces was much lower than on the unmodified PU, and significantly lower than on the PU/PO surfaces with the same poly(OEGMA) chain length; adsorption decreased with increasing poly(OEGMA) chain length for both graft types. The absolute levels of protein adsorption at a given protein concentration were also comparable to those for the single protein systems. A clear effect of surface EO density on protein resistance of the OEG layers was again observed in the binary protein adsorption experiments. Thus the adsorbed quantities of each protein from all three binary combinations decreased in the sequence PU/PO5 > PU/PO50 > PU/PH/PO5 ≈ PU/PO100 > PU/PH/PO50 > PU/PH/PO100.

Table 5.4 Adsorption from binary protein solutions. Molar ratios in solution, 1:1.

	Lys/Fg				Lac/Fg				Lac/Lys			
	0.05 mg/ml		1.0 mg/ml		0.05 mg/ml		1.0 mg/ml		0.05 mg/ml		1.0 mg/ml	
Surface	Lys	Fg	Lys	Fg	Lac	Fg	Lac	Fg	Lac	Lys	Lac	Lys
PU	60 ± 11	999 ± 68	69 ± 17	1301 ± 74	76 ± 4	648 ± 30	804 ± 108	922 ± 69	1074 ± 68	138 ± 18	3860 ± 225	94 ± 25
PU/PO5	13 ± 6	53 ± 3	15 ± 3	153 ± 68	2 ± 3	25 ± 10	23 ± 12	135 ± 85	36 ± 15	62 ± 12	54 ± 22	31 ± 18
PU/PO50	5 ± 2	18 ± 4	12 ± 2	54 ± 19	1.8 ±1	7± 3	4 ± 2	28 ± 9	25 ±4	36 ± 8	35 ± 5	18 ± 3
PU/PO100	3 ± 2	16 ± 2	9 ± 3	32 ± 6	0.6 ± 0.1	4 ± 2	2 ± 1	20 ± 3	16 ± 2	28 ± 7	28 ± 3	10 ± 6
PU/PH/PO5	1.8 ± 1.5	12 ± 5	3 ± 2	37 ± 24	0.5 ± 0.2	6 ± 3	3 ±2	31 ± 9	9 ± 3	17 ± 11	37 ±6	11 ± 3
PU/PH/PO50	0.5 ± 0.2	9 ± 4	2 ± 1	23 ± 4	0.2 ± 0.2	4 ± 3	1.4 ± 0.7	16 ± 10	5 ± 2	9 ± 5	23 ± 3	9 ± 6
PU/PH/PO100	0.1 ± 0.1	4 ± 1	1 ± 1	12 ± 4	0.02 ± 0.01	2 ± 1	0.3 ± 0.4	13 ± 3	3 ± 2	7 ± 4	18 ± 7	8 ± 2

Data are mean ± SD, n = 4.

The molar ratios of the proteins in the adsorbed layers are shown in Figure 5.4. For the unmodified PU surface, the ratios were about 1:1 at both total concentrations for the Lys:Fg system, suggesting no preference for either protein on this hydrophobic surface. For the Lac:Fg system the molar ratios were 3:1 and 20:1, respectively, at 0.05 and 1 mg/ml; and for the Lac:Lys system the ratios were 8:1 and 42:1. These are much greater than the solution molar ratios, indicating surface enrichment of Lac in both systems and suggesting a higher affinity of Lac than either Fg or Lys for the hydrophobic PU surface. For both Lac and Fg, the absolute adsorption levels were higher at the higher total protein concentration (Table 5.4). At this concentration (1 mg/ml), Fg adsorption was again in the range of a close-packed monolayer; Lac adsorption was much greater than close-packed-monolayer; and Lys was slightly less (<200 ng/cm^2).

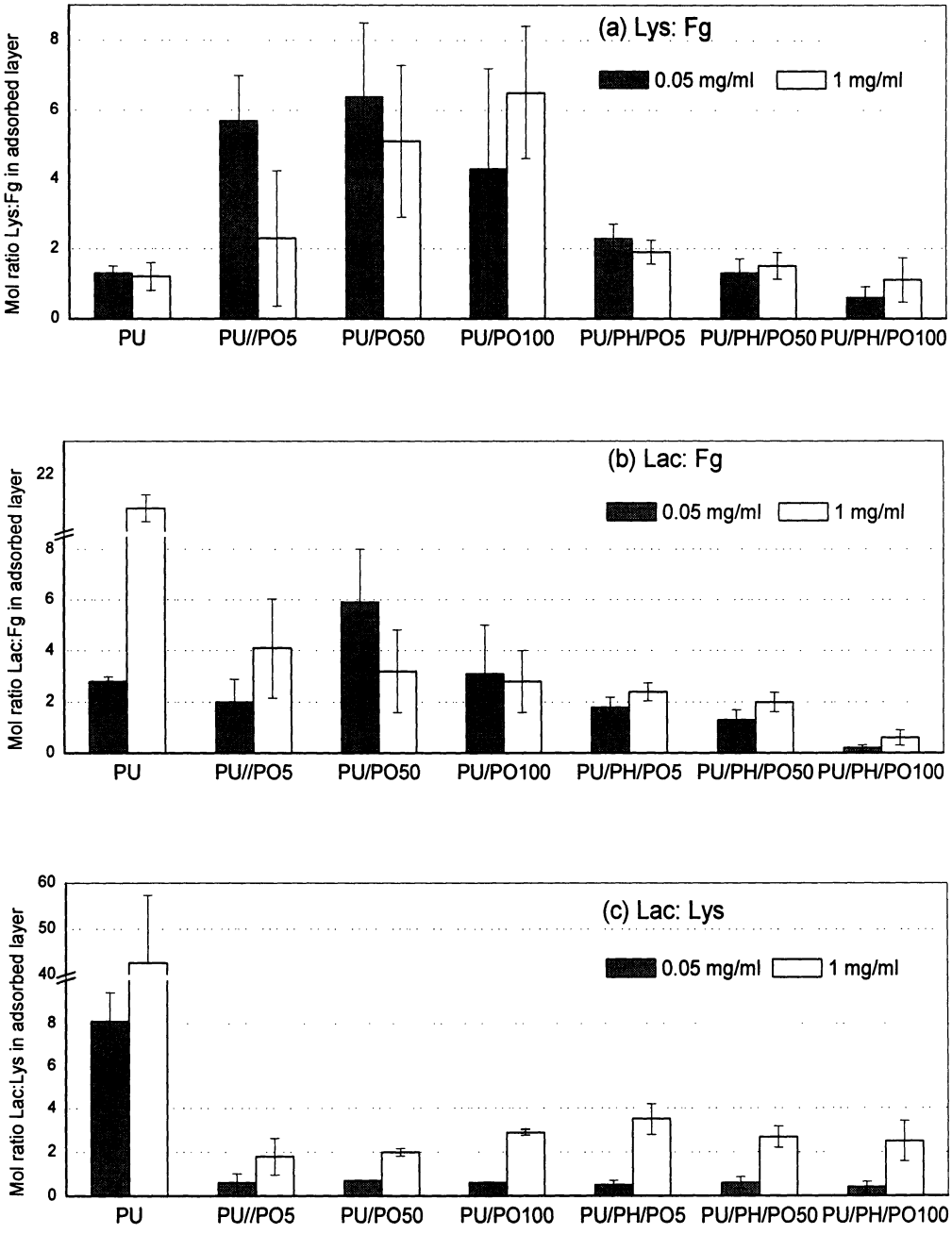

Figure 5.4 Protein adsorption from binary solutions of 0.05 and 1.0 mg/ml total concentration. (a) Lys, Fg; (b) Lac, Fg; (c) Lac, Lys. Molar ratios in solution, 1:1 in all cases. Data are mean ± SD, n = 4.

For the PU/PO surfaces in the Lys:Fg and Lac:Fg systems, the ratios in the layers were in the range of 2 to 6.5 (Figures 5.4a and 5.4b) indicating a preference for the smaller proteins. "Discrimination" among proteins based on size suggests that the graft structure allowed the smaller proteins to more easily penetrate the layer. For the PU/PH/PO surfaces in the Lys:Fg and Lac:Fg systems, the surface molar ratios decreased with increasing poly(OEGMA) chain length and were in the vicinity of 1:1 at both total concentrations. The adsorbed layer compositions were thus close to those of the solutions, suggesting that the PU/PH/PO surfaces resist these proteins equally independent of protein size. The loss of size-sensitivity may be due to the increased density of EO residues on the PU/PH/PO surfaces compared to the PU/PO surfaces, as suggested by the XPS data. The absolute adsorption levels for all three proteins on the PU/PH/PO surfaces were very low and much lower than on the PU/PO surfaces (Table 5.4). In the case of Lys, adsorption ranged from less than 0.1 to about 20 ng/cm^2. Reductions of more than 99% for each protein in the Lys:Fg and Lac:Fg systems were observed on the PU/PH/PO surface with the longest chain length.

Adsorption of Lac and Lys (of similar size but opposite charge) from binary solutions followed the same trends on both the PU/PH/PO and PU/PO surfaces (Figure 5.4c). At the lower total concentration, the Lac:Lys ratio was approximately 1:1, indicating no preference for either Lac or Lys. At the higher concentration, the Lac:Lys ratios ranged from 2 to 3.5, indicating a preference for Lac. At the higher total concentration, the absolute adsorption of Lac (Table 5.4) increased somewhat, but was still at low levels of less than 50 ng/cm^2; the adsorption of Lys, surprisingly, decreased slightly on a given PU/PO or PU/PH/PO surface at the higher total concentration. The clear preference for Lac over Lys may be due to the lower conformational stability of the "soft" Lac compared to the "hard" Lys[32]. Conformational changes have been reported for α-lactalbumin adsorbed on hydrophobic surfaces and were attributed to hydrophobic interactions.[33-36] This "soft", conformationally fragile protein, negatively charged at

neutral pH, was also observed to adsorb on negatively charged surfaces and to lose its structure to some degree.[33,37] The hydrophobic effect thus appeared to be more important than the expected repulsive electrostatic interactions. In the present work, both the unmodified PU and the OEG grafted surfaces are neutral, suggesting that electrostatic interactions should be minimal. Therefore it is reasonable to assume that the hydrophobic effect plays a more important role than protein charge in adsorption to these surfaces. The presence of hydrophilic OEG grafts should reduce hydrophobic interactions and thus also the potential for protein conformational change associated with the hydrophobic effect. This may explain the lower "discrimination" of Lac and Lys on the OEG grafts compared to the unmodified hydrophobic PU surface. The adsorbed quantities of Lac and Lys on the PU/PH/PO surfaces are again much lower than on the unmodified PU and clearly lower than on the PU/PO surfaces (Table 5.4), indicating the strongly protein-repellent properties of the PU/PH/PO surfaces regardless of protein size and charge.

There is no clear effect of protein solution concentration on the surface molar ratios Lys:Fg and Lac:Fg in the binary adsorption experiments, although the absolute adsorbed amounts of all proteins were greater at the higher solution concentration. For the Lac-Lys system, the Lac:Lys ratio on the surfaces increased at the higher solution concentration; moreover the ratio was <1 at the low concentration and >1 at the high concentration, suggesting a switch in "preference". The absolute adsorbed quantities of Lac increased while Lys decreased, suggesting greater surface activity of Lac compared to Lys.

5.4 General Discussion

The sequential poly(HEMA)-poly(OEGMA) grafts have branched structures (Scheme 5.1). The primary carbon backbones were formed via a first ATRP of HEMA. The hydroxyl end groups of the HEMA chains were then reacted with BIBB to form the PU/PH/initiator surface with a 3-D ATRP-initiator layer. The 3-D initiator layer

contained more initiator than the 2-D initiator layer on the PU/initiator surface, as indicated by XPS (Table 5.2). The poly(OEGMA) chains were formed via a second ATRP of OEGMA from the 3-D initiator layer and constitute side chains on the main chains of the grafts. Most of the poly(OEGMA) chains would be expected to grow in a direction more-or-less parallel to the substrate surface, thus increasing the zone of influence or coverage of the poly(OEGMA). At a given primary graft density the surface coverage of PH/PO grafts is thus expected to be greater than that of analogous single-grafted poly(OEGMA). The densities of EO moieties on the PU/PH/PO surfaces were higher than those on PU/PO surfaces with the same poly(OEGMA) chain length, as indicated by XPS data (Table 5.2).

The protein resistance of PEO-based surfaces is generally believed to arise from the compression of the flexible PEO chains (steric repulsion) and/or the existence of water layers tightly associated with EO moieties.[38] Both the primary HEMA grafts and the secondary OEGMA grafts have carbon backbones which are less flexible than the -C-C-O- backbone of PEO. In addition, the PEO chains in the OEGMA grafts are short with an average of 4.5 EO units per chain. Thus steric repulsion resulting from chain compression is expected to be relatively unimportant for the protein resistance of these surfaces. It seems more likely that the "water barrier" associated with EO units is primarily responsible[39-44]. The water content should increase with increasing EO surface density, and the effectiveness of the water barrier should thus depend on the surface density of EO units, regardless of the "architectural" differences in the two types of OEG grafts (PU/PH/PO and PU/PO). The surface density of EO increased in the sequence PU/PO5, PU/PO50, PU/PH/PO5, PU/PO100, PU/PH/PO50, PU/PH/PO100, and the amounts of adsorbed protein decreased in the same sequence in every single and binary adsorption experiment, thus supporting the water barrier mechanism for protein resistance.

5.5 Conclusion

Highly protein-resistant polyurethane surfaces were prepared by sequential grafting of poly(HEMA) and poly(OEGMA) via s-ATRP. The surfaces were prepared in five steps including oxygen plasma treatment, initiator immobilization, s-ATRP of HEMA, multi-functional macro-initiator formation, and s-ATRP of OEGMA. Before and after each step the polyurethanes were characterized by advancing water contact angle and XPS. The data were consistent with successful grafting of poly(HEMA) and poly(OEGMA) and indicated that high surface densities of EO residues and a range of poly(OEGMA) chain lengths were achieved.

The protein resistance of the grafted surfaces was evaluated in single and binary protein systems using Fg, Lys and Lac as model proteins. Adsorption from single protein systems on PU/PH/PO surfaces showed the same trends as for surfaces on which OEGMA was grafted directly to PU by ATRP (PU/PO). Adsorption levels on the modified PU surfaces were significantly lower than on the unmodified surface, and adsorbed quantities decreased with increasing poly(OEGMA) graft length. The adsorption levels on the PU/PH/PO surfaces were clearly lower than on the corresponding PU/PO surfaces. On the PU/PH/PO100 surface with the longest poly(OEGMA) chain length of 100, the reduction of Lys adsorption was in the range of 95 to 98% and the reduction of Fg and Lac adsorption was more than 99% compared to the unmodified PU.

In binary protein adsorption experiments on the PU/PH/PO surfaces, the Lys:Fg and Lac:Fg molar ratios in the adsorbed layer decreased with increasing poly(OEGMA) chain length and were in the vicinity of 1:1 at both total concentrations investigated, i.e. close to that of the solution, suggesting that the PU/PH/PO surfaces resist these proteins equally. In the Lac:Lys system the ratio in the adsorbed layers was slightly higher than in solution at high total concentration, indicating a preference for Lac over Lys on the

PU/PH/PO surfaces under these conditions. This may be due to the lower conformational stability of Lac compare to Lys.

Acknowledgments: This work was supported by a Strategic Grant of the Natural Sciences and Engineering Research Council of Canada (NSERC). We also thank the Canada Foundation for Innovation (CFI) for support of the research facilities in our laboratories.

5.6 References

1 Brash J. L., Exploiting the current paradigm of blood-material interactions for the rational design of blood-compatible materials, J. Biomater. Sci. Polym. Edn., 11, 1135 (2000).

2 Lee J. H., Ju Y. M., Kim D. M., Platelet adhesion onto segmented polyurethane film surfaces modified by addition and crosslinking of PEO-containing block copolymers, Biomaterials, 21, 683 (2000).

3 Anderson J. M., Biological responses to materials, Ann. Rev. Mater. Res., 31, 81 (2001).

4 Ratner B. D., Bryant S. J., Biomaterials: where we have been and where we are going, Annual Review of Biomedical Engineering, 6, 41 (2004).

5 Lee J. H., Lee H. B., Andrade J. D., Blood compatibility of polyethylene oxide surfaces, Prog. Polym. Sci., 20, 1043 (1995).

6 Bearinger J. P., Terrettaz S., Michel R., Tirelli N., Vogel H., Textor M., Hubbell J. A., Chemisorbed poly(propylene sulphide)-based copolymers resist biomolecular interactions, Nat. Mater., 2, 259 (2003).

7 Shen M. C., Wagner M. S., Castner D. G., Ratner B. D., Horbett T. A., Multivariate surface analysis characterization of plasma polymerized tetraglyme surface chemistry for reduction of protein adsorption and monocyte adhesion, Langmuir, 19, 1692 (2003).

8 Lopez G. P., Ratner B. D., Tidwell C. D., Haycox C. L., Rapoza R. J., Horbett T. A., Glow discharge plasma deposition of tetraethylene glycol dimethyl ether for fouling-resistant biomaterial surfaces, J. Biomed. Mater. Res., 26, 415 (1992).

9 Jeon S. I., Andrade J. D., Protein-surface interactions in the presence of polyethylene oxide: II. Effect on protein size, J. Coll. Interf. Sci., 142, 159 (1991).

10 Elbert D. L., Hubbell J. A., Surface treatments of polymers for biocompatibility, Annu. Rev. Mater. Sci., 26, 365 (1996).

11 Unsworth L. D., Sheardown H., Brash J. L., Protein resistance of surfaces prepared by sorption of end-thiolated poly(ethylene glycol) to gold: Effect of surface chain density, Langmuir, 21, 1036 (2005).

12 Han D-K., Park K-D., Ahn K-D., Jeong S-Y., Kim Y-H., Preparation and surface characterization of PEO-grafted and heparin-immobilized polyurethanes, J. Biomed. Mater. Res., 23, 87 (1989).

13 Maechling-Strasser C., Dejardin P., Galin J. C., Schmitt A., Preadsorption of polymers on glass and silica to reduce fibrinogen adsorption, J. Biomed. Mater. Res., 23, 1385 (1989).

14 Korematsu A., Takemoto Y., Nakaya T., Inoue H., Synthesis, characterization and platelet adhesion of segmented polyurethanes grafted phospholipid analogous vinyl monomer on surface, Biomaterials, 23, 263 (2002).

15 Lee J. H., Kopecek J., Andrade J. D., Protein-resistant surfaces prepared by PEO-containing block copolymer surfactants, J. Biomed. Mater. Res., 23, 351 (1989)..

16 Ma X., Su Y., Sun Q., Wang Y., Jiang Z., Preparation of protein-adsorption-resistant polyethersulfone ultrafiltration membranes through surface segregation of amphiphilic comb copolymer, J. of Membr. Sci., 292, 116 (2007).

17 Ma H. W., Wells M., Beebe T. P., Chilkoti A., Surface-initiated atom transfer radical polymerization of oligo(ethylene glycol) methyl methacrylate from a mixed self-assembled monolayer on gold, Adv. Funct. Mater., 16, 640 (2006).

18 Feng W., Zhu S., Ishihara K., Brash J. L., Protein resistant surfaces: Comparison of acrylate graft polymers bearing oligo-ethylene oxide and phosphorylcholine side chains, Biointerphases, 1, 50 (2006).

19 Jin Z., Feng W., Zhu S., Sheardown H., Brash J. L., Protein-resistant polyurethane via surface-initiated atom transfer radical polymerization of oligo(ethylene glycol) methacrylate, J. Biomed. Mater. Res. A, 91A, 1189 (2009).

20 Jin Z., Feng W., Beisser K., Zhu S., Sheardown H., Brash J. L., Protein-resistant polyurethane prepared by surface-initiated atom transfer radical graft polymerization (ATRgP) of water-soluble polymers: Effects of main chain and side chain lengths of grafts, Coll. Surf. B: Biointerfaces, 70, 53 (2009).

21 Feng W., Zhu S., Ishihara K., Brash J. L., Adsorption of fibrinogen and lysozyme on silicon grafted with poly(2-methacryloyloxyethyl phosphorylcholine) via surface-initiated atom transfer radical polymerization, Langmuir, 21, 5980 (2005).

22 Siow K. S., Britcher L., Kumar S., Griesser H. J., Plasma methods for the generation of chemically reactive surfaces for biomolecule immobilization and cell colonization: A review, Plasma Process and Polym., 3, 392 (2006).

23 Jin X., Shen Y., Zhu S., Atom transfer radical block copolymerization of 2-(N,N-dimethylamino)ethyl methacrylate and 2-hydroxyethyl methacrylate, Macromol. Mater. Eng., 288, 925 (2003).

24 Beers K. L., Boo S., Gaynor S. G., Matyjaszewski K., Atom transfer radical polymerization of 2-hydroxyethyl methacrylate, Macromolecules, 32, 5772 (1999).

25 Norde W., Haynes C. A., Reversibility and the mechanism of protein adsorption, In: Proteins at Interfaces II: Fundamentals and Applications, Horbett T. A. and Brash J. L. (eds.), American Chemical Society, Washington, DC, P26-40 (1995).

26 Shiba E., Lindon J. N., Kushner L., Matsueda G. R., Hawiger J., Kloczewiak M., Kudryk B., Salzman E. W., Antibody-detectable changes in fibrinogen adsorption affecting platelet activation on polymer surfaces, Am. J. Physiol. Cell. Physiol., 260, C965 (1991).

27 Feng L., Andrade J. D., Protein adsorption on low temperature isotropic carbon: III. isotherms, competitivity, desorption and exchange of human albumin and fibrinogen, Biomaterials, 15, 323 (1994).

28 Tegoulia V. A., Cooper S. L., Leukocyte adhesion on model surfaces under flow: Effects of surface chemistry, protein adsorption, and shear rate, J. Biomed. Mater. Res., 50, 291 (2000).

29 Gurkov T. D., Russev S. C., Danov K. D., Ivanov I. B., Campbell B., Monolayers of globular proteins on the air/water interface: Applicability of the volmer equation of state, Langmuir, 19, 7362 (2003).

30 van der Veen M., Stuart M. C., Norde W., Spreading of proteins and its effect on adsorption and desorption kinetics, Coll. Surf. B: Biointerfaces, 54, 136 (2007)

31 Engel M. F. M., van Mierlo C. P. M., Visser A. J. W. G., Kinetic and structural characterization of adsorption-induced unfolding of bovine alpha-lactalbumin, J. Biol. Chem., 277, 10922 (2002).

32 Pasche S., Voros J., Griesser H. J., Spencer N. D., Textor M., Effects of ionic strength and surface charge on protein adsorption at PEGylated surfaces, J. Phys. Chem. B, 109, 17545 (2005).

33 Larsericsdotter H., Oscarsson S., Buijs J., Thermodynamic analysis of proteins adsorbed on silica particles: Electrostatic effects, J. Coll. Interf. Sci., 237, 98 (2001).

34 Noppe W., Haezebrouck P., Hanssens I., De Cuyper M., A simplified purification procedure of alpha-lactalbumin from milk using Ca^{2+}-dependent adsorption in hydrophobic expanded bed chromatography, Bioseparation, 8, 153 (1999).

35 Lindahl L., Vogel H. J., Metal-ion-dependent hydrophobic-interaction chromatography of alpha-lactalbumins, Anal. Biochem., 140, 394 (1984).

36 Norde W., Anusiem A. C. I., Adsorption, desorption and readsorption of proteins on solid-surfaces, Coll. Surf., 66, 73 (1992).

37 Haynes C. A., Sliwinsky E., Norde W., Structural and electrostatic properties of globular-proteins at a polystyrene water interface, J. Coll. Interf. Sci., 164, 394 (1994).

38 Morra M., Poly(ethylene oxide) coated surfaces, In: Water in Biomaterials Surface Science, Morra M. (ed.), Wiley, New York P307-332 (2001).

39 Harder P., Grunze M., Dahint R., Whitesides G. M., Laibinis P. E., Molecular conformation in oligo(ethylene glycol)-terminated self-assembled monolayers on gold and silver surfaces determines their ability to resist protein adsorption, J. Phys. Chem. B, 102, 426 (1998).

40 Ostuni E, Chapman R. G., Holmlin R. E., Takayama S., Whitesides G. M., A survey of structure-property relationships of surfaces that resist the adsorption of protein, Langmuir, 17, 5605 (2001).

41 Feldman K., Hahner G., Spencer N. D., Harder P., Grunze M., Probing resistance to protein adsorption of oligo(ethylene glycol)-terminated self-assembled monolayers by scanning force microscopy, J. Am. Chem. Soc., 121, 10134 (1999).

42 Pertsin A. J., Grunze M., Computer simulation of water near the surface of oligo(ethylene glycol)-terminated alkanethiol self-assembled monolayers, Langmuir, 16, 8829 (2000).

43 Pertsin A. J., Hayashi T., Grunze M., Grand canonical Monte Carlo Simulations of the hydration interaction between oligo(ethylene glycol)-terminated alkanethiol self-assembled monolayers, J. Phys. Chem. B, 106, 12274 (2002).

44 Luk Y. Y., Kato M., Mrksich M., Self-assembled monolayers of alkanethiolates presenting mannitol groups are inert to protein adsorption and cell attachment, Langmuir, 16, 9604 (2000).

CHAPTER 6 Protein-resistant Materials via Surface-initiated ATRP of 2-Methacryloyloxyethyl Phosphorylcholine (MPC)

Authors: **Z. Jin,** W. Feng, S. Zhu, H. Sheardown, and J.L. Brash

Publication Information: Journal of Biomaterial Science, Polymer Edition

Accepted Date: Jul 27, 2009

A simple three-step method was used as a general strategy to achieve high-density grafts on various polymeric substrate surfaces of interest for biomaterials applications

Protein-resistant Materials via Surface-initiated Atom Transfer Radical Polymerization of 2-Methacryloyloxyethyl Phosphorylcholine (MPC)

Abstract: Poly(2-methacryloyloxyethyl phosphorylcholine) (poly(MPC)) was grafted from various polymeric substrates to prepare protein-resistant materials. The poly(MPC) chain length was adjusted via the ratio of monomer to sacrificial initiator in solution. The surfaces were characterized by water contact angle and X-ray photoelectron spectroscopy (XPS). The protein resistant properties of the poly(MPC)-grafted surfaces were evaluated by single adsorption experiments with fibrinogen and lysozyme. It was shown that the simple three-step grafting method could be applied to modify various biomaterial surfaces including polyurethane and silicones. The adsorption of fibrinogen and lysozyme to the modified surfaces was greatly reduced compared to the unmodified surfaces, and adsorption decreased with increasing poly(MPC) chain length. On polyurethane film grafted with poly(MPC) of chain length 100, the reduction in adsorption was ~96% for lysozyme and ~99% for fibrinogen.

Keywords: surface modification; atom transfer radical polymerization (ATRP); protein resistant surface; phosphorylcholine; MPC.

6.1 Introduction

Polymeric materials have been widely used in the biomedical field. For example, polydimethylsiloxane (PDMS)-based materials have been used in cardiovascular and ophthalmic applications[1,2], and polyurethane (PU)-based materials, well known for their excellent mechanical properties, have been used extensively in blood contacting applications.[3-5] These polymers have desirable physical and mechanical properties and convenient processability. However, biofouling on these hydrophobic polymeric surfaces may trigger serious problems including foreign body reactions, bacterial infection and blood coagulation.[6] Thus, there is much current interest in developing methods that would eliminate or reduce protein adsorption on these materials.

Surfaces modified with water-soluble or hydrophilic polymers such as poly(ethylene oxide) (PEO) and phosphorylcholine (PC)-based polymers, have shown excellent resistance to protein adsorption.[7-10] The anti-biofouling properties and biocompatibility of these polymers are generally believed to be attributable to the "water barriers" associated with the EO and PC groups.[10] Surfaces rich in the zwitterionic phosphorylcholine head groups of lipids, which mimic the natural surface of cell plasma membranes, have been shown to be resistant to biological interactions such as protein adsorption, platelet adhesion and cell adhesion generally.[11] It has also been found that PC-based polymers have relatively high *in vivo* stability in long-term biomedical applications.[12] Indeed long-term *in vivo* biostability may be one of the major advantages of PC-based polymers over PEO-based polymers, which are known to undergo oxidation at the ether groups in the presence of oxygen and transition metal ions.[13,14]

There are many methods for modifying polymer surfaces, including coating[15], physical adsorption[16], blending with surface active components[17], surface tethering ("grafting to" method)[18] and graft polymerization ("grafting from" method).[19] Among these methods, surface-initiated atom transfer radical polymerization (s-ATRP) has attracted much attention mainly due to characteristics such as tolerance of impurities,

mild reaction conditions, achievability of high grafting density, and of uniform and tuneable graft chain lengths.[20,21] Despite all these advantages, however, the use of s-ATRP for modifying polymeric biomaterial surfaces is limited to some degree due to the challenge of introducing ATRP initiators into these chemically inert surfaces.

In this work, a simple three-step method was used as a general strategy to achieve high-density grafts on various polymeric substrate surfaces of interest for biomaterials applications: polyurethane (PU) film, polyurethane catheter, PDMS film, and a silicone based hydrogel. Oxygen plasma treatment was first carried out to introduce reactive functional groups into the substrates, followed by ATRP initiator immobilization and s-ATRP on the initiator surfaces using MPC as monomer. The poly(MPC) chain length was regulated by varying the molar ratio of monomer to sacrificial initiator in solution. Protein adsorption experiments with fibrinogen and lysozyme were carried out to investigate the protein-resistance of the surfaces. The effect of poly(MPC) chain length on the protein-resistance of the PU surfaces was also investigated.

6.2 Materials and Methods

6.2.1 Materials

MPC was kindly provided by Professor K. Ishihara (School of Engineering, University of Tokyo, Japan). Fibrinogen (340 kDa, plasminogen-free) was purchased from Enzyme Research Laboratories and dialyzed against isotonic Tris buffer (pH 7.4), aliquoted, and stored at -70°C. Lysozyme (14.3 kDa, from chicken egg white) was purchased from Sigma-Aldrich and used as received. Deionized water with a resistivity of 18.2 MΩ·cm was prepared using a Millipore water purification system. Toluene (reagent grade, Caledon Laboratories) was double-distilled over CaH_2 before use. Nitrogen gas was of high-purity grade. 2-Bromoisobutyryl bromide (BIBB) (98%, Sigma-Aldrich), ethyl 2-bromoisobutyrate (EBIB) (98%, Sigma-Aldrich), 2,2'-bipyridyl (bpy) (99%, Sigma-Aldrich), Cu(I)Br (99.999%, Sigma-Aldrich), pyridine (99.9%, Fisher Scientific),

and methanol (HPLC grade, Caledon Laboratories) were used as received. Other reagents were commercially available and also used as received.

Substrate No. 1

PU (Tecothane, TT-1095A)

Substrate No. 2

PU catheter (Tecothane)

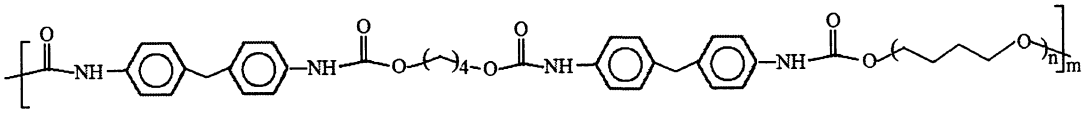

Substrate No. 2 has the same major component, Tecothane, as substrate No. 1; and contains barium sulfate as a radiopaque additive (20% by weight).

Substrate No. 3

cross-linked PDMS

Substrate No. 4

model lens surface (silicone hydrogel)

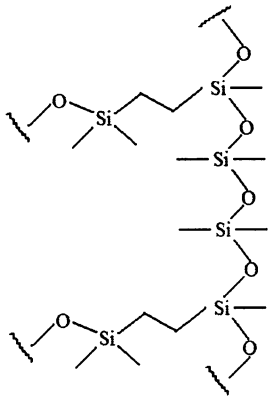

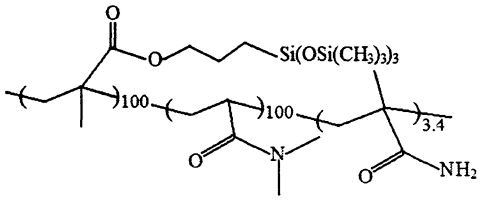

Figure 6.1 The chemical structures of four polymeric substrates used in surface grafting of poly(MPC) via s-ATRP.

Four polymeric substrates were used for surface-initiated ATRP grafting: polyurethane (PU) film (Tecothane TT-1095A, Thermedics), was prepared by solution casting as described in previous work;[22] PU catheter (Tecothane, Arrow International), was commercially available and used as received; cross-linked polydimethylsiloxane

(PDMS) film was prepared from Sylgard 184 silicone elastomer kit (Dow Corning, Midland, MI) according to the manufacturer's directions;[23] a model silicone hydrogel film prepared from 3-methacryloxypropyl tris(trimethylsiloxy) silane (TRIS), N,N-dimethylacrylamide (DMAA), and methacrylamide (MAA). The chemical structures of these materials are shown in Figure 6.1.

6.2.2 Preparation of Poly(MPC)-grafted Surfaces

Grafting of MPC by ATRP was carried out in three steps.[22]

(1) *Surface treatment with oxygen plasma*[22,24,25]: Oxygen plasma treatment (Micro-RIE Series 800, Technics, USA) was carried out on both sides of the substrates for 5 min at 100 W and 200 mTorr pressure. PU catheter segments (d_{in} = 1 mm, d_{out} = 2 mm, length = 6 mm) were slit lengthwise. The PU film, PDMS film and silicone hydrogel were in the form of disks of diameter 6 mm. The surfaces were then exposed to air for 5 min after the oxygen plasma treatment and stored in toluene prior to use.

(2) *Formation of initiator monolayer on surfaces*:[22] The freshly oxygen-plasma-treated surfaces (~20 samples) were immersed in dry toluene (40 ml) in a round-bottomed flask. The flask was de-aerated in a steam of nitrogen for 30 min and cooled to -15°C in a NaCl-ice bath. Pyridine (26 mmol, 2.1 ml) was first added via a nitrogen-purged syringe. 2-Bromoisobutyryl bromide (BIBB, 22 mmol, 2.72 ml) dissolved in 10 ml of toluene was added dropwise over a period of 1 h. The reaction was gently stirred at 0°C overnight and then at room temperature (23°C) for 3 h. After reaction, the ATRP initiator-immobilized surfaces were removed from the reaction mixture and extracted in methanol overnight. The surfaces were finally dried in vacuum at 40°C for 1 day.

(3) *s-ATRP of MPC*: In a typical ATRP grafting experiment with a molar ratio of MPC:EBIB (ethyl 2-bromoisobutyrate) = 100:1, a flask containing MPC (10.0 mmol, 3.0 g), Cu(I)Br (0.1 mmol, 14.3 mg) and 2,2'-bipyridyl (bpy, 0.2 mmol, 31.8 mg) was first de-aerated by three evacuation-nitrogen backfilling cycles. De-aerated methanol (5 ml)

was added to the flask, forming a dark brown liquid mixture. The mixture was degassed for another 10 min and transferred to a nitrogen-filled glove box. De-aerated EBIB initiator (0.1 mmol, 14.7 μL) was then added. The reaction mixture was stirred vigorously for 1 min and immediately transferred to vials containing ATRP-initiator-immobilized surfaces. s-ATRP grafting was carried out at room temperature in the glove box for 14 h. The poly(MPC)-grafted surfaces were then removed from the glove box, extracted (Soxhlet) with boiling ethanol for 24 h and dried in vacuum at 65°C for 2 days.

6.2.3 Graft and Surface Characterization

The MPC conversion and theoretical MW of poly(MPC) ($M_{n,NMR}$) produced by EBIB in solution was determined from ^{1}H-NMR spectra (Bruker AC-P200 spectrometer, D_2O solvent). Aqueous gel permeation chromatography (GPC, Waters 2690 separations module with a Waters 2410 refractive index detector, PEO calibration standards) was used to measure the MW and polydispersity (PDI) of poly(MPC) formed in solution. Static water contact angles on the surfaces were determined using the sessile drop method on a Rame-Hart NRL goniometer (Mountain Lakes, NJ). All surfaces were immersed in ethanol at room temperature for 24 h and dried in a nitrogen stream immediately prior to measurement. The surface composition of samples was investigated by XPS using a ThermoFisher Theta Probe spectrometer with monochromatic Al K-alpha source. Survey spectra and low-resolution spectra were recorded in standard mode via a multi-channel detector with 60° angular acceptance. The elemental compositions to a depth of ~9 nm in the uppermost surface were obtained.

6.2.4 Protein Adsorption

The adsorption of fibrinogen and lysozyme was measured in TBS buffer (pH 7.4) at room temperature (22°C) using radioiodinated proteins. Solutions for adsorption experiments contained 90% unlabeled protein and 10% ^{125}I-radiolabeled protein.[22,26,27] Two protein concentrations, 0.05 and 1.0 mg/ml, were used. All samples were immersed in TBS overnight to achieve complete hydration and then transferred to the protein

solution. Adsorption was allowed to proceed under static conditions for 2h. The samples were then immersed in fresh TBS for 5 min (three cycles) to remove solution and loosely adsorbed protein. The final samples were placed in counting vials and the radioactivity determined (Wizard 3" 1480 automatic gamma counter, Perkin–Elmer Life Sciences). Four replicate samples were measured for each concentration in a given experiment. Experiments were performed at least twice.

6.3 Results and Discussion

6.3.1 PU Film Prepared by s-ATRP of MPC

6.3.1.1 Preparation of Poly(MPC)-grafted PU film Surfaces

A three-step process was performed to graft poly(MPC) from various polymeric substrates, as shown in Scheme 6.1. The process included oxygen plasma treatment, initiator immobilization, and s-ATRP. In the first step, various reactive species were introduced onto the surfaces by oxygen plasma treatment; hydroxyl and hydro-peroxide groups were then formed on the surfaces after a short exposure to air.[22,28-30]. In the second step, BIBB was added to form an ATRP-initiator layer on the surfaces. As we discussed in our previous work,[19,22] the hydroxyl and/or carboxyl groups reacted with BIBB to form ATRP-initiator on the substrate. The residual peroxide groups on the surface may play a role similar to that of the initiator in the ATRP process, reacting with Cu(I) complex to form Cu(II) complex and radicals. The polydispersity of the grafts may increase slightly due to the difference between the activation rate of peroxides and ATRP-initiator. The initiator density was expected to vary with the surface chemistry of the substrates, although the values were not determined due to the lack of suitable methods. In the final step, poly(MPC) grafts were formed by s-ATRP with Cu(I)Br/bpy complex as catalyst and methanol as solvent. Free/sacrificial initiator (EBIB) was added to the reaction. The ATRP of MPC thus occurred in solution as well as on the surface.

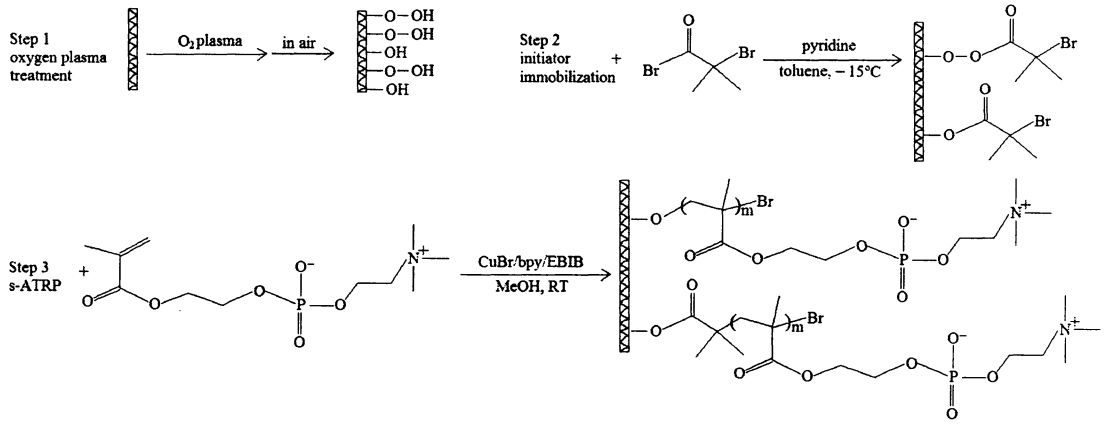

Scheme 6.1 Surface-initiated ATRP of MPC from polymeric biomaterial surfaces.

Table 6.1 Conversion and molecular weight in s-ATRP of MPC from PU/initiator surface with sacrificial initiator in solution.

Surface	MPC MW	Molar Ratio MPC:EBIB	Conversion (%)	DP	$M_{n,NMR}$ (g/mol)
PU/MPC10	300	10	> 99[a]	10	3,000
PU/MPC50	300	100	52	52	15,600
PU/MPC100	300	150	64	96	28,800

[a] No residual monomer signal detected in 1H NMR spectrum.

The MPC conversion and molecular weight of poly(MPC) formed in solution are shown in Table 6.1. Monomer conversions of >99%, 52% and 64% were achieved after 14 h reaction with MPC:EBIB ratios of 10:1, 100:1 and 150:1, respectively. The corresponding degrees of polymerization (DP) of MPC formed in solution were estimated as 10, 52 and 96, respectively, based on the MPC:EBIB ratios and conversions. Since the ATRP of MPC was performed in solution and on the surface at the same time and under the same conditions, it was assumed that the polymer chains formed in solution were

representative of the grafts on the surface, and thus that the poly(MPC) chains on the surface had similar length and length distribution as those in the solution.[31,32] The poly(MPC)-grafted PU surfaces were thus referred to as PU/MPC10, PU/MPC50 and PU/MPC100 with 10, 50 and 100 indicating the respective DPs.

6.3.1.2 Properties of PU/poly(MPC) Surfaces

Water contact angles (advancing) for the unmodified and poly(MPC)-grafted PU film surfaces are shown in Figure 6.2. A high advancing water contact angle of ~92° was observed on the unmodified surface. The contact angles were significantly lower after poly(MPC) grafting and decreased with increasing chain length. The surfaces with the longest chain length of ~100 had angles as low as 33°. The observation of increasing hydrophilicity with increasing poly(MPC) chain length is presumably due to increasing coverage of the surface by hydrophilic phosphorylcholine (PC) moieties.

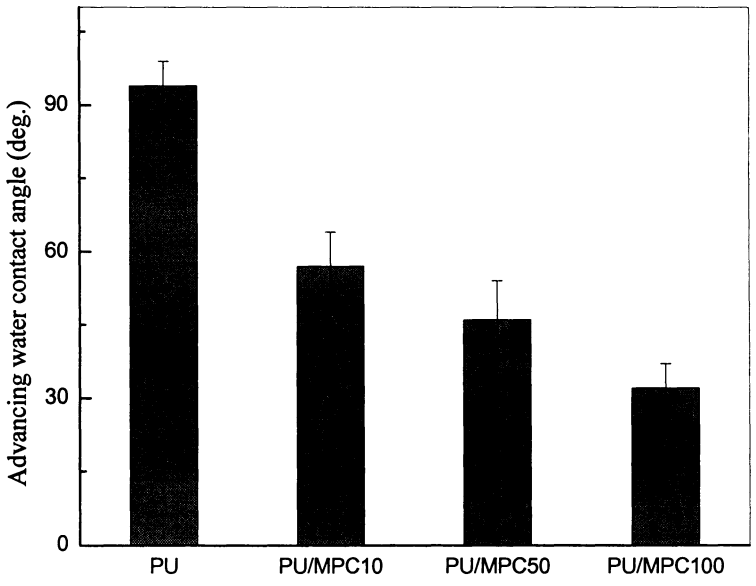

Figure 6.2 Water contact angles (advancing) of poly(MPC)-grafted PU surfaces. Error bars represent one standard deviation, n = 6.

Table 6.2 Elemental composition of the poly(MPC)-grafted surfaces determined from XPS

	Elemental Composition (atom%)					
Surfaces	C	N	O	Br	Si	P
PU	78.4	2.7	18.9	0	0	0
PU/initiator	77.9	1.6	20.2	0.3	0	0
PU/MPC10	75.6	2.4	21.0	0.2	0	0.9
PU/MPC50	74.1	2.5	21.9	0.3	0	1.2
PU/MPC100	71.6	3.2	22.7	0.2	0	2.4
Catheter/MPC50	71.7	3.7	23.8	0.2	0	0.6
PDMS/MPC50	46.5	0.9	29.9	0.1	21.8	0.8
Sil/MPC50	69.2	4.0	25.5	0.1	0.5	0.6
PDMS[a]	44	0	26	0	30	0
Sil[b]	72.4	3.5	20.7	0	3.4	0
MPC[b]	57.9	5.3	31.6	0	0	5.3

Data precision ±5%.

[a] See Ref. [40].

[b] Theoretical composition.

The elemental composition of the poly(MPC)-grafted surfaces was determined by XPS (Table 6.2). No bromine was detected in the unmodified PU film surface but bromine signals were clear in the PU/initiator and PU/MPC surfaces (atomic concentration ~0.3%), indicating the presence of ATRP initiator residues. Whereas no phosphorus was detected in the unmodified PU and PU/initiator surfaces, clear phosphorus signals were observed in the PU/MPC surfaces. The signal intensity, proportional to the phosphorus atomic concentration, increased with increasing poly(MPC) chain length. The nitrogen and oxygen contents were also observed to increase with increasing chain length of poly(MPC), which is rich in P, N and O atoms compared to the

PU film substrate. The increase of P, N and O concentration with increasing chain length suggests increasing coverage of phosphorylcholine moieties.

6.3.1.3 Protein Adsorption on the Modified PU Film Surfaces

Fibrinogen, a key protein in blood coagulation (dimensions 450×90×90 Å), and lysozyme, a small protein found in the front of the eye (dimensions, 45×30×30 Å) were chosen as model proteins to investigate the protein resistant properties of the poly(MPC)-grafted surfaces. Figure 6.3a shows fibrinogen adsorption on the PU surfaces before and after modification. The adsorbed quantities on all surfaces were greater at 1.0 than at 0.05 mg/ml. At both concentrations, the unmodified PU surface showed the highest adsorbed quantities, which were in the range expected for close-packed monolayers.[24,33] The PU/MPC surfaces adsorbed much less than the unmodified PU surface, and adsorption decreased as the poly(MPC) chain length increased. A reduction of 99% compared to the unmodified PU was seen on the PU/MPC100 surface.

The adsorption of lysozyme from single protein solutions to poly(MPC) grafts is shown in Figure 6.3b. Lysozyme adsorption on these surfaces followed the same trend as fibrinogen: adsorption was greatest on the unmodified PU film surface and decreased with increasing chain length of the poly(MPC) grafts. The adsorbed quantity of lysozyme on the PU/poly(MPC)100 surface at 1.0 mg/ml concentration was about 27 ng/cm^2, representing a 96% reduction from the unmodified PU. The protein (fibrinogen and lysozyme) adsorption levels on the poly(MPC) grafts were similar to those on poly(OEGMA) grafts with same chain lengths (for example, fibrinogen and lysozyme adsorption on the PU/poly(OEGMA)100 surface were 46 ± 7 ng/cm^2 and 34 ± 9 ng/cm^2 respectively at 1.0 mg/ml concentration),[19,22] and were comparable to the values seen on model silicon surfaces similarly modified by ATRP grafting of MPC.[26] It seems likely that water associated with the PC and PEO moieties, acting as a "barrier", is responsible for the protein resistance of these surfaces. The effect of chain length might then be due

to the increasing surface density of PC or EO moieties resulting in increasing bound water content as the chain length increases at a constant chain density.

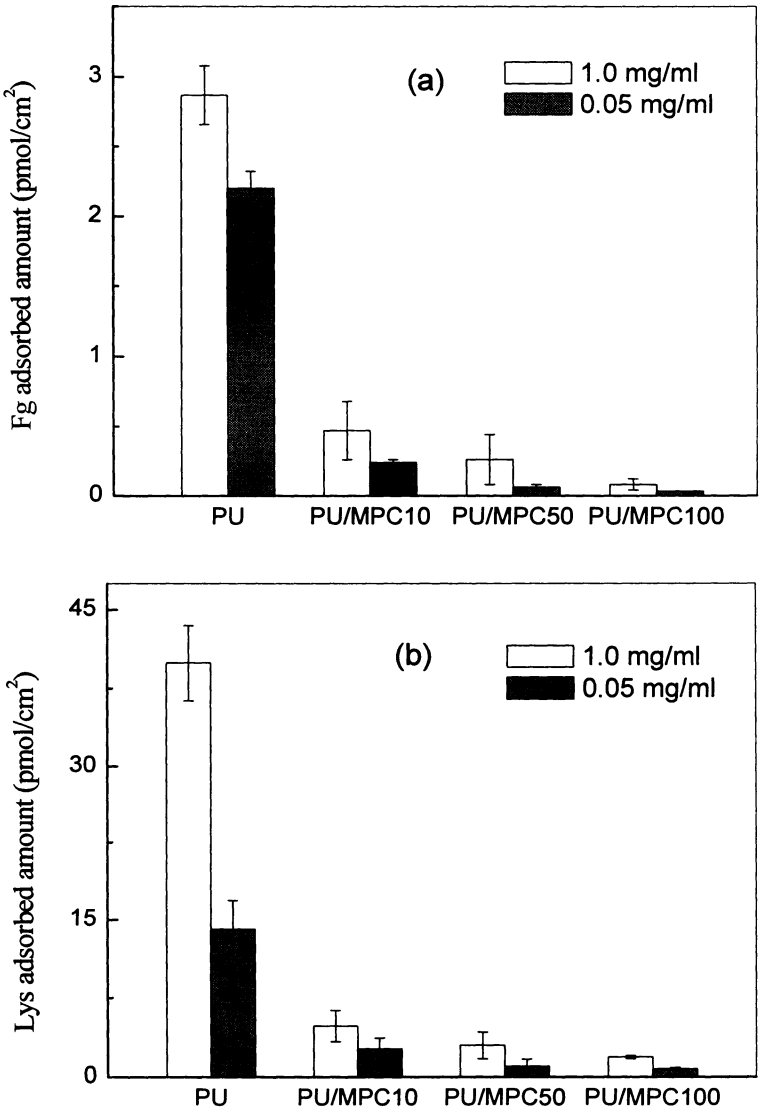

Figure 6.3 Protein adsorption from TBS with concentrations of 0.05 and 1.0 mg/ml. (a) Fg; (b) Lys. Adsorption time 2h. Error bars represent one standard deviation, n = 4.

6.3.2 s-ATRP of MPC on Various Substrates for Improved Protein-resistance

6.3.2.1 Preparation and Characterization of Poly(MPC)-grafted Surfaces

The simple three-step modification process developed in this work was used to form poly(MPC) grafts on other polymeric substrates. The four selected substrates include PU film, a commercially available PU catheter as an example of a vascular biomaterial, PDMS film, and an experimental silicone hydrogel (referred to as Sil) as an example of an ophthalmic biomaterial. The ATRP grafting of MPC on these surfaces was again carried out in the presence of free (EBIB) initiator in solution. Table 6.3 shows the polymerization data, including monomer conversion, molecular weight and polydispersity of the polymer formed in solution. Monomer conversion in the range of 40-50% was achieved after 14 h reaction with an MPC:EBIB ratio of 100:1. The polydispersity was in the range of 1.10 to 1.20, indicating good control of the ATRP process. The poly(MPC) chains grafted on the surfaces were thus expected to be relatively uniform with DP ~50. These poly(MPC)-grafted surfaces are referred to as PU/MPC50, Catheter/MPC50, PDMS/MPC50 and Sil/MPC50.

Table 6.3 Conversion and molecular weight in s-ATRP of MPC from various polymeric substrates with sacrificial initiator in solution.

Surface	Molar Ratio of MPC:EBIB	Conversion (%)[a]	$M_{n,NMR}$ (g/mol)	$M_{n,GPC}$ (g/mol)[b]	Mw/Mn
PU/MPC50	100	52	15,600	11,900	1.17
Catheter/MPC50	100	40	12,000	9,400	1.14
PDMS/MPC50	100	43	12,900	11,100	1.20
Sil/MPC50	100	47	14,100	10,600	1.19

[a] Conversion calculated from ^{1}H-NMR data.

[b] Based on PEO calibration standards.

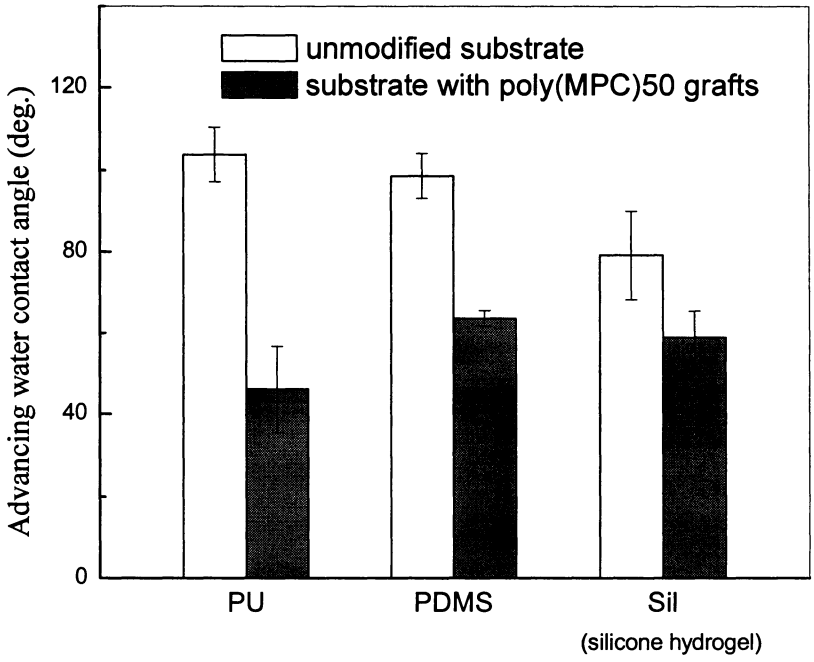

Figure 6.4 Water contact angles (advancing) of various polymeric substrates before and after ATRP grafting of MPC. Error bars represent one standard deviation, n = 4.

The water contact angles of the polymeric substrates before and after MPC grafting are shown in Figure 6.4. The unmodified PU film, PDMS film and Sil surfaces showed high advancing water contact angles ≥80°. The angles decreased after poly(MPC) grafting to values in the range of 45-65 ° depending on the substrate type. The lower angle of ~45° for PU/MPC50 may indicate higher poly(MPC) surface coverage than for PDMS/MPC50 and Sil/MPC50. The contact angles of the catheter surfaces were not determined due to the difficulty of measuring in tube geometry at small diameter.

The elemental compositions of these substrates before and after ATRP grafting of MPC are shown in Table 6.2. Bromine and phosphorus were not detected in the

unmodified surfaces. However, clear bromine and phosphorus signals were observed on the poly(MPC)-grafted surfaces. The nitrogen and oxygen contents of the grafted surfaces were higher than those of the unmodified surfaces. The presence of phosphorus and the increased nitrogen and oxygen contents suggested successful grafting of poly(MPC).

6.3.2.2 Protein Adsorption on the Poly(MPC)-grafted Surfaces

Figure 6.5 shows fibrinogen adsorption data for these substrates before and after ATRP grafting of MPC. Adsorption on the unmodified surfaces was again in the range of close-packed monolayers (0.2 to 1.6 $\mu g/cm^2$). The unmodified PDMS film surface adsorbed somewhat less (~0.6 $\mu g/cm^2$) than the unmodified PU film surface (~0.8 to 1.2 $\mu g/cm^2$), in agreement with previous reports.[19,34] The quantities adsorbed on the poly(MPC) grafted surfaces were significantly lower than on the unmodified materials, with reductions of 97%, 77%, 86% and 90%, respectively, on the grafted PU film, Catheter, PDMS film and Sil surfaces compared to the corresponding unmodified surfaces at a fibrinogen concentration of 0.05 mg/ml. The lowest fibrinogen adsorption and the greatest reduction in adsorption occurred on the PU/MPC50 surface suggesting the highest surface coverage of poly(MPC) on this surface. High surface coverage could result from the long chain length (DP of 52) and possibly high graft density on the carbon-rich PU surface compared to the silicone.

Data on the adsorption of lysozyme are shown in Figure 6.6. On the unmodified substrates, the adsorbed quantity was relatively high and much greater at 0.5 than at 0.05 mg/ml. At 0.5 mg/ml lysozyme concentration, the adsorbed quantities on all four unmodified surfaces were greater than 0.4 $\mu g/cm^2$, suggesting formation of multilayer or tight (compressed) monolayer. The poly(MPC) grafts adsorbed much less lysozyme with reductions of 92%, 83%, 77% and 80%, respectively, on the PU, Catheter, PDMS and Sil surfaces. The PU/MPC50 surface again showed higher resistance to lysozyme adsorption than the other grafted surfaces.

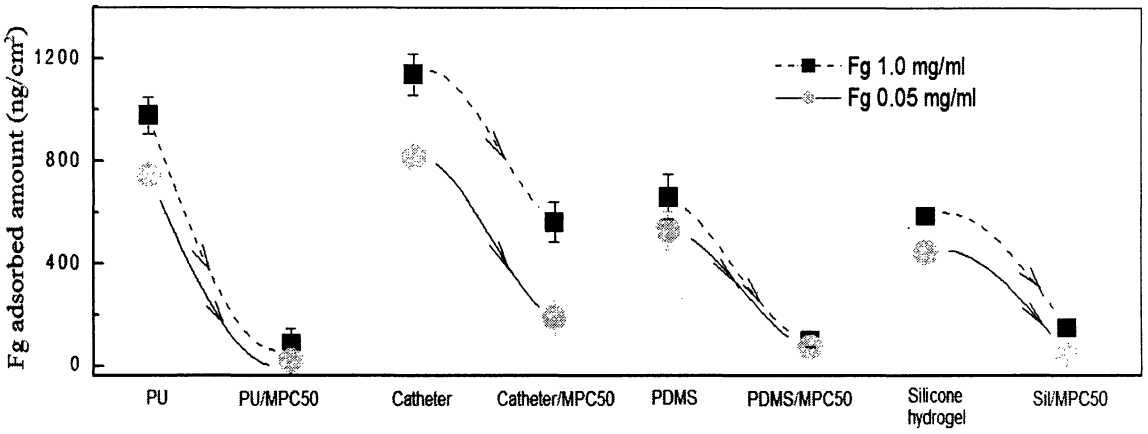

Figure 6.5 Fibrinogen adsorption on various substrates before and after ATRP grafting of MPC. Error bars represent one standard deviation, n = 4.

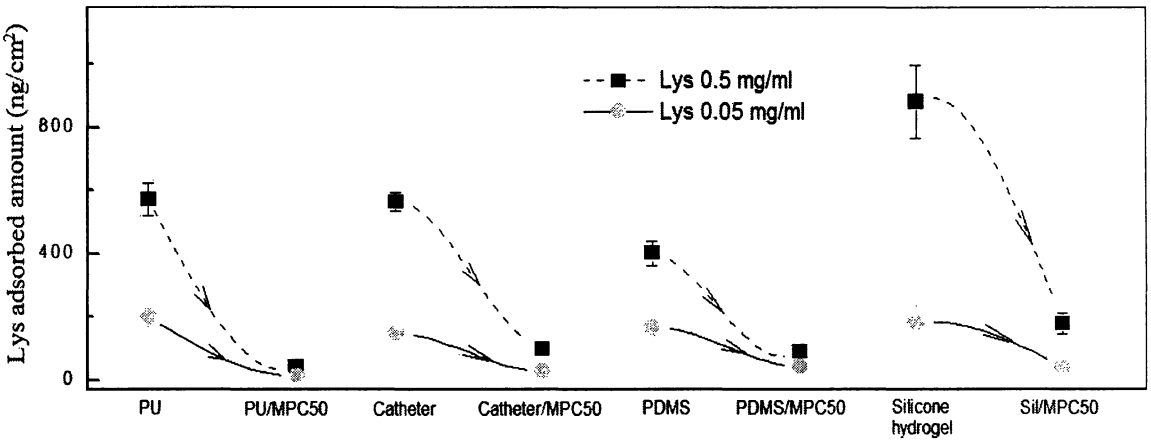

Figure 6.6 Lysozyme adsorption on various substrates before and after ATRP grafting of MPC. Error bars represent one standard deviation, n = 4.

The unmodified PU catheter and PU film adsorbed similar amounts of protein, despite the differences in chemical composition of the two materials (Catheter: ~80% Tecothane and ~20% barium sulphate; PU: 100% Tecothane). However, poly(MPC) grafts of given chain length on the PU catheter surface adsorbed less protein than the same grafts on the PU film, possibly due to a lower graft density on the catheter surface. The catheter surface may have a lower density of functional groups upon oxygen plasma treatment, and therefore a lower ATRP-initiator density and a lower density of poly(MPC) grafts.

It was also found that poly(MPC) grafts of given chain length on the silicone elastomer surfaces (PDMS and Sil) adsorbed slightly greater amounts of protein than the same grafts on the PU surfaces. These differences may again be due to differences in poly(MPC) graft density on the different substrates. It was reported[35-37] that oxygen plasma treatment on silicone produced surfaces with a high density of Si-O bonds and reduced the hydrogen and carbon contents in the surface region. The oxygen plasma-treated silicone surfaces showed low C-OH density compared to the relatively carbon-rich PU surfaces; this is expected to result in relatively low ATRP-initiator density and therefore low graft density of poly(MPC).

Several methods have been reported to immobilize ATRP initiators on silicone surfaces. For example, Xiao et al[38] used UV/ozone plasma to oxidize the PDMS surface and then reacted the resulting silanol groups with a gaseous trichlorosilane (1-trichlorosilyl-2-(*m-p*-chloromethylphenyl)ethane). Another method was to simply mix a vinyl-terminated ATRP-initiator with the reactants used in preparing a PDMS-based substrate.[39] Since the ATRP-initiator was distributed throughout the material, the total amount of initiator used was much larger than that present on surface. In the present work, ATRP initiator immobilization was achieved by a facile plasma-based technique, with many advantages such as ability to operate at room temperature, relatively short treatment

time, reproducibility and relatively low cost. Furthermore we have shown that this method is applicable to various practically used biomaterials typified by polyurethanes and silicones.

6.4 Conclusions

It was demonstrated that surface-initiated ATRP of MPC could be used to modify various types of polymeric substrates for improved protein resistance. Highly protein-resistant PU film, PU catheter, PDMS film and silicone hydrogel surfaces were prepared via a three-step procedure that included oxygen plasma treatment, initiator immobilization, and s-ATRP of MPC. The surfaces before and after modification were characterized by advancing water contact angle and XPS. The data confirmed successful grafting of poly(MPC), and showed that, on the PU surfaces, a range of poly(MPC) chain lengths were achievable by varying the monomer/initiator molar ratio.

The effect of poly(MPC) chain length on the protein-resistance of the PU surfaces was investigated in single protein experiments using fibrinogen and lysozyme as model proteins. It was found that protein adsorption on the poly(MPC) grafts was significantly lower than on the unmodified PU film surface, and that the adsorbed amounts decreased with increasing poly(MPC) graft length. Moreover, the poly(MPC) grafts were of comparable protein resistance to poly(OEGMA) grafts of similar chain length.

Fibrinogen and lysozyme adsorption experiments on the four modified substrates showed that ATRP grafting of MPC improved the protein resistance of these surfaces significantly. Grafts of poly(MPC) of chain length ~50 reduced both fibrinogen and lysozyme adsorption by 75 to 97%. The modified PU film showed the greatest reduction.

Acknowledgments: This work was supported by a Strategic Grant of the Natural Sciences and Engineering Research Council of Canada (NSERC). We also thank the Canada Foundation for Innovation (CFI) for supporting the research facilities in our laboratories. We thank Professor K. Ishihara for providing the MPC monomer used in this research.

6.5 References

1 Motomura T., Maeda T., Kawahito S., Matsui T., Ichikawa S., Ishitoya H., Kawamura M., Shinohara T., Sato K., Kawaguchi Y., Taylor D., Oestmann D., Glueck J., Nose Y., DeBakey M. E., Development of silicone rubber hollow fiber membrane oxygenator for ECMO, Artif. Organs, 27, 1050 (2003).

2 Goda T., Konno T., Takai M., Moro T., Ishihara K., Biomimetic phosphorylcholine polymer grafting from polydimethylsiloxane surface using photo-induced polymerization, Biomaterials, 27, 5151 (2006).

3 Zdrahala R. J., Zdrahala I. J., Biomedical applications of polyurethanes: a review of past promises, present realities, and a vibrant future, J. Biomater. Appl., 14, 67 (1999).

4 Xue L., Greisler H. P., Biomaterials in the development and future of vascular grafts, J. Vasc. Surg., 37, 472 (2003).

5 Yoo H-J., Kim H-D., Characteristics of crosslinked blends of Pellethene® and multiblock polyurethanes containing phospholipid, Biomaterials, 26, 2877 (2005).

6 Brash J. L., Exploiting the current paradigm of blood-material interactions for the rational design of blood-compatible materials, J. Biomater. Sci. Polym. Edn., 11, 1135 (2000).

7 Ishihara K., Nomura H., Mihara T., Kurita K., Iwasaki Y., Nakabayashi N., Why do phospholipid polymers reduce protein adsorption? J. Biomed. Mater. Res., 39, 323 (1998).

8 Ishihara K., Ziats N. P., Tierney B. P., Nakabayashi N., Anderson J. M., Protein adsorption from human plasma is reduced on phospholipids polymers, J. Biomed. Mater. Res., 25, 1397 (1991).

9 Ishihara K., Oshida H., Endo Y., Ueda T., Watanabe A., Nakabayashi N., Hemocompatibility of human whole-blood on polymers with a phospholipids polar group and its mechanism, J. Biomed. Mater. Res., 26, 1543 (1992).

10 Feng W., Zhu S., Ishihara K., Brash J. L., Protein resistant surfaces: Comparison of acrylate graft polymers bearing oligo-ethylene oxide and phosphorylcholine side chains, Biointerphases, 1, 50 (2006).

11 Lewis A. L., Phosphorylchoine-based polymers and their use in the prevention of biofouling, Coll. Surf. B: Biointerf., 18, 261 (2000).

12 Lewis A. L., Furze J. D., Small S., Robertson J. D., Higgins B. J., Taylor S., Ricci D. R., Long-term stability of a coronary stent coating post implantation, J. Biomed. Mater. Res. B: Appl. Biomater., 63, 699 (2002).

13 Claire P. de S., Degradation of PEO in the solid state: a theoretical kinetic model, Macromolecules, 42, 3469 (2009).

14 Lee S-H., Kim S-H., Kim Y-H., Han Y-K., Synthesis and degradation Behaviors of PEO/PL/PEO tri-block copolymers, Macromolecular Research, 10, 85 (2002).

15 Maechling-Strasser C., Dejardin P., Galin J. C., Schmitt A., Preadsorption of polymers on glass and silica to reduce fibrinogen adsorption, J. Biomed. Mater. Res., 23, 1385 (1989).

16 Lee J. H., Kopecek J., Andrade J. D., Protein-resistant surfaces prepared by PEO-containing block copolymer surfactants, J. Biomed. Mater. Res., 23, 351 (1989).

17 Ma X., Su Y., Sun Q., Wang Y., Jiang Z., Preparation of protein-adsorption-resistant polyethersulfone ultrafiltration membranes through surface segregation of amphiphilic comb copolymer, J. of Membr. Sci., 292, 116 (2007).

18 Han D-K., Park K-D., Ahn K-D., Jeong S-Y., Kim Y-H., Preparation and surface characterization of PEO-grafted and heparin-immobilized polyurethanes, J. Biomed. Mater. Res., 23, 87 (1989).

19 Jin Z., Feng W., Zhu S., Sheardown H., Brash J. L., Protein-resistant polyurethane via surface-initiated atom transfer radical polymerization of oligo(ethylene glycol) methacrylate, J. Biomed. Mater. Res. A, 91A, 1189 (2009).

20 Liu P., Su Z., Surface-initiated atom transfer radical polymerization (SI-ATRP) of MMA from PANI powders, Polym. Bullet., 55, 411 (2005).

21 Zhang H., Shouro D., Itoh K., Takata T., Jiang Y., Grafting polymer from poly(ethylene terephthalate) films by surface-initiated ATRP, J. Appl. Polym. Sci., 108, 351 (2008).

22 Jin Z., Feng W., Beisser K., Zhu S., Sheardown H., Brash J. L., Protein-resistant polyurethane prepared by surface-initiated atom transfer radical graft polymerization (ATRgP) of water-soluble polymers: Effects of main chain and side chain lengths of grafts, Coll. Surf. B: Biointerfaces, 70, 53 (2009).

23 Klenkler B. J., Griffith M., Becerril C., West-Mays J. A., Sheardown H., EGF-grafted PDMS surfaces in artificial cornea applications, Biomaterials 26, 7286 (2005).

24 Siow K. S., Britcher L., Kumar S., Griesser H. J., Plasma methods for the generation of chemically reactive surfaces for biomolecule immobilization and cell colonization: A review, Plasma Process and Polym., 3, 392 (2006).

25 Cvelbar U., Pejovnik S., Mozetie M., Zalar A., Increased surface roughness by oxygen plasma treatment of graphite/polymer composite, Appl. Surf. Sci., 210, 255 (2003).

26 Feng W., Zhu S., Ishihara K., Brash J. L., Adsorption of fibrinogen and lysozyme on silicon grafted with poly(2-methacryloyloxyethyl phosphorylcholine) via surface-initiated atom transfer radical polymerization, Langmuir, 21, 5980 (2005).

27 Unsworth L. D., Sheardown H., Brash J. L., Protein-reistant poly(ethylene oxide)-grafted surfaces: chain density-dependent multiple mechanisms of action, Langmuir, 24, 1924 (2008).

28 Swaraj S., Oran U., Lippitz A., Friedrich J. F., Unger W. E. S., Surface analysis of plasma deposited polymer films, 6: analysis of plasma deposited allyl alcohol films before and after aging in air, Plasma Process Polym., 2, 572 (2005).

29 France R. M., Short R. D., Plasma treatment of polymers: effects of energy transfer from an argon plasma on the surface chemistry of PS, LDPE, PP and PET, J. Chem. Soc. Faraday Trans., 93, 3173 (1997).

30 Kang I. K., Kwon O. H., Lee Y. M., Sung Y. K., Preparation and surface characterization of functional group-grafted and heparinimmobilized polyurethanes by plasma glow discharge, Biomaterials, 17, 841 (1996).

31 Marutani E., Yamamoto S., Ninjbadgar T., Tsujii Y., Fukuda T., Takano M., Surface-initiated atom transfer radical polymerization of methyl methacrylate on magnetite nanoparticles, Polymer, 45, 2231 (2004).

32 Couet J., Biesalski M., Surface-initiated ATRP of N-isopropylacrylamide from initiator-modified self-assembled peptide nanotubes, Macromolecules, 39, 7258 (2006).

33 Unsworth L. D., Sheardown H., Brash J. L., Protein resistance of surfaces prepared by sorption of end-thiolated poly(ethylene glycol) to gold: Effect of surface chain density, Langmuir, 21, 1036 (2005).

34 Chen H., Zhang Z., Chen Y., Brook M. A., Sheardown H., Protein repellant silicone surfaces by covalent immobilization of poly(ethylene oxide), Biomaterials, 26, 2391 (2005).

35 Langowski B. A., Uhrich K. E., Oxygen plasma-treatment effects on Si transfer, Langmuir, 21, 6366 (2005).

36 Roth J., Albrecht V., Nitschke M., Bellmann C., Simon F., Zschoche S., Michel S., Luhmann C., Crundke K., Voit B., Surface functionalization of silicone rubber for permanent adhesion improvement, Langmuir, 24, 12603 (2008).

37 Millare B., Thomas M., Ferreira A., Xu H., Holesinger M., Vullev V. I., Dependence of the quality of adhesion between poly(dimethylsiloxane) and glass surfaces on the conditions of treatment with oxygen plasma, Langmuir, 24, 13218 (2008).

38 Xiao D., Zhang H., Wirth M., Chemical modification of the surface of poly(dimethylsiloxane) by atom-transfer radical polymerization of acrylamide, Langmuir, 18, 9971 (2002).

39 Wu Y., Huang Y., Ma H., A facile method for permanent and functional surface modification of poly(dimethylsiloxane), J. Am. Chem. Soc., 129, 7226 (2007).

40 van Poll M. L., Zhou F., Ramstedt M., Hu L., Huck W. T. S., A self-assembly approach to chemical micropatterning of poly(dimethylsiloxane), Angew. Chem. Int. Ed., 46, 6634 (2007).

CHAPTER 7 Summary and Recommendations for Future Work

7.1 Summary of Thesis Work

A method employing oxygen plasma treatment followed by s-ATRP of OEGMA was developed to prepare polymer brushes of high graft density and controlled, uniform molecular weight from PU surfaces. The main chain length of grafted polymers was adjusted by varying the molar ratio of monomer (OEGMA, MW 300) to sacrificial initiator in solution from 5:1 to 200:1. The PU surfaces were characterized before and after each step of modification by water contact angle, AFM, and XPS. Polymer brushes having high grafting density and well controlled graft length were achieved using this method.

Protein adsorption experiments from tris-buffered saline (TBS) and plasma were carried out to evaluate the protein resistance of the surfaces. Adsorption from single and binary protein solutions as well as from plasma was found to be significantly reduced after surface modification. Adsorption decreased with increasing poly(OEGMA) main chain length. On the surface with the highest main chain length of 200, fibrinogen adsorption from buffer was reduced by 96-99%. From plasma, levels as low as 1-5 ng/cm^2 were observed. In binary protein adsorption experiments with mixed solutions of lysozyme and fibrinogen, the Lys:Fg ratios in the layers adsorbed to the PU/poly(OEGMA) surfaces were found to be higher than those in the solution, indicating that resistance to adsorption of the larger protein was greater than to the smaller one.

The effect of poly(OEGMA) side chain length on the protein-resistant properties of polymer brushes was investigated using monomers of MW 300, 475, 1100 g/mol. It was found that the surface with the longest main chain and shortest side chain grafts had

the highest resistance to protein adsorption. For a given main chain length, the Fg adsorption level did not change significantly with increasing side chain length. However, Lys adsorption increased with increasing side chain length, possibly due to decreasing graft density as monomer size and chain "footprint" on the surface increased. Adsorption resistance was generally greater for the bigger protein.

To achieve a wide range of EO densities including high levels that were not possible with simple grafting, we developed a method for double or sequential grafting. This involved grafting of poly(HEMA) to the surface followed by grafting of poly(OEGMA) to the poly(HEMA) grafts. Both steps used s-ATRP. Protein adsorption on the double grafted surfaces was greatly reduced compared to the unmodified PU, and was lower than on the corresponding single grafted OEGMA surfaces. On the double grafted surface with the highest poly(OEGMA) chain length of 100, the reduction of Lys adsorption was in the range of 95 to 98% and the reduction of Fg and Lac adsorption was more than 99% compared to the unmodified PU. Adsorption from binary protein solutions showed that the double grafted surfaces resisted the three proteins equally, i.e. independent of protein size.

The simple three-step grafting method was used as a general strategy to achieve high-density grafts on various polymeric substrates including polyurethane and silicone films and commercially available polyurethane catheters. Poly(MPC) grafts having various chain lengths were grafted from these substrates and were found to reduce protein adsorption significantly. On polyurethane surface grafted with poly(MPC) of chain length 100, the reduction in adsorption was ~96% for lysozyme and ~99% for fibrinogen, i.e. comparable to the reductions seen for poly(OEGMA) grafts of similar chain length.

7.2 Recommendations for Future Work

Much more work on the biointeractions of these materials should be carried out. Examples of in vitro studies related to blood compatibility include effects on coagulation, and platelet interactions. Stability of the grafted layers over time should also be investigated. Eventually in vivo evaluations to determine tissue and blood responses and to ascertain long term stability will be required.

Broader extensions of this work should also be considered. The simple three-step ATRP-grafting procedure with OEGMA could be used as a general strategy to achieve high-density grafts on various polymeric substrate surfaces. Therefore since ATRP has the potential to be used with a wide variety of monomers to produce polymers of controlled architecture including block copolymers,[1,2] this simple three-step procedure could be used more broadly for the preparation of biocompatible and/or bioactive polymer brushes for biomedical applications.

For example, positively charged quaternized poly (2-(dimethylamino)ethyl methacrylate) (poly(DMAEMA)) has significant antibacterial properties.[3,4] The three-step ATRP-grafting of tertiary amine-containing DMAEMA could be performed on polyurethane or other polymeric substrates. Subsequent quaternization of the amino groups by an alkyl halide may provide a poly(DMAEMA) surface with antibacterial properties. Poly(OEGMA)-b-poly(DMAEMA) block-copolymer brushes could also be formed by the same strategy and may be expected to be not only protein-resistant, but also antibacterial.

Other types of bioactive surface could also be prepared based on this general procedure. For example, poly(glycidyl methacrylate) (poly(GMA)) and/or poly(OEGMA)-b-poly(GMA) brushes could be formed on polymeric biomaterial surfaces. Pyridyl disulfide moieties could be attached to the polymer brushes by reaction with

epoxy groups in the GMA units.[5] Thiol-containing biomolecules such as proteins or antibodies could then be immobilized on these polymer brushes via a thiol-disulfide interchange reaction.[5] Biomolecule-immobilized surfaces are of great interest for applications in biosensors and biotechnology,[6] and may provide a way to determine the graft density of polymer chains on polymeric substrates, which remains unknown in this work due to the lack of techniques for quantification.

7.3 References

1. Coessens V., Pintauer T., Matyjaszewski K., Functional polymers by atom transfer radical polymerization, Prog. Polym. Sci., 26, 337 (2001).
2. Matayjaszewski K., Xia J., Atom transfer radical polymerization, Chem. Rev., 101, 2921 (2001).
3. Kochkodan V. M., Hilal N., Goncharuk V. V., Al-Khatib L., Levadna T. I., Effect of the surface modification of polymer membranes on their microbiological fouling, Colloid J., 683, 267 (2006).
4. Lee S. B., Koepsel R. R., Morley S. W., Matyjaszewski K., Sun Y., Russell A. J., Permanent, nonleaching antibacterial surfaces. 1. Synthesis by atom transfer radical polymerization, Biomacromolecules, 5, 877 (2004).
5. Iwata R., Satoh R., Iwasaki Y., Akiyoshi K., Covalent immobilization of antibody fragments on well-defined polymer brushes via site-directed method, Coll. Surf. B: Biointerf., 62, 288 (2008).
6. Goddard J. M., Hotchkiss J. H., Polymer surface modification for the attachment of bioactive compounds, Prog. Polym. Sci., 32, 698 (2007).

APPENDIX A List of Publications

Publications

(1) **Jin Z**, Feng W, Zhu S, Sheardown H, Brash J L, "Protein-Resistant Polyurethane via Surface-Initiated Atom Transfer Radical Polymerization of Oligo(ethylene glycol) Methacrylate", *Journal of Biomedical Materials Research A.*, 2009, 91A, 1189-1201.

(2) **Jin Z**, Feng W, Beisser K, Zhu S, Sheardown H, Brash J L, "Protein-Resistant Polyurethane Prepared by Surface-initiated ATRgP of Water-soluble Polymers: Effects of Main Chain Length and Side Chain Length of Graft", *Colloids and Surfaces B: Biointerfaces*. 2009, 70, 53-59.

(3) **Jin Z**, Feng W, Zhu S, Sheardown H, Brash J L, "Protein-Resistant Polyurethane by Sequential Grafting of Poly(2-hydroxyethyl methacrylate (HEMA)) and Poly(oligo(ethylene glycol) methacrylate (OEGMA)) via Surface-Initiated ATRP", Submitted to *Journal of Biomedical Materials Research A*.

(4) **Jin Z**, Feng W, Zhu S, Sheardown H, Brash J L, "Protein-Resistant Materials via Surface-Initiated Atom Transfer Radical Polymerization of 2-Methacryloyloxyethyl Phosphorylcholine", *Journal of Biomaterial Science, Polymer Edition*, accepted.

(5) **Jin Z**, Brash J L, Zhu S, "ATRP Grafting of Oligo(ethylene glycol) Methacrylates from Gold Surface: Effect of Monomer Size on Grafted Chain and EO Unit Densities", *Canadian Journal of Chemistry*, accepted.

Conference Presentations

(1) **Jin Z**, Feng W, Brash J L, Zhu S, "High-performance Non-biofouling Biomaterials Prepared by Surface-initiated Atom Transfer Radical Polymerization", Emerging Materials Knowledge Network 3rd Annual Conference, Toronto, Canada, June 15, **2007**. (Poster presentation, **the First Prize**)

(2) **Jin Z**, Feng W, Zhu S, Brash J L, "Protein-Resistant Polyurethane Prepared by Surface Initiated Atom Transfer Radical Polymerization of Oligo(ethylene glycol) Methacrylate (OEGMA)", 26th Canadian Biomaterials Society (CBS) Conference, London, Canada, May 25-27, **2007**. (Oral presentation)

(3) **Jin Z**, Feng W, Brash J L, Zhu S, "High Protein-Resistant Biomaterials Prepared by Surface Initiated Atom Transfer Radical Polymerization of Water-Soluble Polymers", 57th Canadian Chemical Engineering Conference, Edmonton, Alberta, Canada, October 28-31, **2007**. (Oral presentation)

(4) **Jin Z**, Feng W, Zhu S, Brash J L, "Protein-Resistant Polyurethane Prepared by Surface Initiated ATRP of Oligo(ethylene glycol) Methyl Ether Methacrylate (OEGMA): Effects of Main Chain Length and Side Chain Length of Graft", 8th World Biomaterials Congress 2008, Amsterdam, Netherlands, May 28-June 1, **2008**. (poster presentation, **2008 CBS Student Travel Award**)

(5) **Jin Z**, Feng W, Brash J L, Zhu S, "Protein-Resistant Polyurethane Prepared by Surface Initiated Atom Transfer Radical Polymerization", 2009 Chemical Engineering Graduate Student Seminar Day, McMaster University, Canada, April 8, **2009**. (oral presentation, **A.E. Hamielec Award**)

(6) **Jin Z**, Feng W, Zhu S, Brash J L, "Protein-Resistant Polyurethane by Sequentially-Grafted Poly(2-Hydroxyethyl Methacrylate) and Poly(Oligo(Ethylene Glycol)

Methacrylate) via Surface-Initiated ATRP", Society For Biomaterials (SFB) 2009 Annual Meeting and Exposition, San Antonio, Texas, USA, April 22-25, **2009**. (poster presentation)

(7) **Jin Z**, Feng W, Brash J L, Zhu S, "Atom Transfer Radical Polymerization Grafting with Well-Defined Polymer Brush for High Protein-Resistant Surfaces", Polymer Reaction Engineering 7 (PRE7), Niagara Falls, Canada, May 3-8, **2009**. (oral presentation)

(8) **Jin Z**, Feng W, Zhu S, Brash J L, "Protein-Resistant Polyurethane by Sequential Graft Polymerization of HEMA and OEGMA via Surface-Initiated ATRP", 27th Conference of the Canadian Biomaterials Society, Quebec City, Canada, May 20-23, **2009**. (oral presentation, **2009 CBS Student Travel Award**)

(9) **Jin Z**, Feng W, Brash J L, Zhu S, "Surface Modification via Atom Transfer Radical Polymerization Grafting for Protein-Resistant Polyurethane", 8th World Congress of Chemical Engineering, Montreal, Canada, August 23-27, **2009**. (oral presentation)

Awards and Scholarships

2009	A.E. Hamielec Award
2009	CBS Student Travel Award
2008 - 2009	Ontario Graduate Fellowship – McMaster Prestige Award
2008	CBS Student Travel Award
2007	The First Prize for Poster Competition on EMK 3rd Annual Conference

APPENDIX B ATRP Grafting of Oligo(ethylene glycol) Methacrylates from Gold Surface: Effect of Monomer Size on Grafted Chain and EO Unit Densities

Authors: **Z. Jin**, J.L. Brash, S. Zhu

Publication Information: Canadian Journal of Chemistry, accepted
honouring Mitchell A. Winnik

In this thesis work, the effects of poly(OEGMA) main chain length (Chapter 3) and side chain length (Chapter 4) on the protein-resistant properties of polymer brushes were investigated. However, the grafted chain density and EO unit density, which are crucial factors in determining the protein resistance of a grafted surface, remain unknown due to the lack of techniques for quantification.

In this appendix work, instead of polyurethane (the main target substrate of the work) or other polymeric substrate, we chose a flat, smooth gold substrate, which allows characterization of the grafted layer by ellipsometry. The chain density and EO unit density were calculated from the thickness of the grafts as determined by ellipsometry, and the effects of monomer MW and initiator density on surface chain density and EO unit density were investigated. In related work we are examining the impact of surface EO density on the protein resistance of these surfaces.

Abstract: Oligo(ethylene glycol) methacrylate (OEGMA) was grafted from Au surface via surface-initiated atom transfer radical polymerization (s-ATRP). The initiator density was adjusted by the mole fractions of surface-attachable ATRP initiator and diluting agent. Three OEGMA monomers of MW 300, 475, 1100 g/mol were used. The Au surfaces before and after modification were characterized by water contact angle and ellipsometry. The effect of monomer MW and initiator density on surface chain density and EO unit density was investigated. It was found that at low initiator density (mole fraction of initiator of 2-5%), poly(OEGMA) grafts had comparable surface chain density independent of OEGMA MW. However, at high initiator density (mole fraction of initiator >10%), poly(OEGMA)$_{1100}$ had obviously lower chain densities than poly(OEGMA)$_{300}$ and poly(OEGMA)$_{475}$ which could be attributed to the size difference of the monomers. The low chain length and surface chain density of poly(OEGMA)$_{1100}$ resulted in its relatively low surface EO unit density.

Keywords: Au surface; poly(ethylene glycol); atom transfer radical polymerization (ATRP); grafting; surface chain density; surface EO unit density; monomer MW.

Introduction

Poly(ethylene oxide) (PEO) and oligo(ethylene glycol) (OEG)-containing polymers (e.g. poly(oligo(ethylene glycol) methacrylate) (OEGMA)) have attracted much attention as a biomaterial coating due to its high ability to resist non-specific protein adsorption, biofouling and its high biocompatibility.[1] It has been shown that many factors including PEO chain length, surface chain density, polymer conformation and surface EO unit density, have strong effects on the protein-resistant and biocompatible performance.[2-4] However, details of these effects are still a matter of debate. A significant barrier to elucidate these factors to protein resistance and/or biocompatiblity is the lack of techniques to control and accurately measure these properties.

Recently, the development of atom transfer radical polymerization (ATRP) method provides a facile way to achieve uniform and tunable graft chain length on surface.[5-8] It has also been found that chain density of polymer grafts can be varied by adjusting the initiator density on surface,[9,10] and the monomer size has an effect on the polymer chain density formed via surface-initiated ATRP (s-ATRP).[11] Recently, the surface-initiated ATRP of PEO-containing molecules (such as OEGMA) has been performed on well-defined model substrates such as silicon and gold,[9,10] which allow relatively accurate characterization of polymer grafts via ellipsometry and/or AFM compared to other substrates such as polymeric substrate. However, there is very little work where surface chain density and surface EO unit density are finely tuned by varying monomer MW and initiator density, and where the effect of monomer MW and initiator density was systematically studied.

In this study, oligo(ethylene glycol) methacrylate (OEGMA) was grafted from Au surface via s-ATRP with various initiator densities and three OEGMA monomers of MW 300, 475, 1100 g/mol (eq. 5, 9 and 23 ethylene oxide residues, respectively). The

effect of monomer MW and initiator density on surface chain density and surface EO unit density was investigated.

Experimental

Materials

Gold-coated silicon wafers (500-μm thickness, 100-mm diameter, Au coating layers of 100-nm thickness on both sides) were purchased from SVM (Silicon Valley Microelectronics, Inc.) and cut into 5×5 mm pieces using a Micro Ace Series 3 dicer (Loadpoint Ltd., England). Hydrogen peroxide (30%), ammonia solution (30%) and methanol (HPLC) were obtained from Caledon Laboratories LTD and used as received. Bis[2-(2'-bromoisobutyryloxy) ethyl] disulfide (the structure shown in Scheme B.1) was purchased from ATRP Solutions Inc., and used as received. Butyl disulfide (97%), ethyl 2-bromoisobutyrate (EBIB) (98%), 2,2'-bipyridyl (bpy) (99%), and Cu(I)Br (99.999%) were purchased from Sigma-Aldrich and used as received. OEGMA with molecular weights (MW) of 300, 475 and 1100, were purchased from Sigma-Aldrich and passed over a basic alumina column to remove inhibitor. Basic alumina (Brockman Activity 1, mesh 60-325) was purchased from Fisher Scientific and used as received. Deionized water used in this study had a resistivity of 18.2 MΩ·cm and nitrogen gas was of ultrahigh-purity (UHP) grade.

Pretreatment of Au surfaces

Gold-coated silicon chips (5×5 mm) were immersed in a solution having one part hydrogen peroxide, one part ammonium hydroxide, and five parts water at 80°C for 5 min, sonicated for 1 min, and rinsed in deionized water to remove any carbonaceous contamination. After cleaning, the gold-coated chips were either used immediately for the formation of the initiator self-assembled monolayer (SAM) or stored in ethanol at room temperature.

Formation of initiator monolayer on Au surfaces

The self-assembled monolayer (SAM) of initiator was formed by soaking the freshly cleaned gold-coated chips in an ethanol solution (total concentration 1 mM) containing disulfides for 24h without stirring at room temperature. The mixed disulfide solution contained bis[2-(2'-bromoisobutyryloxy) ethyl] disulfide (the initiator molecule **1** in Scheme B.1), and butyl disulfide as a diluting agent. The mole fraction of the initiator varied from 0, 2, 5, 10, 25, 50, 75, and 100%. The surfaces were removed from the solution, cleaned ultrasonically for 1 min in pure ethanol, and rinsed with THF, and then dried in a nitrogen stream. The gold surfaces with SAMs (referred to as Au/initiator) were either used immediately or stored in glass tubes under nitrogen at room temperature.

s-ATRP of OEGMA from initiator-functionalized gold surfaces

Poly(OEGMA)s with various side chain lengths (EO units) or monomer MWs (300, 475 and 1100 g/mol) were grafted from the Au/initiator surfaces via s-ATRP. The detailed procedure was described previously.[12,13] EBIB was used as a sacrificial initiator. The monomer concentration was fixed at 38% w/v and the molar ratio of OEGMA:EBIB:Cu(I)Br:bpy at 100:1:1:2, with methanol as solvent. 10 g OEGMA was used in an s-ATRP process with 40 pieces of gold-coated chips. The s-ATRP process was performed under nitrogen at room temperature for 48 h. The surfaces were then cleaned ultrasonically for 1 min in methanol, rinsed with methanol, and then dried in a nitrogen stream.

Characterization

Proton NMR spectroscopy (Bruker AC-P200 spectrometer, D_2O solvent) was used to determine OEGMA conversion in the s-ATRP reactions. Gel permeation chromatography (GPC, Waters 2690 separations module with a Waters 2410 refractive index detector, PEO calibration standards) was used to determine the molecular weight and polydispersity index (PDI) of poly(OEGMA) formed in solution. Water contact angle

measurements were performed on the gold surfaces with a Rame-Hart NRL goniometer (Mountain Lakes, NJ) at room temperature, using the sessile drop method.

An Exacta 2000 ellipsometer (Waterloo Digital Electronics) was used to determine the thicknesses of the initiator monolayer and poly(OEGMA) on the gold-coated substrates with single wavelength (6328 Å) and an incident angle of 70°. The gold-coated wafers were considered as the substrate, with refractive index (n_s) and extinction coefficient (k_s) of 0.19 ± 0.02 and 3.52 ± 0.08, respectively. For the initiator-functionalized and poly(OEGMA)-grafted surfaces, the polarizer (P) and analyzer (A) angles for the null condition were measured and thickness values were determined using a three-layer air-grafts-gold model via the Exacta 2000 Variable Theta Simplex Fitting Program. A refractive index of 1.46 was used for initiator SAMs and poly(OEGMA) grafts.[14,15]

The surface chain densities of poly(OEGMA) as well as initiator/diluting agent were calculated based on the following equation:[9,16]

$$\sigma = \frac{h\rho N_A}{\overline{M}_n} \qquad (1)$$

where σ is the surface chain density, h is the layer thickness determined by ellipsometry, ρ is the bulk density of the grafted layer (1.0 g/cm^3 was used for poly(OEGMA) and initiator SAMs), N_A is Avogadro's number, and $\overline{M}_n$ is the number-average molecular weight ($M_{n,GPC}$ was used for poly(OEGMA)). The molecular weight of poly(OEGMA) formed on surface is assumed to be the same as that of poly(OEGMA) formed in solution, and the mole fraction of initiator in the SAMs is assumed to be the same as that in the mixed disulfide solution during initiator-immobilization.

Results and discussion

Mixed SAMs formed on Au surfaces

Scheme B.1 illustrates the two-step reaction procedure for the synthesis of poly(OEGMA)-grafted Au surfaces (referred to as Au/poly(OEGMA)). The chain density of poly(OEGMA) was controlled through the surface initiator density in the SAMs. Bis[2-(2'-bromoisobutyryloxy) ethyl] disulfide (**1**) was used as the grafting initiator and butyl disulfide (**2**) as an inert "diluting agent" that chemisorbs to gold similarly to the initiator. The mole fractions of active initiator in the SAMs ranged from 2 to 100%.

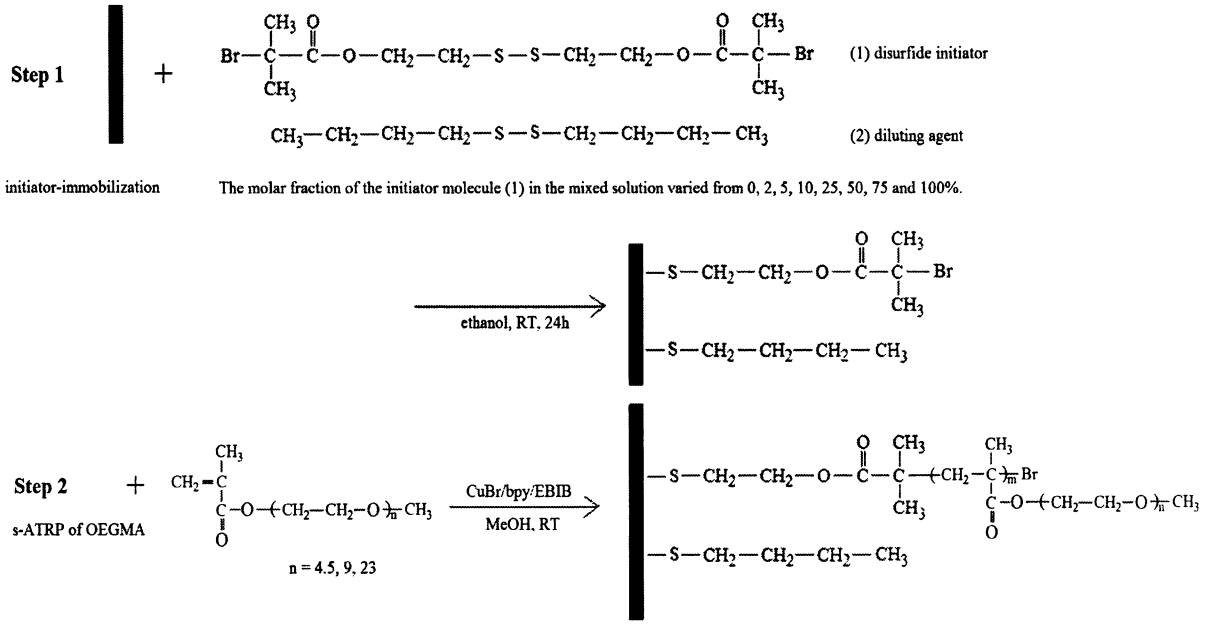

Scheme B.1 Two-step reaction procedure for the synthesis of poly(OEGMA)-grafted Au surface with varying graft chain density.

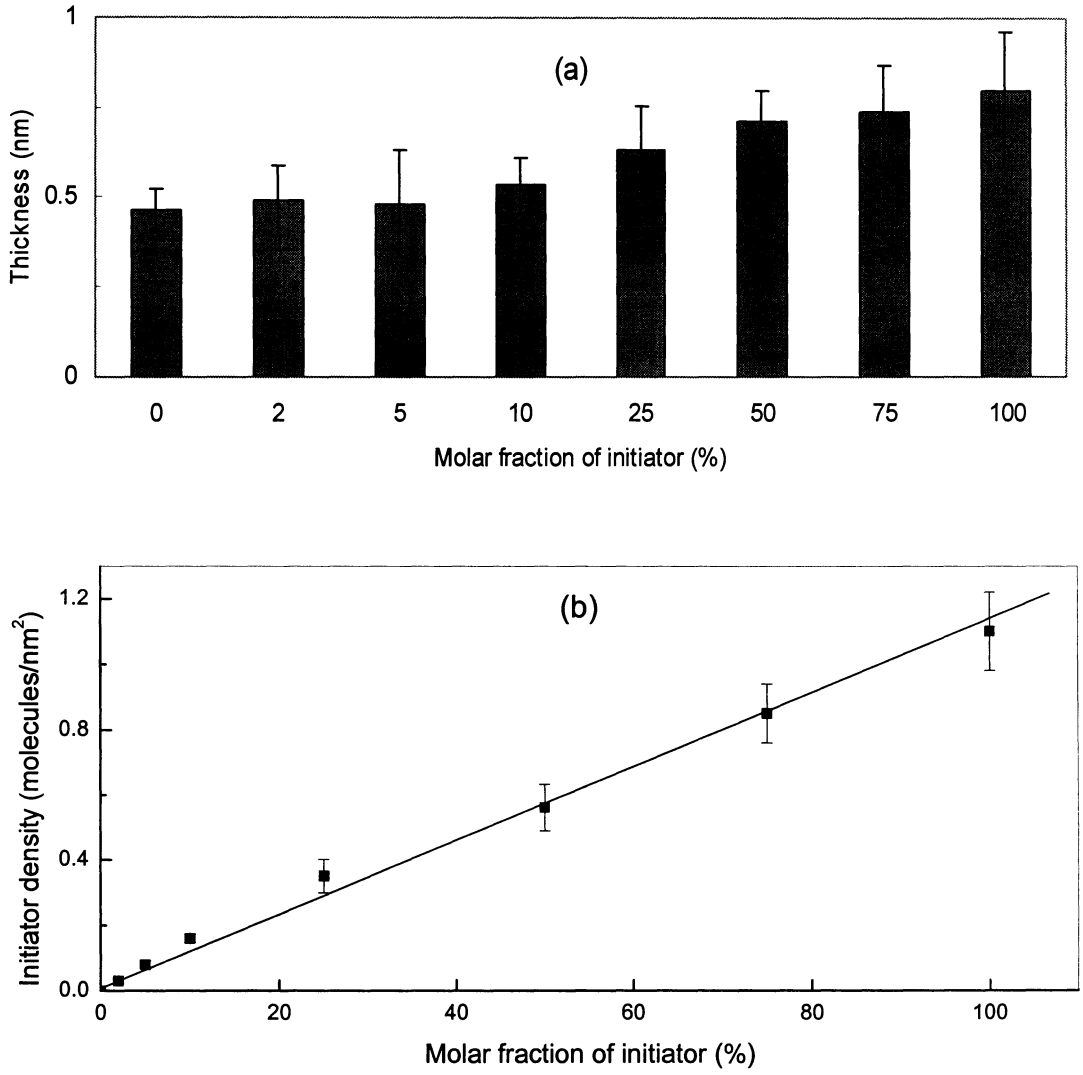

Figure B.1 (a) Ellipsometric thickness of the mixed SAMs of initiator and diluting agent. (b) Surface density of initiator in the mixed SAMs. Error bars represent one standard deviation, n = 4.

Figure B.1a shows the ellipsometric thickness of the SAMs having various mole fractions of initiator; values were in the range <1 nm. The 100% initiator layer was

significantly thicker than the 100% diluting agent layer, in agreement with the dimensions of the two molecules. The surface density (molecules/nm^2) of the SAMs was calculated from the thickness data, and the initiator density was estimated from the SAM density and the mole fraction of initiator. The initiator density (Figure B.1b) was found to increase linearly with increasing mole fraction of initiator in the mixed disulfide solution.

Poly(OEGMA) grafts via s-ATRP

ATRP grafting of OEGMA was carried out on the Au/initiator surfaces with Cu(I)Br/2bpy complex as catalyst and free/sacrificial initiator (EBIB) in solution. The free initiator in solution was in very large amounts compared to the initiator covalently-attached on surface. For a well-controlled ATRP process, the polymer chains formed by the free initiator in solution may be assumed to have the same chain length and distribution as the chains grafted on the surface.[17] The monomer conversion, molecular weight and polydispersity of the polymers formed in solution are shown in Table B.1. Complete conversion was achieved for the ATRP grafting of OEGMA of MW 300 and 475. However, for OEGMA of MW 1100, the conversion was limited to ~48%. Polydispersities determined by GPC were in the range of 1.05 to 1.19, indicating good control of the ATRP process.

Table B.1 Conversion and molecular weight in s-ATRP of OEGMA from Au/initiator surfaces with sacrificial initiator in solution.

OEGMA MW	Molar ratio OEGMA/EBIB	Conversion (%)[a]	Theoretical M_n (kg/mol)	$M_{n,GPC}$ (kg/mol)[b]	Mw/Mn
300	100	> 99	30	28.7	1.06
475	100	> 99	47.5	39.5	1.13
1100	100	48	52.8	49.0	1.05

[a] Conversion calculated from ^{1}H-NMR data.

[b] Based on PEO calibration standards.

The advancing water contact angles (θ_{Adv}) of the Au surfaces before and after modification are shown in Figure B.2. The contact angle of unmodified Au surface was about 65° and clearly decreased after poly(OEGMA) grafting. For a given monomer MW, especially for MW of 300 and 475, θ_{Adv} decreased slightly from ~55° to ~40° with increasing initiator fraction from 2% to 100%, presumably due to the increased surface density of the hydrophilic EO units at higher initiator density. For OEGMA of MW 1100, the contact angle leveled off at initiator fraction > 50%; this is in agreement with the thickness and density variation of the poly(OEGMA) grafts (Figure B.3).

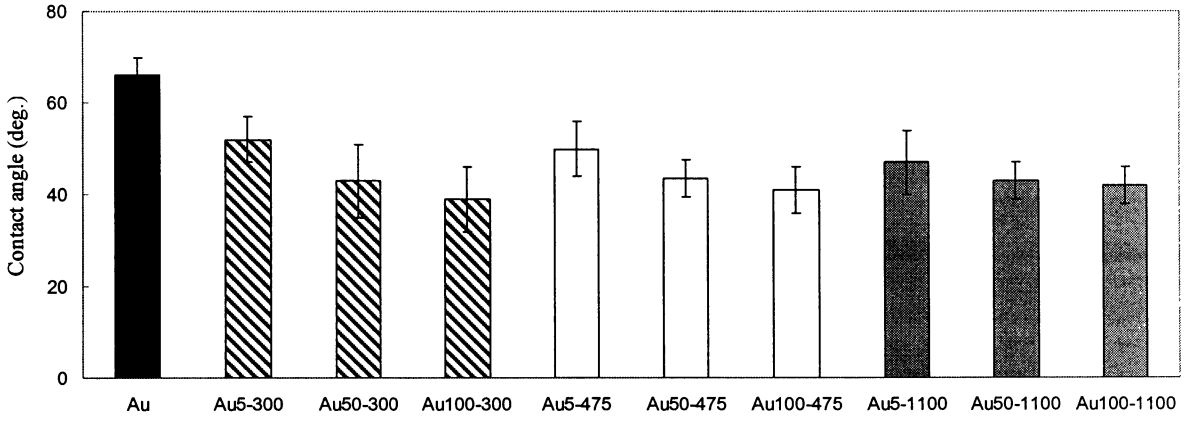

Figure B.2 Water contact angles (advancing) of poly(OEGMA)-grafted Au surfaces. The surfaces are named by the mole fraction of initiator (%) (first number) and the monomer MW (second number). Error bars represent one standard deviation, n = 4.

The thickness of poly(OEGMA) grafts was determined by ellipsometry and the data are shown in Figure B.3a. For a given monomer MW, the thickness of the grafts increased significantly with increasing initiator fraction or initiator density, and leveled off above an initiator fraction of 50%, especially for OEGMA of MW 1100. At relatively low surface initiator density (initiator fraction ~2%), poly(OEGMA)$_{1100}$ grafts showed a slightly higher thickness than poly(OEGMA)$_{300}$ presumably reflecting higher MW but

similar chain density. On surfaces with initiator fraction >10%, the poly(OEGMA)$_{1100}$ layer was obviously thinner than the poly(OEGMA)$_{300}$ and poly(OEGMA)$_{475}$ for a given initiator density. The low DP (~48) or short backbone length of poly(OEGMA)$_{1100}$ is one possible reason for the relatively low thickness of poly(OEGMA)$_{1100}$ layers.

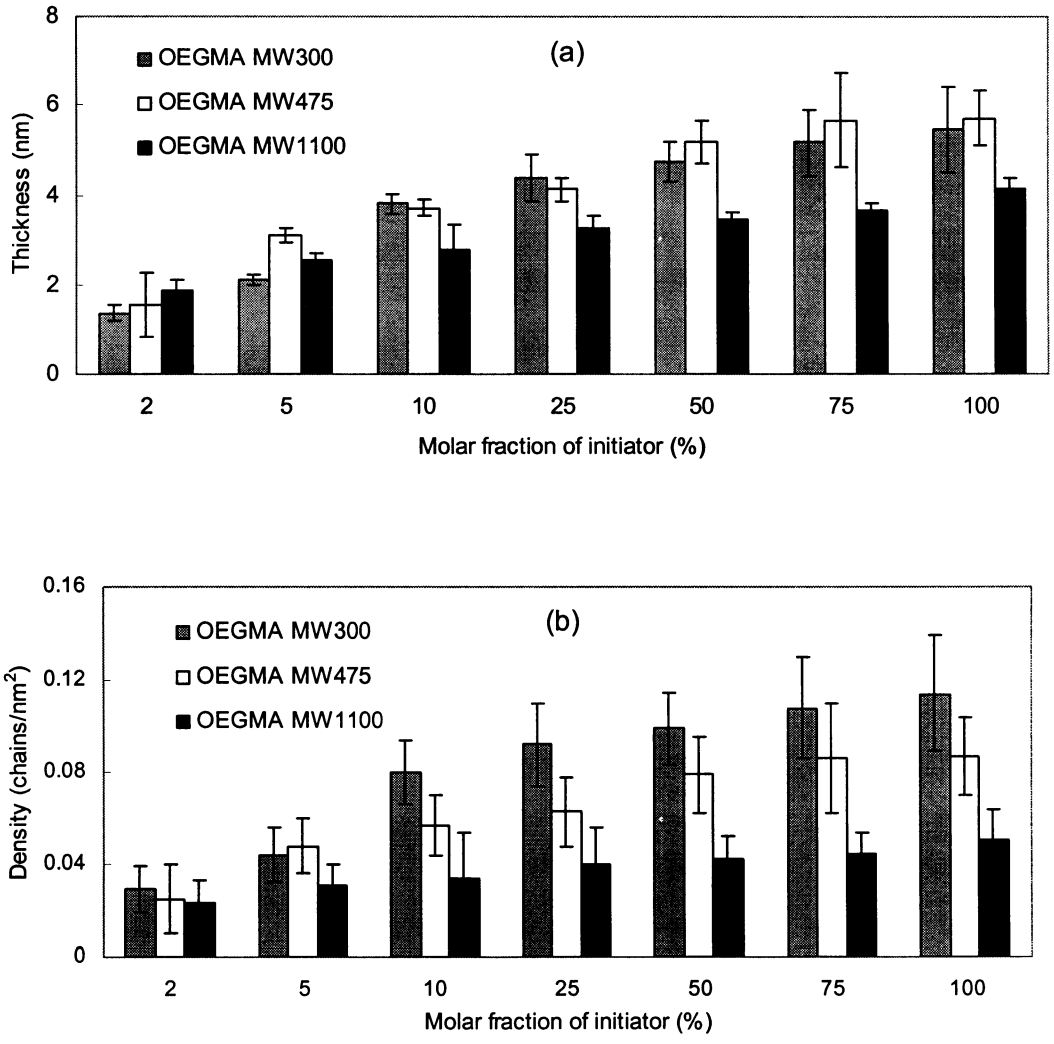

Figure B.3 (a) Ellipsometric thickness and (b) density (chains/nm^2) of the poly(OEGMA) grafts with various OEGMA MW 300, 475 and 1100. Error bars represent one standard deviation, n = 4.

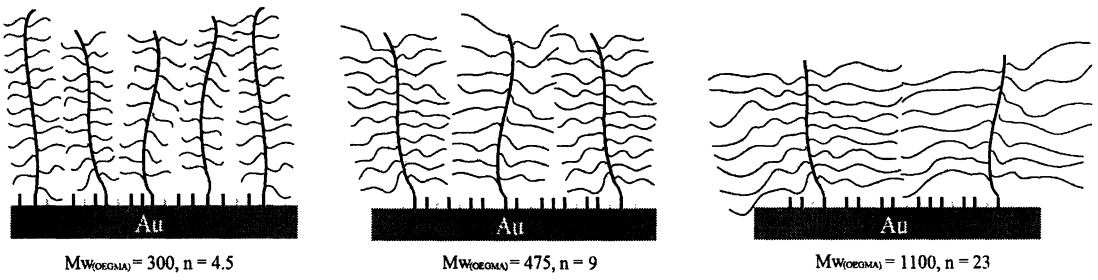

Scheme B.2 Highly stretched poly(OEGMA) brushes with various OEGMA MW.

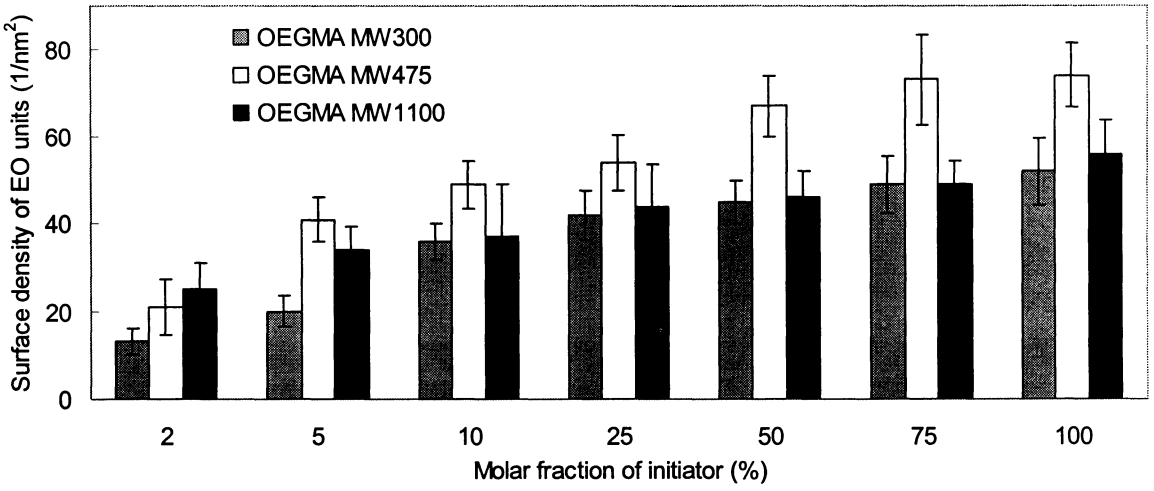

Figure B.4 Surface density of EO monomer units on Au surfaces for various OEGMA MW and initiator density. Error bars represent one standard deviation, n = 4.

The surface densities (chains/nm^2) of the poly(OEGMA) grafts calculated from the ellipsometric thickness data are shown in Figure B.3b. For a given monomer MW, the poly(OEGMA) density increased significantly with increasing initiator fraction from 2% to ~50%, and leveled off at higher initiator fractions. At low initiator density (mole fraction 2-5%), poly(OEGMA) grafts had comparable surface density (chains/nm^2)

independent of OEGMA MW; however at high initiator density (mole fraction > 10%), significant differences were seen in the densities of poly(OEGMA) grafts for the different monomer MWs. Poly(OEGMA)$_{300}$ and poly(OEGMA)$_{475}$ showed higher graft densities than poly(OEGMA)$_{1100}$, possibly attributable to the size difference of the monomers. Scheme B.2 shows a schematic of the stretched out structures of poly(OEGMA) brushes (the expected configuration at relatively high initiator density) and the effect of monomer MW on surface density of polymer chains. The larger monomer with larger footprint, once adsorbed, may restrict access of the catalyst complex and monomer to nearby initiator sites, thus reducing initiation efficiency and graft chain density.

The surface densities of EO repeat unit residues (estimated from monomer MW, polymer chain length and polymer chain density) are shown in Figure B.4. For a given monomer MW, the surface EO unit density generally increased with increasing initiator density in the range (0.03-1.1/nm^2) investigated. For a given high initiator density (initiator fraction >10%), the poly(OEGMA)$_{475}$ layer had the highest EO unit density. The poly(OEGMA)$_{300}$ and poly(OEGMA)$_{1100}$ layers had similar EO unit density. The low DP and low surface chain density of poly(OEGMA)$_{1100}$ relative to poly(OEGMA)$_{475}$ and poly(OEGMA)$_{300}$ probably account for its relatively low surface EO unit density. Poly(OEGMA)$_{300}$ had the similar chain density to poly(OEGMA)$_{475}$ at the relatively low initiator density and obviously higher chain density than poly(OEGMA)$_{475}$ at the relatively high initiator density. However, Poly(OEGMA)$_{300}$ has much shorter PEO side chain length, about half of side chain length of Poly(OEGMA)$_{475}$, which resulted in the lower EO unit density than Poly(OEGMA)$_{475}$.

Conclusions

Poly(OEGMA) was grafted from Au surface via a two-step procedure including initiator-chemisorption and surface-initiated ATRP. The initiator density was adjusted by mixing initiator with an inert surface-attachable diluting agent. Three OEGMA monomers

of MW 300, 475, 1100 g/mol were used. The Au surfaces were characterized by water contact angle and ellipsometry before and after modification. The data indicated successful formation of initiator and poly(OEGMA) layers with a range of surface densities.

The surface densities of initiator and poly(OEGMA) were calculated from the ellipsometric thickness of the layers. The initiator density was found to increase linearly with increasing mole fraction of initiator in the initiator/diluting agent mixture. For a given monomer MW, the poly(OEGMA) thickness and density increased with increasing initiator fraction from 2% to ~50%, and leveled off at higher initiator fractions. At low initiator density (mole fraction of initiator 2-5%), poly(OEGMA) grafts had comparable surface chain density independent of OEGMA MW; at high initiator density (mole fraction >10%), poly(OEGMA)$_{1100}$ showed lower graft densities than poly(OEGMA)$_{300}$ and poly(OEGMA)$_{475}$ which could be attributed to the size difference of the monomers.

Surface EO unit density was estimated from monomer MW, polymer chain length and polymer chain density and was found generally to increase with increasing initiator density in the range (0.03-1.1/nm^2) for a given monomer MW. For a given high initiator density (initiator fraction >10%), poly(OEGMA)$_{475}$ layers showed the highest EO unit density. Poly(OEGMA)$_{300}$ and poly(OEGMA)$_{1100}$ layers showed similar, but lower, EO unit density.

Acknowledgments

This work was supported by a Strategic Grant of the Natural Sciences and Engineering Research Council of Canada (NSERC). We also thank the Canada Foundation of Innovation (CFI) for supporting the research facilities in our laboratories.

References

1 Harris J. M., Introduction to biotechnical and biomedical applications of poly(ethylene glycol), In: Poly(ethylene glycol) Chemistry: Biotechnical and Biomedical Applications, Harris J. M. (ed), Plenum Press, NY, P1-14 (1992).

2 Szleifer I., Protein adsorption on surfaces with grafted polymers: A theoretical approach, Biophys. J., 72, 595 (1997).

3 Jeon S. I., Andrade J. D., Protein-surface interactions in the presence of polyethylene oxide: II. Effect on protein size, J. Coll. Interf. Sci., 142, 159 (1991).

4 Unsworth L. D., Sheardown H., Brash J. L., Protein resistance of surfaces prepared by sorption of end-thiolated poly(ethylene glycol) to gold: Effect of surface chain density, Langmuir, 21, 1036 (2005).

5 Liu P., Su Z., Surface-initiated atom transfer radical polymerization (SI-ATRP) of MMA from PANI powders, Polym. Bullet., 55, 411 (2005).

6 Zhang H., Shouro D., Itoh K., Takata T., Jiang Y., Grafting polymer from poly(ethylene terephthalate) films by surface-initiated ATRP, J. Appl. Polym. Sci., 108, 351 (2008).

7 Ma H., Wells M., Beebe T. P., Chilkoti A., Surface-initiated atom transfer radical polymerization of oligo(ethylene glycol) methyl methacrylate from a mixed self-assembled monolayer on gold, Adv. Funct. Mater., 16, 640 (2006).

8 Feng W., Zhu S., Ishihara K., Brash J. L., Protein resistant surfaces: Comparison of acrylate graft polymers bearing oligo-ethylene oxide and phosphorylcholine side chains, Biointerphases, 1, 50 (2006).

9 Feng W., Brash J. L., Zhu S., Non-biofouling materials prepared by atom transfer radical polymerization grafting of 2-methacryloloxyethyl phosphorylcholine: separate effects of graft density and chain length on protein repulsion, Biomaterials, 27, 847 (2006).

10 Ma H., Hyun J., Stiller P., Chilkoti A., 'Non-fouling' oligo(ethylene glycol)-functionalized polymer brushes synthesized by surface-initiated atom transfer radical polymerization, Adv. Mater., 16, 338 (2004).

11 Ejaz M., Ohno K., Tsujii Y., Fukuda T., Controlled grafting of a well-defined glycopolymer on a solid surface by surface-initiated atom transfer radical polymerization, Macromolecules, 33, 2870 (2000).

12 Jin Z., Feng W., Beisser K., Zhu S., Sheardown H., Brash J. L., Protein-resistant polyurethane prepared by surface-initiated atom transfer radical graft polymerization (ATRgP) of water-soluble polymers: Effects of main chain and side chain lengths of grafts, Coll. Surf. B: Biointerfaces, 70, 53 (2009).

13 Jin Z., Feng W., Zhu S., Sheardown H., Brash J. L., Protein-resistant polyurethane via surface-initiated atom transfer radical polymerization of oligo(ethylene glycol) methacrylate, J. Biomed. Mater. Res. A, 91A, 1189 (2009).

14 Kim E., Lee B. S., Pyo H. B., Song H. W., Kim Y. P., Choi I. S., Kim H. S., Fabrication of nonbiofouling surface and its application to surface plasmon field-enhanced fluorescence spectroscopy, Biochip J., 2, 103 (2008).

15 Lee B. S., Chi Y. S., Lee K. B., Kim Y. G., Choi I. S., Functionalization of poly(oligo(ethylene glycol) methacrylate) films on gold and Si/SiO_2 for immobilization of proteins and cells: SPR and QCM studies, Biomacromolecules, 8, 3922 (2007).

16 Feng W., Chen R. X., Brash J. L., Zhu S. P., Surface-initiated atom transfer radical polymerization of oligo(ethylene glycol) methacrylate: effect of solvent on graft density, Macromol. Rapid Commun., 26,1383 (2005).

17 Pyun J., Kowalewski T., Matyjaszewski K., Synthesis of polymer brushes using atom transfer radical polymerization, Macromol. Rapid Commun., 24,1043 (2003).